UNIVERSITÀ DEGLI STUDI DI UDINE

Dipartimento di Scienze Mediche e Biologiche

CORSO DI DOTTORATO DI RICERCA IN SCIENZE E TECNOLOGIE CLINICHE
XXIV CICLO

TESI DI DOTTORATO DI RICERCA

Role of $p27^{KIP1}$ in cancer progression: new insight into its post-translational regulation

DOTTORANDA
Dott.ssa Sara Lovisa

RELATORE
Prof. Alfonso Colombatti

CORRELATORI
Dott. Gustavo Baldassarre
Dott.ssa Monica Schiappacassi

COORDINATORE
Prof. F.S. Ambesi Impiombato

Anno Accademico 2011/2012

Alla mia famiglia

Alle mie preziosissime Amiche

This work was performed in the Division of Experimental Oncology 2
at Centro di Riferimento Oncologico (CRO, National Cancer Institute) of Aviano,
directed by Prof. Alfonso Colombatti.

I am grateful to S.C.I.C.C. group and in particular to
Dr. Monica Schiappacassi and Dr. Gustavo Baldassarre.

I thank Dr. Susanna Chiocca and Dr. Simona Citro (IFOM-IEO Campus, Milan)
for performing the first part of the analysis of p27 SUMOylation.

TABLE OF CONTENTS

ABSTRACT

The tumor suppressor gene $p27^{Kip1}$ plays a fundamental role in human cancer progression. Its expression and/or functions are altered in almost all the different tumor histotype analyzed. p27 is mainly regulated at post-translational level and its deregulation in human cancer is mainly due to its accelerated proteasomal degradation. It has been demonstrated that the tumor suppression function of p27 resides not only in the ability to inhibit Cyclins/CDKs complexes through its N-terminal domain, but also in the capacity to modulate cell motility through its C-terminal portion. Particular interest has been raised by the last amino-acid (threonine 198) in the regulation of both protein stability and cell motility. Here, we describe that the presence of threonine in position 198 is of primary importance for the regulation of the protein stability and for the control of cell motility. However, while the control of cell motility is dependent on the phosphorylation of T198, the stability of the protein is specifically controlled by the steric hindrance of the last amino acid. The effects of T198 modification on protein stability are not linked to the capacity of p27 to bind Cyclins/CDKs complexes and/or the F-box protein Skp2. Conversely, our results support the hypothesis that conformational changes in the disorder structure of the C-terminal portion of p27 are important in its ability to be degraded via a proteasome-dependent mechanism. On the other hand T198 phosphorylation favors p27/stathmin interaction eventually contributing to the regulation of cell motility.

Our results also indicate that p27 functions are affected by SUMOylation, a reversible post-translational modification that plays an important role in regulating protein localization, stability and activity. We demonstrate that p27 is SUMOylated *in vitro* on lysine 134 and that p27 SUMOylation affects protein stability, since the un-SUMOylated $p27^{K134R}$ mutant is less stable when compared to the WT protein. p27 SUMOylation is increased by TGFβ, an important stimulus regulating p27 stability and localization. Accordingly, TGFβ treatment induces p27-SUMO colocalization into the nucleus and stimulates nuclear accumulation of endogenous p27. Moreover, TGFβ induces nuclear accumulation of p27 WT but not of the SUMO-defective $p27^{K134R}$. Since TGFβ has been described to induce G1-arrest by accumulating nuclear p27 and by preventing its proteasomal degradation our results suggest that TGFβ regulation of p27 function and localization could be exerted through the modulation of its SUMOylation.

Collectively this thesis work provides new insight into p27 regulation by both conformational changes in its unstructured C-terminal domain and post-translational modifications.

INTRODUCTION

1. Cell cycle

The term “cell cycle” defines the process by which a cell correctly divides into two daughter cells and is central to the understanding of all life (Nurse, 2000). It is in fact largely accepted that is essential for their survival that the two daughter cells receive a full complement of all the organelles and a copy of the genome correctly duplicated. To ensure that DNA faithfully replicates and that the replicated chromosomes correctly segregate into the two newly divided cells, in all eukaryotic cells, cell cycle progression is stringently controlled (Heichman et al., 1994; Wuarin et al., 1996). In particular several mechanisms ensure that S phase is completed before mitosis begins and that M phase started only if the DNA has been faithfully replicated. This is possible since two Gap phases (the G1 separating the M and S phases, and the G2 between the S and M phases) are present in somatic cells and dictate the timing of cell division during which the control mechanisms principally act. However, in early embryonic cells that need to fast replicate, these two Gap phases seem to be absent. In living organisms the cells are usually in a state of quiescence called G0 and can re-enter into the cell cycle after stimuli derived from the local microenvironment such us growth factors stimulation, a process that can be reproduced in *in vitro* experiments. The beginning of the G1 phase is the only part of the cell cycle that seems to be dependent on growth factors stimulation. When cells are stimulated by growth factors to enter the cycle from G0, they generally require continuous mitogenic stimulation to be driven to the restriction point, after which mitogens can be withdrawn and cells will enter S phase and complete the cycle in their absence. This landmark study has been carried out about 40 years ago by Arthur Pardee (1974) that was able to demonstrate that, in a normal cell, growth factors are necessary to initiate and maintain the transition from early to late G1 phase since to the so called “restriction point” or G1 phase checkpoint. Once the cell had passed the restriction point it is irreversibly committed to complete cell division even if growth factor stimulation is removed. Once the restriction point has been passed, the cell enters S phase during which the DNA is duplicated. At this point, in the G2 phase, before the mitosis (M phase) could start, the cell controls that DNA has been faithful duplicated and checks the internal signalling events necessary for a successful division. Progression of mitosis is controlled by signalling pathways that monitor the integrity of microtubule function, to ensure the fidelity of chromosome segregation. Regulation by growth factors would be damaging for a cell, and consequently, mitosis is a growth factors-independent phase of the cell cycle. As cells exit mitosis, the cell cycle is reset, allowing the establishment of a new, competent replication state in G0 or G1 phases.

1.1 Cyclins and CDKs

Progression through the cell cycle is orderly driven by Cyclin-Dependent Kinases (CDK) activity (Figure 1). CDKs are serine and threonine kinases, and their actions are dependent on associations with their activating subunits, cyclins (Sherr, 1995). Cyclin abundance is regulated by protein synthesis and degradation; the activity of CDKs is therefore regulated to a large degree by the presence of different cyclins. Also, cyclins possess overlapping, but distinct, functional activities, allowing further refinement of control and probably the timely and irreversible occurrence of cell-cycle transitions. Cyclin specificity can be achieved in various ways: cyclins are expressed or are present at stable levels at different times; they are differentially sensitive to cell-cycle-regulated inhibitors; they are differentially restricted to specific subcellular locations; or they bind specifically to only some phosphorylation targets. In some cases, intrinsic cyclin specificity has been traced to specific modular sequences in the cyclin protein (for example, nuclear localization sequences (NLS), destruction boxes that regulate proteolysis or hydrophobic patches that can mediate interactions with substrates). Cyclins are regulated at the level of protein degradation by ubiquitin-mediated proteolysis. The sensitivity of different cyclins to different ubiquitin ligases constitutes an important mechanism for cyclin specificity in controlling the cell-cycle engine. Restriction point control is mediated by two families of enzymes, the cyclin D- and E-dependent kinases. The D-type cyclins (D1, D2, and D3) interact combinatorially with two distinct catalytic partners: CDK4 and CDK6. Whereas CDK4 and CDK6 are relatively long-lived proteins, the D-type cyclins are unstable, and their induction, synthesis, and assembly with their catalytic partners all depend upon persistent mitogenic signalling. In this sense, the D-type cyclins act as growth factor sensors, forming active kinases in response to extracellular cues (Sherr et al., 1993). Indeed, the major function of the cyclin D pathway is to provide this link between mitogenic cues and the potentially autonomous cell cycle machinery which is composed primarily of CDK2 and CDK1 and their associated regulators. Thus D-type cyclins are usually absent from cell cycles that proceed independently of extrinsic mitogenic signals. Conversely, constitutive activation of the cyclin pathway can reduce or overcome certain requirements for cell proliferation and thereby contribute to oncogenic transformation. (Weinberg et al., 1995). The activities of these kinases are regulated also by integrins. The expression of cyclin D1 and thus, the activation of CDK4/6 are suppressed in cells that are not anchored to ECM. Integrin signalling may be needed for the transcription of cyclin D1, because the cyclin D1 promoter is co-ordinately regulated by JNK and ERK. Integrins also stimulate the p70 S6-kinase, which may promote cyclin D1 translation. Finally,

anchorage to the ECM is necessary for the down-regulation of the CDK2 inhibitors p21 and p27 and, thus, the activation of cyclin E-CDK2.

The mitogen-dependent accumulation of the cyclin D-dependent kinases triggers the phosphorylation of the Retinoblastoma protein (Rb), thereby helping to cancel its growth-repressive functions. Rb represses the transcription of genes whose products are required for DNA synthesis. It does so by binding transcription factors such as the E2Fs and recruiting repressors such as histone deacetylases (Brehm et al., 1998; Luo et al., 1998; Magnaghi et al., 1998) and chromosomal remodelling SWI/SNF complexes (Zhang et al., 2000) to E2F-responsive promoters on DNA. Rb phosphorylation by the G1 CDKs disrupts these interactions (Harbour et al., 1999), enabling released E2Fs to function as transcriptional activators. Apart from a battery of genes that regulate DNA transcription, E2Fs induce the cyclin E and A genes. Cyclin E enters into a complex with its catalytic partner CDK2 and collaborates with the cyclin D-dependent kinases to complete Rb phosphorylation (reviewed in Belletti et al., 2005). This shift in Rb phosphorylation from mitogen-dependent cyclin D-CDK4/6 complexes to mitogen-independent cyclin E-CDK2 accounts in part for the loss of dependency on extracellular growth factors at the restriction point. Cyclin E-CDK2 also phosphorylates substrates other than Rb, and its activity is somehow linked to replication origin firing. The activity of the cyclin E-CDK2 complex peaks at the G1-S transition, after which cyclin E is degraded and replaced by cyclin A. Cyclin A is particularly interesting among the cyclin family, because it can activate two different CDKs and function in both S and M phases. In mitosis, the precise role of cyclin A is obscure, but it may contribute to the control of cyclin B stability. Cyclin A starts to accumulate during S phase and is abruptly destroyed before previous to cyclin B which persists until metaphase plate is formed.

Other levels of CDKs regulation are represented by phosphorylation and de-phosphorylation of specific threonine and/or tyrosine residues that results either in the activation or in the inhibition of CDKs catalytic activity. In particular, CDKs have to be phosphorylated (on the threonine residue located in its 'T-loop') to fully open its catalytic cleft. In fact, CDK7 together with cyclin H and the assembly factor MAT1 forms the CDK-activating kinase (CAK) complex, responsible for the activating phosphorylation of CDK1, CDK2, CDK4 and CDK6. This phosphorylation is removed by the phosphatase KAP after the cyclin partner has been degraded, i.e. KAP binds to CDK2 and dephosphorylates Thr160 when the associated cyclin subunit is degraded or dissociated.

On the other hand, the cyclin−CDK complexes can be kept in an inactive state by phosphorylation on one, or sometimes two, residues in the ATP-binding site of the CDK. These residues are a conserved tyrosine in many CDKs that is phosphorylated by Wee1/Mik1, and an adjacent threonine residue that is phosphorylated in animal cells by Myt1. Members of the Cdc25 family of

phosphatases remove the phosphates from the ATP-binding site tyrosine and/or threonine of the CDK, and thus activate the cyclin-CDK complex. Finally, the cyclin-CDK complexes are further regulated by the binding of specific CDK inhibitor proteins (CKI) (reviewed in Nigg, 2001).

1.2 CKIs

The CKIs can be divided into 2 families on the basis of sequence: the INK4 family and the Kip/Cip family (reviewed in Belletti et al., 2005). The INK4 proteins are almost entirely composed of ankyrin repeats, a putative protein-protein interaction motif and this family comprises four members: $p15^{INK4b}$, $p16^{INK4a}$, $p18^{INK4c}$ and $p19^{INK4d}$. In humans, INK4a and INK4b are closely linked on the short arm of chromosome 9, whereas INK4c maps to chromosome 1 and INK4d maps to chromosome 19. In mice, the INK4c and INK4d genes are expressed in stereotypic patterns in different tissues during development in uterus, whereas INK4a and INK4b expression has not been detected prenatally. These inhibitors are specific for the CDK4 and CDK6 kinases that bind the D-type cyclins. These kinase complexes have been most closely linked to the control of G1 phase, especially with regard to the decision to proliferate or not according to the presence of growth factors, and to cell size control. The INK4 family inhibits the CDK4 subfamily by competing for binding with the D-type cyclins. By preventing the D-type cyclins from binding CDK4 and 6, the INK4 proteins could be predicted to keep these kinases in an inactive state, because, in analogy with what has been demonstrated for the activation of CDK2 by cyclin A, CDK4 and 6 should neither be able to bind their substrates nor to hydrolyse ATP without the conformational change induced by binding with the cyclin Ds. However, to confirm this hypothesis it will require the resolution of the structures of the INK4 proteins and the CDK4/6 subfamily that up to now has not been reported. The INK4 proteins are also able to inhibit CDK4/6 in a complex with cyclin D (Jeffrey et al., 2000), and it will be interesting to see whether this inhibition bears any relation to the inhibitory mechanisms employed by the Kip/Cip family. The Kip/Cip family comprises three proteins; $p21^{Cip1/Waf1/Sdi1}$ (Xiong et al., 1993; el-Deiry et al., 1993; Harper et al., 1993; Noda et al., 1994), $p27^{Kip1}$ (Polyak et al., 1994; Toyoshima et al., 1994) and $p57^{Kip2}$ (Lee et al., 1995; Matsuoka et al., 1995). These inhibitors show tissue specific distribution patterns. For example in gastrointestinal tract, the best organ characterized, p21, p27 and p57 are not expressed in the basal cells, which are the proliferating stem cells of keratinocytes, whereas there are well expressed in the suprabasal nonproliferative compartment (el-Deiry et al., 1995; Fredersdorf et al., 1996). Intense co-staining of p27 and p57 has been detected in some specialized tissue, such as neurons (postmitotic neurons in the intermediate zone), lens, skeletal muscle, cartilage, lung (bronchial epithelium), kidney

(podocytes) and skin (superbasal cells) during their development. However, some tissue express only p27, such as most lymphocytes, the retina, and the adrenal medulla (reviewed in Nakayama et al., 1998). Their expression regulation is also differently regulated following specific stimuli. Indeed p57 is imprinted (Matsuoka et al., 1996), and have been implicated in cell differentiation (Elledge et al., 1996), and in the response to stress. p21 transcription is upregulated in response to DNA damage by wild type but not mutant p53, and p27 was initially identified as the factor responsible for inhibiting proliferation in contact-inhibited and TGF*β*-treated cells (Koff et al., 1993). Until now the Kip/Cip family had been considered specific for the cyclin-CDK complexes (for the G1 and S phase kinases) (Harper et al., 1995). However, there is a report showing that p21, a DNA-damage-inducible cell-cycle inhibitor, acts also as an inhibitor of the SAPK (kinases stress-activated protein), group of mammalian MAP, such as JNK (Shim et al., 1996), suggesting that p21 may participate in regulating signalling cascades that are activated by cellular stresses such as DNA damage. The Kip/Cip family are 38–44% identical in the first 70 amino acid region of their amino terminus, and this region is sufficient to inhibit cyclin-CDK activity (Nakanishi et al., 1995; Chen et al., 1995; Chen et al., 1996). In fact the kinase inhibitory domain maps to the N-terminus (1-82) and contains the CDK binding site (28-82). A functional characterization of p21 mutants in the N-terminal domain reveals that cyclins bind to this domain independently of CDK2. Fotedar et al. (1996) find that p21 can associate with cyclin-CDK kinases in two functionally distinct forms, one in which the kinase activity is inhibited and the other one in which the kinase is still active. The first one requires that p21 bind both the CDK and the cyclin. In the second type of interaction, p21 bind only the cyclin or the CDK.

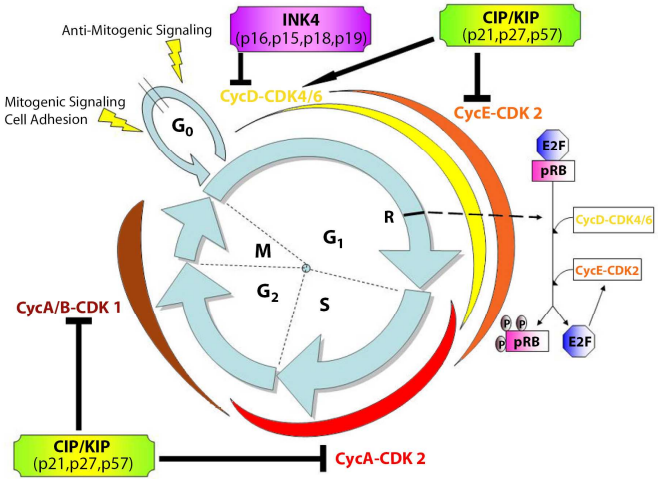

Figure 1. *Schematic representation of cell cycle regulation.* Mitogenic stimuli promote cell cycle progression from G0 to G1 inducing the expression of D type cyclins and lowering the expression of p27. Sequential activation of cyclin E-CDK2, cyclin A-CDK2, cyclin A-CDK1 and cyclin B-CDK1 allow the cells to pass through the restriction point (R) and to complete the mitotic division. The passage through the R point is due to the inactivation of the pRB protein by CDKs-dependent phosphorylation (*from Belletti et al., 2005).*

2. $p27^{Kip1}$

$p27^{Kip1}$ (hearafter p27) was first identified as a CDK2 activity inhibitor detected in contact-inhibited or TGFβ treated cells (Polyak et al., 1994). At the same time, it was cloned in a tri-hybrid screen as a cyclin D-CDK4 interacting protein (Toyoshima et al., 1994).

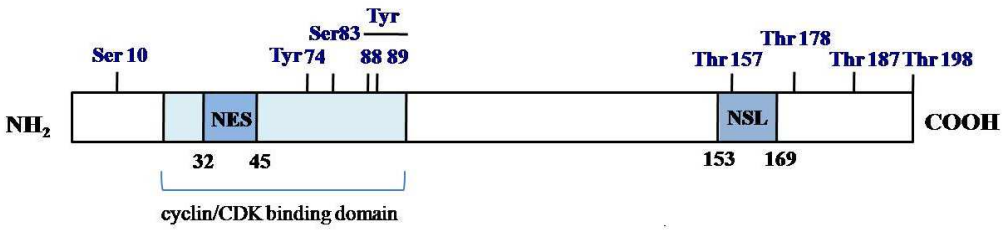

Figure 2. *Schematic representation of the principal p27 domains and its major phosphorylation sites.*

2.1 p27 in G1/S transition

p27 has a crucial role in the G1-S transition by interacting with and inhibiting cyclin E-CDK2 and cyclin A-CDK2 activity, thus blocking cell cycle progression (reviewed in Belletti et al., 2005). In early G1 p27 promotes cyclin D-CDK4/6 complex assembly and nuclear import, increasing cyclin D stability, all without inhibiting CDK4 kinase activity. In proliferating cells, p27 is primarily associated with cyclin D-CDK4/6 complexes, but these complexes are catalytically active, whereas in G1 arrested cells p27 preferentially binds and inhibits cyclin E-CDK2. The sequestration of p27 by cyclin D-CDK4/6 complexes effectively frees CDK2 from inhibition and allows both CDK4/6 and CDK2 to remain active. In this way mitogen induction of cyclin D expression determines cell cycle progression both by activating CDK4 and by sequestering p27 thus favouring cyclin E-CDK2 activation. Activation of cyclin E by E2F, after hyper-phosphorylation of pRB, enables the formation of the active cyclin E-CDK2 complex. This is accelerated by the continued sequestration of Cip/Kip proteins into complexes with assembling cyclin D-CDK complexes. Cyclin E-CDK2 completes the phosphorylation of Rb, further enabling activation of E2F-responsive genes, including cyclin A. Once cyclin E-CDK2 is activated, it phosphorylates p27. This phosphorylation on threonine 187 allows p27 to be recognized by the ubiquitin ligases and to be targeted for destruction by the 26S proteasome (reviewed in Lu et al., 2010). Therefore, cyclin E-CDK2 antagonizes the action of its own inhibitor. Once cyclin E-CDK2 is activated, p27 is rapidly degraded, contributing to the irreversibility of passage through the restriction point. If cells are persistently stimulated with mitogens, cyclin D-dependent kinase activity remains high in the

subsequent cell cycles, p27 levels stay low, and virtually all p27 can be found in complexes with the cyclin D-CDK4/6. However, when mitogens are withdrawn, cyclin D is rapidly degraded, and the pool of previously sequestered Cip/Kip proteins are mobilized to inhibit cyclin E-CDK2, thereby arresting progression usually within a single cycle.

Multiple extracellular stimuli regulate p27 abundance, which functions as a sensor of external signals to cell cycle regulation. In normal cells p27 is expressed at high levels in quiescence phase, whereas it decreases rapidly after mitogen triggering and cell cycle re-entry. A number of studies have shown that many anti-mitogenic signals induce the accumulation of p27, including cell–cell contact, growth factor deprivation, loss of adhesion to extracellular matrix, TGFβ, cAMP, rapamycin or lovastatin treatment (Hengst et al., 1998) (Figure 1).

2.2 p27 in G2/M transition

Several works on p27 regulation during cell cycle preogression have revealed a role for p27 also in G2/M transition. Historically p27 was discovered as universal inhibitor of CDKs, able to downregulate *in vitro* not only cyclin E/A-CDK2 activity but also CDK1, whose kinase activity is crucial for mitosis entry (Toyoshima et al., 1994). However, the latter *in vitro* evidence remained for long time unexplored *in vivo*, becoming almost irrelevant to p27 cellular physiology. Nakayama and col. have demonstrated *in vivo* how p27 accumulation at G2/M transition induces a strong decrease in CDK1 associated activity. The prolonged G2 arrest induced by p27, through the suppression of CDK1 activity, was shown to be responsible for centrosome duplication, cell endoreplication (increase in cell genomic content without an associated cell division) and cell polyploidy (Nakayama et al., 2004). As an alternative mechanism, others proposed that these mitotic defects could be due to the ability of high p27 protein levels to prevent the expression of CDK1 rather than to act as CDK1 inhibitor, leaving the effective role of p27 in mitosis regulation unsolved (Kossatz et al., 2004).

2.3 Regulation of p27

In normal cells, the amount of p27 protein is high during G0 phase but decreases rapidly on re-entry of cells into G1 phase. This rapid removal of p27 at the G0-G1 transition is required for effective progression of the cell cycle to S phase. The abundance of p27 is thought to be controlled by multiple mechanisms that operate at level of its synthesis (transcription, translation), degradation and localization. In particular, a change in the subcellular localization of p27 induced by the exposure of quiescent cells to growth stimuli is crucial for the down-regulation of this protein at the G0-G1 transition. In G0 phase, p27 accumulates in the nucleus, where it inhibits the cyclin-CDK complexes. However, p27 undergoes rapid translocation from the nucleus into the cytoplasm by yet unspecified mechanism that seems to involve phosphorylation of Serine 10 by KIS (Kinase-interacting stathmin) or by MAPK and /or phosphorylation of Threonine 198 by Akt or RSK. The translocation of p27 from the nucleus to the cytoplasm is follow by its degradation by the ubiquitin-proteasome pathway involving the KPC1 and KPC2 proteins. This ubiquitin dependent degradation of p27 is different from the one observed into the nucleus and that requires p27 phosphorylation on T187 by the cyclin E-CDK2 complex and the binding to the SKP2 F-box protein (reviewed in Belletti et al., 2005) (Figure 3).

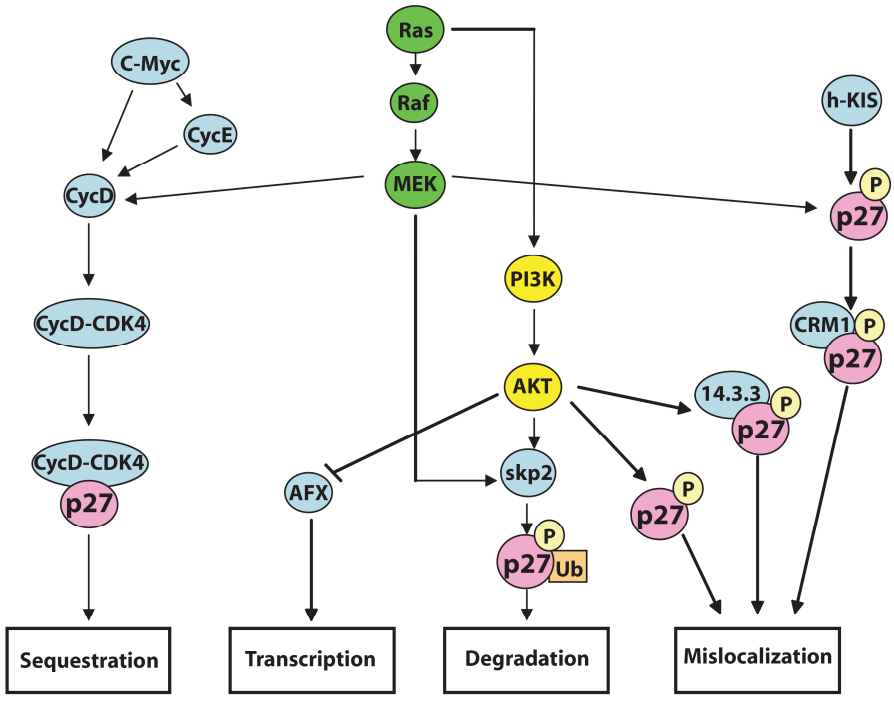

Figure 3. *Representation of the different intracellular pathways known to regulate p27 expression and function* (*from Belletti et al., 2005*).

2.3.1 Transcriptional regulation of p27

Although p27 mRNA levels are usually constant, there are some exceptions to this rule. p27 promoter activity has been shown to be positively regulated by Interleukin-6 signaling through STAT3 activation in melanoma cells (Kortylewski et al., 1999) and negatively regulated by PI3K and Akt through the inhibition of the AFX forkhead transcription factor (Medema et al., 2000). Recently Chassot et al. (2007), using a wounding model that induces cell-cycle entry of human dermal fibroblasts, demonstrated that p27 mRNA is downregulated when cells progress into the G1 phase, and then it returns to its basal level when cells approach the S phase. By using a quantitative PCR screening they identified inhibitors of differentiation (Id3), a bHLH transcriptional repressor, as a candidate mediator accounting for p27 mRNA decrease. Id3 silencing, using a small interfering RNA approach, reversed the injury mediated p27 downregulation demonstrating that Id3 is involved in the transcriptional repression of p27.

2.3.2 Post-translational modifications: p27 phosphorylation

The analysis of p27 by 2D electrophoresis has definitely demonstrated that the protein is phosphorylated at multiple sites. It is generally accepted that these post-synthetic modifications are phosphorylations on threonine and serine residues. However, a number of papers has also recently reported the phosphorylation of p27 on tyrosine residues. Altogether the well-characterized phosphorylated sites on p27 are: serine 10, threonines 157, 187, 198 and tyrosines 74, 88, 89. The phosphorylation in serine 178 has also been described. However, its role and function is, at present, scarcely characterized. Phosphorylation of p27 has been studied extensively and for each of the phosphorylation sites several kinases have been reported and different functions have been ascribed (Borriello et al., 2007).

Furthermore, bidimensional analyses showed the occurrence of a p27 isoform with a pI not due to a phosphorylation (Borriello et al., 2006). Thus p27 could undergo other post-translational modifications.

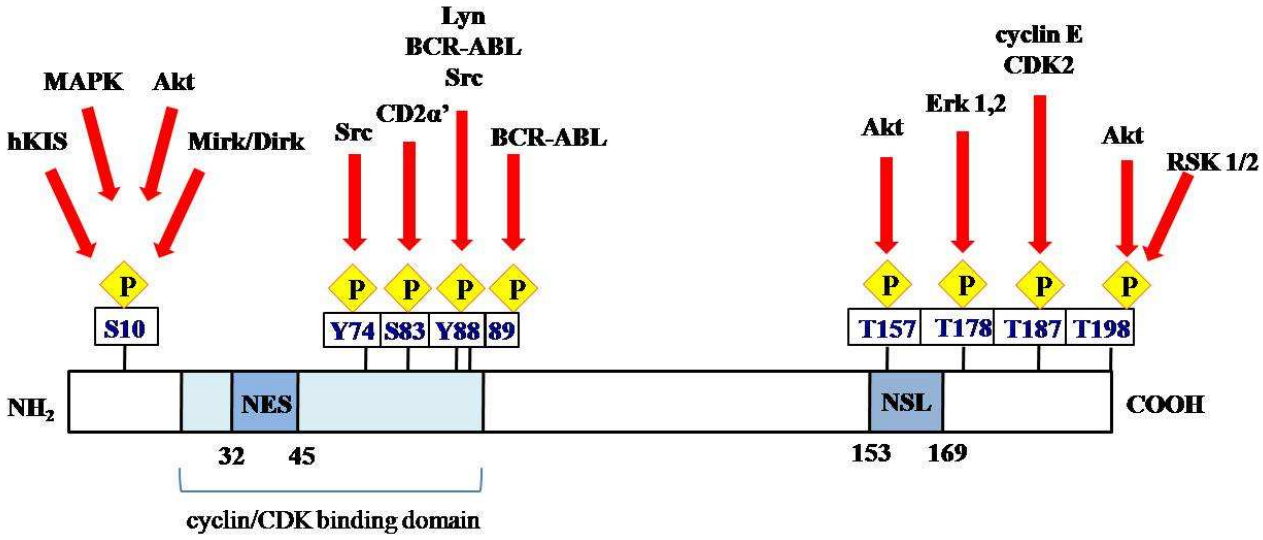

Figure 4. *Summary of the phosphorylation sites observed in p27 with known kinases that modify individual sites.*

2.3.2.1 Serine 10

The phosphorylation of p27 on serine 10 was reported for the first time by the Nakayama's group in 2000 and confirmed by numerous studies. It is estimated that 70–75% of phosphate incorporation occurs on this residue that represents the most abundant post-translational p27 modification. Phosphorylation of Ser 10 is regulated in a cell cycle-dependent manner and may function to stabilize p27. In fact the extent of Ser10 phosphorylation was markedly increased in cells in the G0-G1 phase of the cell cycle compared with that for cells in S or M phase. Furthermore, a mutant p27 in which Ser10 was replaced with glutamic acid in order to mimic the effect of Ser10 phosphorylation exhibited a marked increase in stability compared with the wild-type or S10A mutant proteins (Ishida, 2000). Moreover, Ser10 phosphorylation is required for the binding of p27 to CRM1, a carrier protein for nuclear export (Ishida 2002). Both this reports demonstrated that the nuclear export of p27 is regulated by the phosphorylation on Ser10 and plays critical role to decrease the nuclear abundance of p27 protein below a certain threshold, thereby allowing the activation of cyclin-CDKs complexes and perhaps initiating p27 cytoplasmic functions (Alessandrini et al., 1997 and Rodier et al., 2001).

On the other hand, a major complexity exists about the kinase(s) responsible for serine 10 phosphorylation. At least four enzymes have been supposed to catalyze the reaction. These include MAPK, human kinase interacting stathmin (hKis), Akt/PKB and Mirk/Dirk1B. An hypothesis that might explain the large number of enzymes able to phosphorylate the CKI on Ser10 is that they act during diverse processes and in different phenotypes.

hKis has been identified by Bohem and colleagues as putative Ser10 p27 kinase by a two hybrid screen analysis employing the C-terminus of p27 as bait. The enzyme activation causes: i) p27 cytosolic relocalization and subsequent degradation, and ii) the activation of cell proliferation. Thus, hKis activity seems mostly related to p27 removal and S entry from G1/G0 phases. However, the analysis of the various isoforms of the p27 suggests that the CKI is continuously phosphorylated in serine 10 during G1/G2 transition, a period of cell cycle when hKis activity is low. Mirk/dyrk1B kinase also phosphorylates p27 at Ser10 and increases during the entry in G0 phase (Deng X. et al., 2004). Thus, it might be considered the enzyme that is required for phosphorylating the protein when hKis is not operative. However, the distribution of Mirk/dyrk1B is mostly confined to muscle, while S10 phosphorylated p27 is ubiquitous and it is active in G0, while in this phase a scarce phosphorylation of p27 has been reported. The importance of Akt in the phosphorylation of p27 appears quite complex. Initially, Akt has been suggested to modify the CKI in Thr157 or Thr198 but another work suggests that the kinase phosphorylates p27 mostly in serine 10 and then, in additional residue(s) (Nacusi et al., 2006). AKT also regulates the expression of the CKI gene by negatively acting on FOXO transcription factors.

The activation of Erk1/2 causes a p27 level decrease by inducing the translocation of the protein from the nucleus to the cytoplasm, followed by the CKI degradation. However, several findings indicate that the effect is not due to a direct phosphorylation, although *in vitro* experiments showed that activated Erk1/2 might add a phosphate on serine 10.

In brief, the addition of a phosphate on serine 10 is undoubtedly the major post-synthetic modification of p27, but the identification of enzyme(s) responsible for this phosphorylation is still fading.

2.3.2.2 Threonine 157

Three papers published in 2002 described threonine 157 as target of PKB/Akt (Viglietto et al., Shin et al., Liang et al.). The leit motif of these papers is that phosphorylation of p27 by PKB/Akt leads to functional inactivation of p27 by cytoplasmic sequestration without a decrease in steady state level. PKB/Akt is an effector of Ras/PI3 kinase activation, which occurs in response to stimulation of a broad spectrum of growth factor receptors. Interestingly, this pathway becomes hyperactivated in many cancers due to either deregulation of growth factor receptors or Ras, or inactivation of PTEN, a phosphatase that is antagonistic to PKB/Akt. Thus, p27 inactivation may be a significant factor in carcinogenesis mediated by hyperactivation of the Ras/PI3 kinase pathway. When scanning the p27 polypeptide sequence for minimal PKB/Akt consensus phosphorylation sites, all 3 groups found and verified a site at Thr157. From a mechanistic perspective, the fact that

this site was located within the nuclear localization sequence (NLS) of p27 suggested a hypothesis for PKB/Akt regulation of p27. Since the target of p27 regulation, Cdk2 an essential G1/S phase kinase, is exclusively nuclear, interference with p27 nuclear localization would effectively separate p27 from its regulatory target. This indeed was shown to be true in that ectopic expression of activated PKB/Akt caused cytoplasmic accumulation of wild-type p27 and a concomitant reduction of nuclear wild-type p27/Cdk2 complexes, but could not affect the nuclear localization of the S157A mutant p27, resistant to PKB/Akt phosphorylation. Liang et al., in fact, confirmed that S157 phosphorylation directly interfered with nuclear localization of p27 by *in vitro* assay. Furthermore, PKB/Akt expression could neutralize the cell cycle inhibitory effects of ectopic expression of wild-type p27 but not those of the S157A mutant, effectively linking the observed effects on p27 localization to the biology of p27. However a different mechanism of p27 phosphorylation by Akt has been recently proposed, in that it has been suggested that PKB initially modifies the CKI on serine 10 and, secondary to this phosphorylation, it is able to modify p27 on other residue(s) (Nacusi et al., 2006).

2.3.2.3 Serine 83

A work by Hauck et al. (2008) indicate serine 83 as a new residue phosphorylated by the ubiquitous serine-threonine kinase CK2-α' in cardiomyocytes. The lack of regenerative capacity of adult mammalian cardiomyocytes is thought to be caused by the unavailability of G1 cyclin–CDKs, crucial positive modulators of the cell cycle, and high levels of inhibitory p27. Because p27 is highly expressed in adult myocardium despite the lack in thisi tissue of p27's main target, cyclin E/CDK2, they hypothesized that p27 may exert a growth regulatory function in cardiomyocytes through alternative pathways linking extracellular growth stimuli to p27. They show that angiotensin II, a major cardiac growth factor, induces the proteasomal degradation of p27 through protein kinase CK2-α'–dependent phosphorylation. CK2-α'–mediated phosphorylation of p27 at Ser83 and Thr187 relieves CK2-α' from p27 inhibition and converts CK2-α' into an active kinase which target p27 for proteasomal degradation. Conversely, unphosphorylated p27 potently inhibits CK2-α'. Thus, the p27–CK2-α' interaction is regulated by hypertrophic signaling events and represents a regulatory feedback loop in differentiated cardiomyocytes analogous to, but distinct from, the feedback loop arising from the interaction of p27 with Cdk2 that controls cell proliferation. CK2-α'–dependent regulation of p27 represents a new link between extracellular growth signaling and surveillance of p27 activity in cardiac myocytes. In fact these data show that extracellular growth factor signaling regulates p27 stability in postmitotic cells, and that

inactivation of p27 by CK2-α' is crucial for agonist- and stress-induced cardiac hypertrophic growth.

2.3.2.4 Serine 178

The phosphorylation of serine 178 has also been described in a work published in 2003 (Wolf et al.) which described the role of p27 in the high glucose-induced hypertrophy of mesangial cells. Mesangial cell hypertrophy is one of the earliest morphological abnormalities of diabetic nephropathy. High glucose induces p27 by a post-transcriptional mechanism and mesangial cell hypertrophy depends on G1-phase arrest mediated by this CDK-inhibitor. This work showed that high glucose stimulates phosphorylation of MAP kinases Erk 1,2 in p27 +/+ and –/– mesangial cells. Moreover activation of Erk 1,2 leads to phosphorylation of p27 *in vitro* and *in vivo*. The p27 protein contains three consensus sites for MAP kinase-induced phosphorylation (serine10, serine 178, and threonine 187). Mutations of serine 10 or threonine 187 still supported high glucose-induced hypertrophy. In contrast, a mutation of serine178 converted the hypertrophic response into a proliferative phenotype. Mutation of serine 178 leads to the attenuated expression of p27 in the presence of high glucose. This study demonstrated that high glucose stimulates Erk 1,2 that in turn phosphorylates p27 at serine 178 increasing its expression.

2.3.2.5 Threonine 187

The phosphorylation on threonine 187 represents the only post-synthetic modification consistently demonstrated and accepted. The phosphorylation is catalyzed by the cyclin E/A-CDK2 complex and cyclin B-CDK1 (Alessandrini et al. 1997; Sheaff et al. 1997; Vlach et al. 1997) and leads to its degradation via the ubiquitin-proteasome system (Pagano et al., 1995 and Loda et al., 1997). The integration of the results coming from two lines of research, the one which regards p27 phosphorylation by CDK2 and the other which investigates p27 proteasomal degradation, has allowed to understand that these two mechanisms are part of the same pathway. In fact p27 is ubiquitinated and degraded via proteasome upon phosphorylated on T187 residue by its inhibitory target: cyclin E/A-CDK2 complex. The vast majority, if not all, of Cdk-dependent phosphorylation of p27 is on threonine 187 (T187). In fact, (1) the phosphorylation site containing T187 is the only CDK-consensus site in human and mouse p27, (2) amino acid analysis of p27 phosphorylated in vitro by either CDK2 or CDK1 shows phosphorylation exclusively on threonine 187, (3) p27(T187A) is no longer a CDK-substrate, and (4) coexpression of cyclin E/CDK2 and p27, stimulates T187 phosphorylation of p27.

Threonine 187 phosphorylation is required for the binding of p27 to Skp2, the F-box protein component of an SCF ubiquitin ligase (E3) complex, which acts in the p27 ubiquitination and its subsequent degradation by the ubiquitin-proteasome system. SCF complex represents an evolutionary conserved class of E3 enzymes containing four subunits: Skp1, Cul1, Rbx1/Roc1 and Skp2. Skp2, which represents the variable part of the complex, is a F-box protein (Fbp) that recognizes specifically p27 in a phosphorylation-dependent manner characteristic of the Fbp-substrate interaction. Skp2 expression is not appreciable in G0 and early G1, increases in late G1 and peaks during S and G2 phase. Skp2 binds p27 and induces its ubiquitin-mediated degradation only when p27 is phosphorylated on T187 by the cyclin E/CDK2 and cyclin A/CDK2 complexes.
However, the abilities of CDK2 and CDK1 to phosphorylate p27 on T187 and to induce p27 ubiquitination do not correlate. Therefore, although phosphorylation is necessary for p27 ubiquitination, it is not sufficient. In fact, cyclin B/CDK1 in amounts sufficient to phosphorylate but not bind efficiently p27, does not stimulate p27 ubiquitination. Similarly, p27 CK−, a mutant unable to bind cyclin E/CDK2 complex is still phosphorylated by this kinase but cannot be ubiquitinated. Finally, a cyclin E/CDK2 complex that binds p27 but cannot phosphorylate it, stimulates p27 ubiquitination by relying on a CDK present in the G1 extract. The p27/cyclin/CDK complex is very stable and even when phosphorylated on T187, p27 does not appear to dissociate from the cyclin/Cdk complex. These evidences support the conclusion that CDK-dependent phosphorylation of p27 at T187 together with the formation of a stable p27/cyclin/CDK trimeric complex are both required for ubiquitination to occur (Montagnoli et al., 1999).
The discovery, in 1997, that p27 is regulated by its target of action completely reverse the view assumed till that moment. In fact, CKIs have inhibitory functions towards CDKs to block cell cycle, but is also true that CDKs inactivate their inhibitors to promote cell cycle progression. Moreover the timely regulation of p27 cellular abundance and activity derives from a combination of several factors, which include the ability of certain cyclin/CDK complexes to interact stably with p27, the cellular abundance and specific activity of CDK complexes which phosphorylate p27, as well as the availability of p27-specific ubiquitin ligase (Montagnoli et al., 1999).

2.3.2.6 Tyrosines 74, 88, 89

Several groups have described the phosphorylation of p27 on tyrosine residues (reviewed in Kaldis, 2007). Grimmler et al. (2007) find that the non receptor tyrosine kinase Lyn binds to p27 and phosphorylates it on tyrosine 88 when both proteins are overexpressed in cell lines. The nonreceptor tyrosine kinase Abl also phosphorylates p27 on tyrosine 88 and to a lesser extent on tyrosine 89. Grimmler also detected increased threonine 187 phosphorylation of tyrosine-

phosphorylated p27 leading to decreased p27 protein levels presumably through increased ubiquitylation. Mutant p27 Y88F, which cannot be phosphorylated on tyrosine 88, displayed increased stability in cells, probably because phosphorylation of threonine 187 and subsequent degradation would be less efficient.

Chu et al. (2007) investigated primary human breast cancers and found a loose correlation between low levels of p27 and activated Src kinase. In vitro, c-Src—but not inactivated Src—phosphorylated p27 on tyrosine 74 and 88, which leads to decreased binding to CDK2. Therefore, tyrosine-phosphorylated p27 is not an efficient inhibitor of CDK2 activity in comparison to wild-type p27. Inhibition of Src by the phosphatase PP1 or small interfering RNA decreased tyrosine phosphorylation and increased protein stability of p27, which was correlated with decreased phosphorylation of threonine 187.

Kardinal et al. (2006) found in human acute promyelotic leukemia NB4 cells that p27 interacts with the G-CSF receptor and Grb2 when p27 was tyrosine-phosphorylated. Treatment with G-CSF leads to decreased p27 tyrosine phosphorylation and diminished interaction with CDK4, although CDK2 binding was not affected. Phosphorylation of p27 by Abl increased p27's affinity for Cdk4 while decreasing it for CDK2.

All three papers indicate that p27 is phosphorylated on tyrosine, resulting in decreased p27 protein stability, even by different non receptor tyrosine kinases (NRTK). c-Src is one of the most involved NRTK implicated in tumor progression since a lot of its downstream target act in cellular processes as proliferation, migration and invasion. Lyn also belongs to Src family and the fusion gene BCR-ABL generated by Philadelphia translocation encode for an hyperactivated form of the tyrosine kinase Abl whose deregulated activity is involved in the genesis of chronic myeloid leukemia. The tyrosine residues differs (tyrosine 88 and to some extent 74, 89), but the overall effect seems similar. In fact tyrosine-phosphorylated p27 remains bound to CDK2/cyclin complexes, but p27 does not obstruct the ATP binding site of CDK2, thereby allowing efficient phosphorylation of p27 on threonine 187 by CDK2 and subsequent p27 ubiquitination by SCF-Skp2 and proteasomal degradation. Besides giving us a new piece of the p27 "puzzle", this mechanism highlight the connection of extracellular signals (tyrosine kinases) to cell-cycle regulation.

2.3.2.7 Threonine 198

Several papers illustrate the role of threonine 198 phosphorylation in the regulation of p27 protein localization and stability. This residue was described for the first time in a work by Fujita et al. (2002) as a site phosphorylated by Akt. The starting points of this work were the consideration that (i) inhibition of serine/threonine kinase Akt signaling by some pharmacological agents induces

G1 arrest, in part by up-regulating p27, (ii) PTEN (a phosphatase that impairs Akt activation) induces growth arrest in part by up-regulating p27, (iii) inhibition of PI3K activity by the PI3K inhibitor LY294002 results in G1 arrest with p27 up-regulation. Thus, Akt might be involved in the down-regulation of p27 expression but the precise mechanism was not clear. In addition to the previously described Akt target sites, serine 10 and threonine 157, they identified the C-terminal Thr 198 residue as a novel Akt-dependent phosphorylation site. Screening of the p27-binding protein identified that 14-3-3 proteins bound to p27 only when p27 was phosphorylated at Thr198 by Akt. Because Thr198-phosphorylated p27 was localized only in the cytoplasm, they demonstrated that Akt promote 14-3-3 binding to p27 by phosphorylation at Thr198, allowing its cytoplasmic localization. Considering that Akt also phosphorylates p27 at Thr187 and Ser10, which are involved in Skp2-mediated ubiquitinylation and cytoplasmic localization, respectively, Akt contributes to p27 degradation and to its cytoplasmic localization. In particular the cytoplasmatic accumulation of pT198 p27 by Akt has also been observed in breast cancer cell line (Motti et al., 2004). Anyway the fact that the downregulation of the Akt/PI3K pathway was not sufficient to decrease the level of T198 phosphorylation suggested that this residue could be the target site of other kinases. In fact a work published by the same group (2003) indicated that Thr198 is not only target of the Akt/PI3K signaling pathway but also of the Ras/Raf/MAPK cascade. They identified p90 ribosomal protein S6 kinases (RSKs) as the kinase necessary for Thr198 phosphorylation. RSK-dependent phosphorylation induced 14-3-3 binding and cytoplasmic localization of p27 through a Thr198 phosphorylation. Therefore this two works provide evidences that both the Ras/Raf/MAPK and the PI3K/Akt cascades could contribute to nuclear-cytoplasmic shuttling and degradation of p27 by phosphorylating the Thr198 residue.

Furthermore T198 phosphorylation has been linked not only to p27 subcellular localization but also to protein stability. A work by Liang et al. (2007) presented evidence that p27 is phosphorylated at Thr 198 downstream of the Peutz-Jeghers syndrome protein–AMP-activated protein kinase (LKB1–AMPK) energy-sensing pathway, thereby increasing p27 stability and directly linking sensing of nutrient concentration and bioenergetics to cell-cycle progression. Ectopic expression of wild-type and phosphomimetic Thr 198 to Asp 198 (T198D), but not unstable Thr 198 to Ala 198 (p27T198A) is sufficient to induce autophagy. Under stress conditions that activate the LKB1–AMPK pathway with subsequent induction of autophagy, p27 knockdown results in apoptosis. Thus LKB1–AMPK pathway-dependent phosphorylation of p27 at Thr 198 stabilizes p27 and permits cells to survive growth factor withdrawal and metabolic stress through autophagy. This may contribute to tumour-cell survival under conditions of growth factor deprivation, disrupted nutrient and energy metabolism, or during stress of chemotherapy.

Also the paper of Kossatz et al. (2006) reported a molecular mechanism that regulates p27 stability by phosphorylation at T198. In fact phosphorylation of p27 at T198 prevents ubiquitin-dependent degradation of free p27 and also controls progression through the G1 phase of the cell cycle by regulating the association of p27 with cyclin/CDK complexes. Thr 198-phosphorylated p27 is largely restricted to the cytoplasm in cell exposed to growth stimuli, and the nuclear export of p27 during G1 phase is delayed by mutation of this residue to alanine. Phosphorylation of p27 on Thr 198 appears to be required for the timely exit of p27 from the nucleus after mitogenic stimulation and seems to be determinant of p27 stability, preventing ubiquitination and proteasomal turnover. In fact they demonstrated that the half-life of $p27^{T198A}$ (a non-phosphorylatable form of p27) is shorter than the wild-type p27 form and that the increased turnover of $p27^{T198A}$ at steady-state levels was due to increased ubiquitination. In fact $p27^{T198A}$ was able to incorporate more His-ubiquitin when compared with wild-type p27. Treatment with the proteasome inhibitor MG132 stabilized $p27^{T198A}$ leading to expression levels comparable to wild-type p27 but this protein degradation seems to be only partially due to the Skp2 protein pathway.

p27 phosphorylation at T198 has also been linked to cell motility. A work published by Slingerland's group demonstrated that RSK1 drives p27 phosphorylation at T198 to increase RhoA-p27 binding and cell motility (Larrea at al., 2009). They demonstrated that RSK1 transfectants show mislocalization of p27 to cytoplasm, increased motility, and reduced RhoA-GTP, phospho-cofilin, and actin stress fibers, all of which were reversed by shRNA to p27. Phosphorylation by RSK1 increased p27pT198 binding to RhoA *in vitro*. Thus T198 phosphorylation not only stabilizes p27 and mislocalizes p27 to the cytoplasm but also promotes RhoA-p27 interaction and RhoA pathway inhibition. These data support a model in which RSK1-mediated phosphorylation of p27 at T198 increases p27–RhoA interaction to inhibit the RhoA pathway and reduce actin cytoskeleton stability. This interaction may play a role in G1 to prepare cells for the shape changes that must occur during later phases of the cell cycle. In addition, constitutive phosphorylation of p27 at T198 in cancer cells would increase p27 stability and mislocalize p27 to the cytoplasm to promote not-cell-cycle-related functions.

2.4 p27 as a target of proteasome

Proteolysis of many G1 regulatory proteins, including p27, is mediated by SCF ubiquitin ligases, each composed of four major subunits: Skp1, a cullin subunit called Cul1, Rbx1/Roc1 and one of the many F-box protein (Fbps). The substrate specificity of SCFs is due to distinct F-Box proteins that recognize phosphorylated substrates and target them for ubiquitin-mediated degradation. The F-box protein involved in the ubiquitination and degradation of p27 is Skp2, identified together with Skp1 as interactors of the cyclin A-CDK2 complex, hence the name S phase kinase-associated proteins (Skps).

Degradation of p27 through the ubiquitin-proteasome pathway is a three-step process that requires: phosphorylation of p27 at threonine 187 residue by cyclin E-CDK2 complex, recognition of T187-phosphorylated p27 by the ubiquitin ligase SCF-Skp2 and SCF-Skp2-dependent ubiquitination and degradation of T187-phosphorylated p27 (reviewed in Bloom et al., 2003 and Lu et al., 2010).

The importance of Skp2 in control of p27 abundance was confirmed by the observations that p27 accumulates at high levels in the cells of mice that lack Skp2 (Nakayama et al., 2004). It became widely accepted that Skp2 mediates p27 degradation at G0-G1 transition of the cell cycle. However, this apparently simple scenario turned out not to be so simple after all. Whereas mitogenic activation of resting cells induces rapid degradation of p27 at early to mid-G1 phase, Skp2 is not expressed until late G1 to early S phase, unequivocally later than the degradation of p27 (Hara et al., 2001; Ishida et al., 2002). This degradation of p27 occurs in the cytoplasm after export of the protein from the nucleus whereas Skp2 is restricted to the nucleus (Maruyama et al., 2001). These discrepancies between the temporal and spatial patterns of p27 expression and those of Skp2 expression suggested the existence of a Skp2-independent pathway for the degradation of p27. Indeed, the downregulation of p27 at the G0-G1 transition was found to occur normally in Skp2-/- cells and to be sensitive to proteasome inhibition, indicating that p27 is degradated at this time by a proteasome-dependent, but Skp2-indipendent mechanism (Hara et al., 2001). In contrast to the Skp2-dependent degradation occurring in the nucleus at S-G2 phases, this second pathway seems to occur in the cytosol and it is responsible for the G0-G1 degradation of p27. A recent study has described an ubiquitin ligase, named Kip1 ubiquitilation-promoting complex (KPC), that interacts with and ubiquitinates p27 in G1 phase into the cytoplasm of mammalian cells (Kamura et al., 2004; Hara et al., 2005; Kotoshiba et al., 2005). In accord with this point of view, the generation of mice double knock-out for both p27 and Skp2 revealed that the Skp2-dependent p27 degradation participates principally in the S and G2 phases of the cell cycle rather than in G1 phase (Nakayama et al., 2004) (Figure 5).

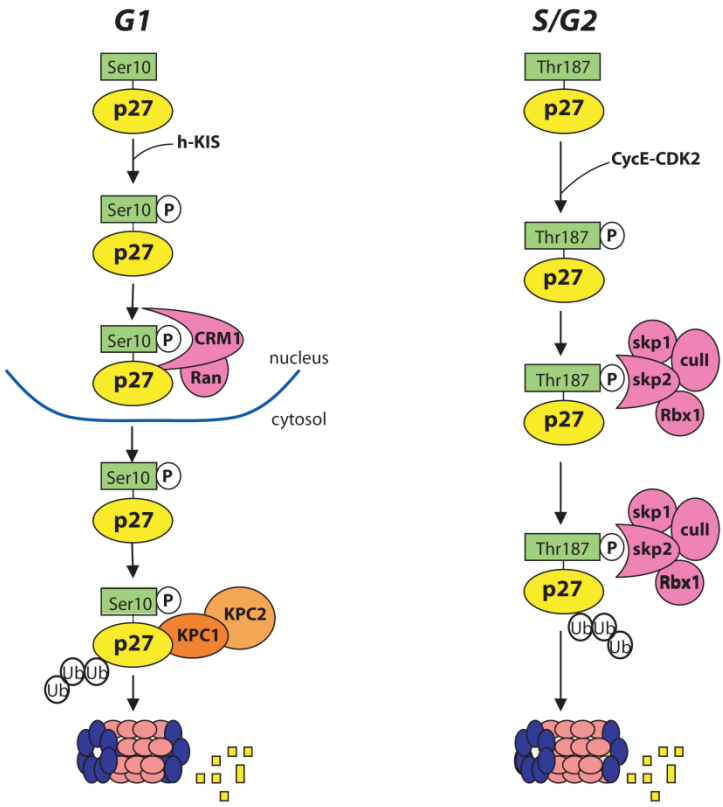

Figure 5. *Proposed models for p27 ubiquitin-dependent degradation*. On the left the proposed cytoplasmic degradation of p27 by the KPC complex, which has been reported to occur in early G1 phase. On the right, the Skp2 dependent p27 proteolysis that occurs in the early S and in G2 phases in the nucleus (*from Belletti et al., 2005*).

2.5 p27 functional inactivation

Besides modulation of its expression levels, subcellular localization also plays a pivotal role in governing p27 function, as mentioned above. It is widely accepted that to act as cell cycle inhibitor p27 must be located in the nucleus, whereas its cytoplasmic sequestration allows cell cycle progression (Belletti et al., 2005; Baldassarre et al., 2005). In fact, to inhibit cyclin E-CDK2, p27 needs to be imported into the nucleus. Nuclear import depends on the presence of a nuclear localization signal (NLS) localized at the C-terminus of the protein (aa 152-166) (Zeng et al., 2000). In particular it has been demonstrated that four are the residues involved in the recognition: K153, R154, K165, R166. Through its NLS sequence, p27 is recognized and targeted to the nucleus by Importin α3 and α5 in a complex with Importin β, and the small GTPase Ran (Sekimoto et al., 2004). Also p27 nuclear export seems to be controlled and regulated, both by the presence of a

leucine rich nuclear export signal (NES) within the CDK binding domain (amino acids 32-45) (Connor et al., 2003) and by the phosphorylation of serine 10. As cells progress along the cell cycle, p27 shuttles between nucleus and cytoplasm. Phosphorylation of p27 at Ser 10 during G0 by Mirk/dyrk1B stabilizes p27 and maintains p27 within the nucleus where it can bind to CDK2. In contrast, phosphorylation of p27 at Ser-10 by the KIS kinase in G1 enables p27 to bind to CRM1 and to be transported into the cytoplasm for destruction (Boehm et al., 2002; Deng et al., 2003).

As discussed above Thr 157 and Thr 198 (Thr 197 in mouse) have also been implicated in the cytoplasmic translocation and localization of p27. Both T157 and T198 phosphorylation by Akt and Akt/RSKs, respectively, prevents the nuclear localization of p27 by promoting its binding to cytoplasmic 14-3-3. The binding of p27 to Jab1 or CRM1 (directly through its NES) has also been implicated in p27 translocation (Tomoda et al., 1999; Connor et al., 2003).

As described for p27 cytoplasmic localization, also p27 sequestration into higher order complexes with cyclin D-CDK4 is important for regulating p27 functions. Various growth signalling pathways stimulate the assembly of these heterotrimeric complexes, containing p27 with cyclin Ds and CDK4/6. Indeed, the MEK/ERK pathway which induces cyclin D transcription, favours the assembly of the cyclin D/CDK4, and sequesters p27 in inactive cytoplasmic complexes (Cheng et al., 1998). Also the proto-oncogene c-Myc, by increasing the expression levels of cyclin D and cyclin E, is responsible for p27 sequestration (Vlach et al., 1996; Perez-Roger et al., 1999; Bouchard et al., 1999), and this molecular event appears essential for Myc-induced cell cycle progression. More importantly, p27 sequestration seems to be one of the relevant mechanisms to human cancerogenesis, at least for lymphomas (Sanchez-Beato et al., 1999) and thyroid carcinomas. Overexpression of cyclin D3 in thyroid cancers caused p27 cytoplasmic sequestration by cyclin D3-CDK complexes (Baldassarre et al., 1999). Moreover, both the Ras/Raf/Mek1 and PI3K/Akt pathways may impinge on p27 localization indirectly by their direct effects on cyclin D levels since, as mentioned above, MAPK activation upregulates cyclin D1 transcripts while Akt-dependent phosphorylation of GSK3-β inhibits cyclin D1 degradation (Pruitt et al., 2001). Both of these mechanisms would increase the subsequent sequestration of p27, and prevent its association with the CDK2 complexes. Additionally, many of the molecules important for the proliferation, differentiation, survival and also adhesion and migration have the ability to modulate and/or downregulate p27, so that its expression may be a powerful prognostic marker since it may represent the readout of multiple different signals transduction pathways known to be involved in the onset and/or the development of human tumours.

2.6 p27 mutations

The inactivation of p27 during tumorigenesis rarely involves genetic mechanisms. However, a study by Pellegata et al. identified p27 as a gene responsible for multiple endocrine neoplasia-like (MENX) syndrome in rats (Pellegata et al., 2006). Mutational analysis of candidate genes, including the *CDKN1B* gene encoding p27, identified a homozygous 8 nucleotide insertion in exon 2 that leads to a frame shift after codon 177 and a p27 protein with a different C terminus (p27_G177fs). Similar to *p27*−/− mice, rats homozygous for this germline mutation were larger compared to their wild-type littermates, and their life span was statistically significantly decreased. Heterozygous rats demonstrated the same phenotype as wild-types confirming the recessive inheritance of MENX. In humans, MEN syndromes are inherited in an autosomal dominant fashion and are due to germline mutations in the *MEN1* tumor suppressor gene (MEN1 syndrome) or the *RET* oncogene (MEN2A and MEN2B syndromes). However, since in 30% of patients with MEN1 syndrome, mutations in *MEN1* could not be identified the rat MENX data raised the hypothesis that p27 could be responsible for the MEN1 phenotype in a subset of these patients. Thus, Pellegata et al. sequenced the human *CDKN1B* gene in multiple members of a suspected MEN1 family without an identifiable MEN1 mutation. In an affected member of this family a germline heterozygous TGG to TGA nonsense mutation at codon 76 leading to a truncated p27 protein (p27_W76X) was identified. The analysis of the renal angiomyolipoma from this patient revealed that the wild-type *CDKN1B* allele appeared to be maintained, and wild-type mRNA was detected, but the tumor cells demonstrated complete lack of p27 protein based on immunohistochemical analysis. To address the potential mechanism underlying the decreased p27 levels and MEN phenotype in rats with the p27_G177fs and in humans with p27_W76X mutations, the authors exogenously expressed these proteins in rat fibroblasts and human MCF-7 and 293T cells together with wild-type and p27_G177X (nonsense mutation at codon 177 to determine if different C terminus influences function) controls and analyzed their levels and cellular localization. Both p27_G177fs and p27_W76X were expressed at significantly lower levels compared to wild-type p27, and p27_W76X was only detected in the cytoplasm and thus could not function as a CDK inhibitor. It is not clear if p27_W76X could act as a dominant negative and lead to the sequestration and downregulation of the wild-type protein, which could potentially explain the lack of p27 in tumors of heterozygous mutation carriers. Recently, a work by Molatore et al. (2010) assessed the functional properties of the MENX-associated p27 mutant protein. *In vitro*, p27fs177 retains some properties of the wild-type p27 protein: it localizes to the nucleus; it interacts with cyclin-dependent kinases and, to lower extent, with cyclins. In contrast to p27WT, p27fs177 is highly unstable and rapidly degraded in every

phase of the cell-cycle, including quiescence. It is in part degraded by Skp2-dependent proteasomal proteolysis, similarly to p27WT. Photobleaching studies showed reduced motility of p27fs177 in the nucleus compared to p27WT, suggesting that in this compartment p27fs177 is part of a multi-protein complex, likely together with the degradation machinery. Studies of primary rat newborn fibroblasts (RNF) established from normal and MENX-affected littermates confirmed the rapid degradation of p27fs177 *in vivo* which can be rescued by Bortezomib (proteasome inhibitor drug).

Recently a germline deletion in the CDKN1B 5'UTR has also been described. This mutation was associated with a significant reduction in the amount of CDKN1B mRNA in peripheral blood leukocytes from the patient with MEN-like phenotype (Malanga et al., 2011).

2.7 p27 and Intrinsically Unstructured Proteins

p27 belongs to the so-called "Intrinsically Unstructured Proteins" (IUPs or IDPs), which comprises many proteins that entirely lack secondary and/or tertiary structure, or posses long segments that lack secondary and/or tertiary structure, under physiological conditions (Dyson et al., 2005). Bioinformatics analyses of whole genome sequences using disorder predictors indicated that 6-33% of proteins in bacteria and 35-51% of proteins in eukaryota contain disordered regions of 40 or more consecutive residues (Dunker et al., 2000; Oldfield et al., 2005). Further, 79% of human cancer-associated proteins have been classified as IUPs, compared to 47% of all eukaryotic proteins in the SWISS-PROT database (Iakoucheva et al., 2002). The latter observation highlights the importance of disorder in the function of proteins that regulate processes often dysregulated in cancer such as cell proliferation, apoptosis, and DNA repair.

Although many IUPs function by folding into an ordered conformation upon binding their biological targets, for many others, disordered conformations mediate biological function. For example, disordered segments serve as linkers in many IUPs. The sequences of intrinsically unstructured proteins exhibit low complexity compared to those of globular proteins. Further, IUPs are depleted in hydrophobic amino acids (i.e. Val, Leu, Ile, Met, Phe, Trp and Tyr) and correspondingly enriched in polar and charged amino acids (i.e. Gln, Ser, Pro, Glu, Lys, Gly and Ala) relative to globular proteins. Consequently, IUPs occupy a different region of "charge-hydrophobicity space" compared to globular proteins and lack tertiary structure because they possess too few hydrophobic residues to independently form a stable hydrophobic core (Galea et al., 2008). NMR studies by many laboratories have now shown that IUPs exhibit varied degrees of nascent structure and disorder. Some IUPs completely lack secondary and tertiary structure while others exhibit partial secondary structure. The inherent flexibility of IUPs is thought to confer

certain functional advantages over more highly structured proteins. First, some IUPs bind specifically to more than one biological target and thus exhibit diverse biological functions, often with involvement in signaling and regulation. It has also been suggested that IUPs are specialized to function as hubs in protein interaction networks due to their propensity for promiscuous interactions. Second, because a large fraction of residues within IUPs are solvent exposed, even within multi-protein assemblies, these sites are accessible for post-translational modification, allowing control of protein function, localization and turnover. Third, disordered polypeptide segments within proteins are often highly susceptible to proteolytic cleavage *in vitro*, and this may be a factor which influences the rate of IUP degradation in cells. Finally, the non compact nature of IUPs may facilitate biomolecular interactions by increasing intermolecular association rates (Galea et al., 2008). Disordered proteins have a greater "capture radius" than compact, folded proteins. According to their so called "fly-casting" mechanism, a segment of an extended, unfolded protein first binds relatively weakly to the surface of a target, followed by folding to reel in the target. By being extended, IUPs sample larger solution volumes, in a sense reducing the dimensionality of the search for their partners. Moreover disordered proteins provide a simple yet elegant solution to having large intermolecular interfaces, but with smaller protein, genome and cell sizes. (Gunasekaran et al., 2003).

Analysis using proteolysis, CD and NMR spectroscopy showed that p27 is largely disordered, with 15-20% α-helical content (Bienkiewicz et al., 2002; Lacy et al., 2004). Secondary structure and disorder prediction also indicated that this protein is predominantly disordered. Although p27 can be categorized as IUPs based on its lack of tertiary structure, CD spectra indicated the presence of a small amount of α-helical secondary structure within the p27 so called "kinase inhibitory domain" (KID). These segments that adopt secondary structure in solution are termed "intrinsically folded structural units", or IFSUs (Sivakolundu et al., 2005). In contrast, results from CD and NMR indicated that p27 C-terminal domain is highly disordered: in fact it lacks secondary and tertiary structure (Galea et al., 2007).

2.7.1 Crystal Structure

The crystal structure of the human p27 kinase N-terminal inhibitory domain bound to the phosphorylated cyclin A-CDK2 complex has been determined in 1996 (Russo et al., 1996). The structure reveals that p27 uses a three-stage approach to bind and inhibit the cyclin A-CDK2 complex. It binds a peptide-binding groove on the conserved cyclin box of cyclin A, it binds the N-

terminal lobe of CDK2 and it also inserts deep inside the catalytic cleft, mimicking ATP. A comparison of CDK2 in this complex with the structure of CDK2 in the binary cyclin A-CDK2 complex reveals that p27 binding causes large conformational changes in and around the catalytic cleft of CDK2. In the complex, the p27 inhibitory domain has a non-globular, extended structure that consists sequentially of a rigid coil, an amphipathic α-helix, an amphipathic β-hairpin, a β-strand and a 3_{10} helix (Figure 6). p27 does not have a hydrophobic core of its own, and its secondary structure elements do not interact significantly with each other. The extended structure of p27 allows it to cover and interact with a large surface area of the cyclin A-CDK2 complex (40% on cyclin A, 60% on CDK2). The majority of the p27 hydrophobic amino acids pack against the cyclin A-CDK2 complex instead of participating in the folding of p27. The extended p27 structure can thus be thought of as refolding on the cyclin A-CDK2 complex. This is consistent with the large buried surface area per aminoacid, which is comparable to that expected from protein folding.

The structure of the cyclin A subunit consists of two five-helix structural repeats, the first of which corresponds to the conserved cyclin box. It is only the cyclin-box repeat that is involved in p27 binding, interacting with the rigid coil and α-helix of p27.

The p27-cyclin interactions are likely to be as important for binding as the p27-CDK2 interactions because they account for 40% of the surface area buried, they include 35% of the short-distance hydrogen bonds, and they involve residues highly conserved among both cyclin and p27 families. The rigid coil of p27, which is 10-aminoacids long and includes the sequence Leu-Phe-Gly conserved among all Kip/Cip family members (the LGF motif), binds a shallow groove on cyclin A, formed by the α1, α3 and α4 helices of the cyclin-box repeat and is lined with amino acids highly conserved among members of the cyclin family. This may explain, in part, the ability of p27 to bind many of the cyclin-CDK complexes. At its N terminus, the coil starts with a reverse turn (residues 26 to 29), followed by a short extended region (residues 29 to 31), and ending with another turn (residues 31 to 34) stabilized by an intramolecular side-chain-backbone hydrogen bond. The second turn contains the Leu 32 and Phe 33 residues of the LGF motif, which bind deeper inside the cyclin A groove. The glycine of the LGF motif has backbone angles that other aminoacids cannot adopt, and in conjunction with the following proline, plays an important role in allowing the polypeptide chain to exit the cyclin A groove and to direct towards CDK2.

The CDK2 structure consists of a N-terminal lobe that is rich in β-sheet, and a larger C-terminal lobe that is mostly α-helical, with the catalytic cleft in between the two lobes. p27 uses three consecutive secondary structure elements its β-hairpin, β-strand and a 3_{10} helix, to clamp around the β-sheet of CDK2. First, the β-hairpin (residues 61-71), which is amphipathic, forms a sandwich with the N-terminal β-sheet of CDK2, burying a large number of hydrophobic and aromatic

aminoacids both from p27 (i.e. Tyr 74) and CDK2, highly conserved in both Kip/Cip and CDK families, respectively. Second, p27 β-strand (residues 75-81) is incorporated into the CDK2 β-sheet through six backbone-backbone β-sheet hydrogen bonds. To accommodate the p27 strand, the first β-strand of CDK2 is displaced and becomes disordered, resulting in a p27-CDK2 hybrid β-sheet. The third portion of the p27-CDK2 interface involves the 3_{10} helix of p27 (residues 85-90) that binds deep inside the catalytic cleft and occupies most of the available space in the cleft, mimicking the position that the ATP occupies in the binary complex. In this region, the most significant contacts are made by Tyr 88, which is conserved in the Kip/Cip family. The crystal structure of the p27-cyclin A-CDK2 complex reveals that p27 has separate binding sites on the cyclin and CDK subunits and this explains how the Kip/Cip inhibitors can bind the isolated subunits. Binding to the cyclin-CDK complex is significantly tigher, consistent with cooperative binding to the two subunits. The LGF motif-cyclin interactions are likely to serve as an initial anchor in complex formation, because these interactions do not need structural rearrangements in cyclin to occur, in contrast to the CDK2 interactions. The interactions with the cyclin may serve as an entry point for the Kip/Cip proteins into the cyclin-CDK complex, but the interactions with the CDK and the accompanying structural changes in the catalytic cleft are likely to be key determinants of inhibition (Russo et al., 1996).

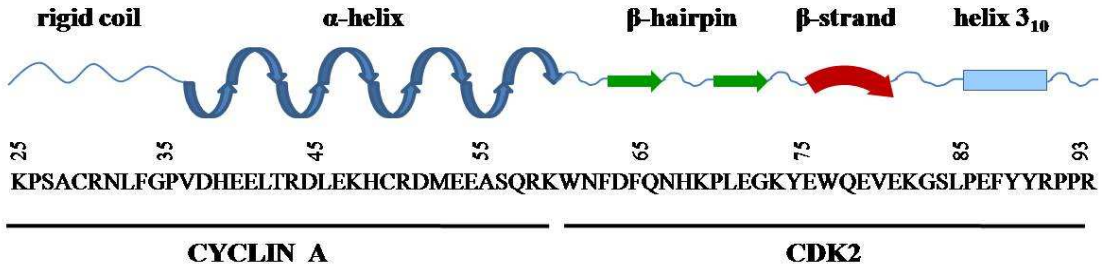

Figure 6. *Sequence of the p27 inhibitory domain showing its secondary structure elements and cyclin A and CDK2 binding domains.*

2.7.2 p27 C-terminal domain

p27 is composed of an N-terminal domain (p27-KID, residues 22-104) that binds and inhibits cyclin/CDKs complexes and a C-terminal domain (residues 105-198, p27-C) that contains several sites of post-translational modifications. Little information is available on the structure of p27-C and how this domain orchestrates all the signals that induce p27 degradation. Recently, NMR spectroscopy studies have provided detailed insights into how the cyclin A/CDK2-bound conformation of p27-KID is altered by phosphorylation of Y88 (Grimmler et al., 2007). In fact this work demonstrated how phosphorylation and ubiquitination of p27 occur in sequential order in a two-step phosphorylation mechanism followed by ubiquitination. The first step involves phosphorylation of Y88 by NRTKs and partial "reactivation" of CDK2 within the p27/CDK2/cyclin A complex. In the second step, reactivated CDK2 phosphorylates T187 located toward the C-terminus of the 100-residue-long C-terminal domain of p27. The intrinsic flexibility of p27 allows its interactions with CDK2/cyclin A and SCF/Skp2 to be modulated by phosphorylation of tyrosine and threonine residues at opposite ends of the p27 polypeptide chain. Prior to phosphorylation, Y88, which is found at the C-terminal end of the KID domain of p27 that binds and inhibits CDK2, is lodged in the ATP binding pocket of Cdk2 thereby inhibiting catalysis by blocking access to ATP. However, due to putative dynamics involving the 3_{10} helix containing Y88 fluctuating into and out of the ATP binding pocket, Y88 within p27/CDK2/cyclin A complexes is accessible for phosphorylation by NRTKs. Following phosphorylation—step 1 of the two-step mechanism—Y88 and the entire 3_{10} helical segment of the KID are ejected from the ATP binding pocket of CDK2. While p27 remains bound to CDK2/cyclin A, ejection of phosphorylated Y88 and the 3_{10} helix restores significant catalytic activity, allowing CDK2 to phosphorylate T187 within the C-terminus of the same p27 molecule that is bound to CDK2 (step 2 of the two-step mechanism). The unimolecular nature of step 2 requires that the C-terminus of p27 "folds back" to allow T187 to be phosphorylated by CDK2. A recent work from Galea et al. provide the first detailed characterization of the structural features of full-length p27 and explain how T187 can be phosphorylated by CDK2 via an unimolecular mechanism. This study showed that the C-terminus of p27 does not interact extensively with the Cdk/cyclin complex, even though it plays an important role in the regulation of p27-mediated cell cycle arrest, and that, in the absence of its cyclin/Cdk binding partners, the N- and C- termini of p27 do not interact. Analysis by NMR spectroscopy showed that the C-terminal domain lacked detectable secondary structure and that, long-range interactions between different regions within p27-C do not occur. Moreover, computational analysis demonstrates that when p27 was bound to cyclin A/CDK2 p27-C remained quite highly extended during the trajectory, rather

than assuming more compact conformations as might be expected. This may be due to electrostatic repulsion between the molecular surface of CDK2/cyclin A and p27-C that "steers" the p27 polypeptide backbone away from the globular core of Cdk2/cyclin A. This work clearly showed that the C-terminal domain of p27 adopts a disordered and quite highly extended conformation when p27 is bound to CDK2/cyclin A. This conformation allows p27 C-terminus to function as a regulatory domain that is structurally independent of the N-terminal domain, which itself binds tightly and specifically to several different CDK/cyclin complexes involved in regulating the G1/S cell cycle transition. The C-terminal domain acts as a flexible "conduit" for signal transduction, which detects a specific signal from NRTKs (phosphotyrosine 88) and, through the catalytic activity of Cdk2, mediates conversion of this signal into a second signal, phosphothreonine 187 (pT187). The pT187 signal, in turn, is functionally transduced through polyubiquitination by SCF/Skp2 that signals the 26S proteasomal degradation of p27.

Based on the observation that the surface of CDK2/cyclin A near the ATP binding site bears negative charge, it has been proposed that electrostatic interactions between this surface and a cluster of positively charged residues at the p27 C-terminus adjacent to T187 facilitate interactions between T187 and the CDK2 substrate binding site. If Y88 of p27 is phosphorylated when these interactions occur, then the oncogenic signal from NRTKs can be transduced through phosphorylation of T187 and subsequent ubiquitination and degradation of p27. If Y88 is not phosphorylated, no signal is transduced and CDK2/T187 encounters are catalytically unproductive. The extended nature and flexibility of the 100-residue-long p27 C-terminus makes it possible for T187 to constantly sense the signaling status of Y88 (i.e., absence or presence of phosphorylation).

Y88 and a second tyrosine residue of p27, tyrosine 74 (Y74), were shown to be phosphorylated by the NRTK, Src, in breast cancer cells. This observation suggests that not only does the Y88-containing segment of p27 experience conformational fluctuations, but that the segment containing Y74, within the β-hairpin that is sandwiched between the N-terminal β-sheet lobe of CDK2, also experiences conformational fluctuations that make its side chain available for phosphorylation by Src. Phosphorylation of Y74 by Src may disrupt local interactions between p27 and CDK2, which may in turn enhance the accessibility of Y88 to NRTKs and its subsequent phosphorylation.

p27 specifically recognizes CDK/cyclin complexes through interactions mediated by multiple short recognition elements connected by flexible polypeptide segments. For example, the RxLFG motif at the N-terminus of the p27 KID binds specifically to cyclin A, a second region within the KID (residues 60–82) binds specifically to the N-terminal β-sheet lobe of CDK2, the Y88 region binds in the ATP binding pocket of CDK2 and, finally, the region near T187 binds the substrate binding site of CDK2. The coupling of post-translational modifications within the multiple, flexible short

recognition elements of p27 affords a level of signaling complexity that has not previously been observed. p27, thus, constitutes a *conduit* for transmission of proliferative signals via post-translational modifications. The term "*conduit*" is used to connote a means of transmission of molecular signals which, in the case of p27, correspond to tyrosine and threonine phosphorylations, ubiquitination and, ultimately, proteolytic degradation. (Galea et al., 2008). The lack of tertiary structure and intrinsic flexibility within p27 allows its many short recognition elements to orchestrate signaling along this conduit. Utilizing intrinsic protein flexibility in this way allows the transduction of multiple signals within a single protein complex due to the ability of different motifs within one polypeptide to "communicate" with each other.

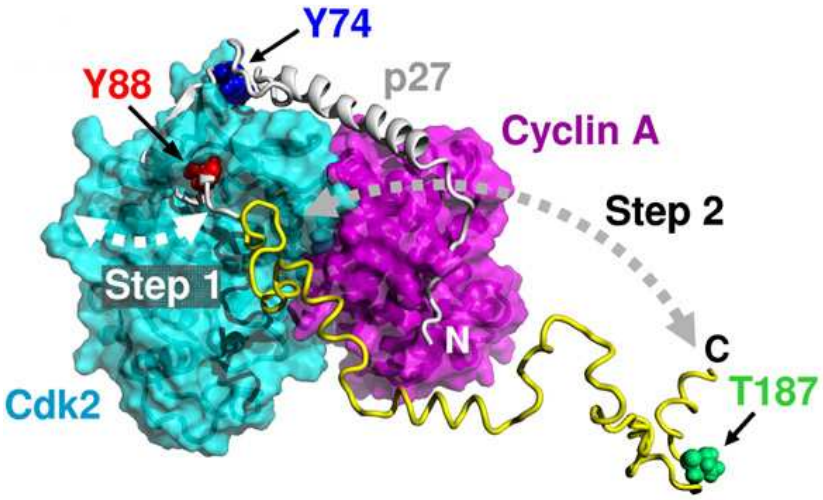

Figure 7. *Structure of the p27/CDK2/cyclin A complex*. Schematic view prepared with the program PyMOL of full-length p27 bound to Cdk2/cyclin A showing the solvent-accessible surface for Cdk2 (cyan) and cyclin A (magenta). The kinase inhibitory domain (KID) (grey) and C-terminal domain (yellow) of p27 are illustrated as ribbons (*from Galea et al., 2007*).

3. Stathmin

Stathmin 1 (also known as oncoprotein 18/Op18 or metablastin) is a ubiquitous 17-kDa cytosolic phosphoprotein, proposed to be a small regulatory molecule and a relay integrating diverse intracellular signalling pathways involved in the control of cell proliferation, differentiation and other activities (reviewed in Belletti et al., 2011). Stathmin 1 (hereafter referred as stathmin) is the prototype member of a phosphoprotein family that also includes stathmin-like 2 (superior cervical ganglion 10; SCG10), stathmin-like 3 (SCG10-like protein; SCLIP), and stathmin-like 4 (RB3 with two splice variants, RB3' and RB3'') . Although stathmin is ubiquitously expressed and is involved in regulating the global dynamics of interphase microtubules, the compartmentalization and restricted tissue distribution of the stathmin-like proteins indicates a more specialized function. All members of the family share a so-called stathmin-like domain that contains up to four phosphorylation sites (stathmin: Ser16, Ser25, Ser38 and Ser63), while displaying a different N-terminal region, that is likely to dictate their sub cellular localization.

Stathmin has been shown to act as a microtubule destabilizing protein. Microtubules consist of α/β tubulin heterodimers that exist in a state of continuous transition between polymerization and depolymerization events. The transition from the phase of growth to the phase of shrinkage is known as "catastrophe" while the transition from the phase of shrinkage to the phase of growth is known as "rescue." Stathmin has been shown to act as a microtubule destabilizer, either by directly promoting the microtubule catastrophe (Belmont et al., 1996) or by sequestering the free α/β tubulin heterodimers in a stable T2S ternary complex, thus preventing tubulin incorporation in growing microtubules (Jourdain et al., 1997).

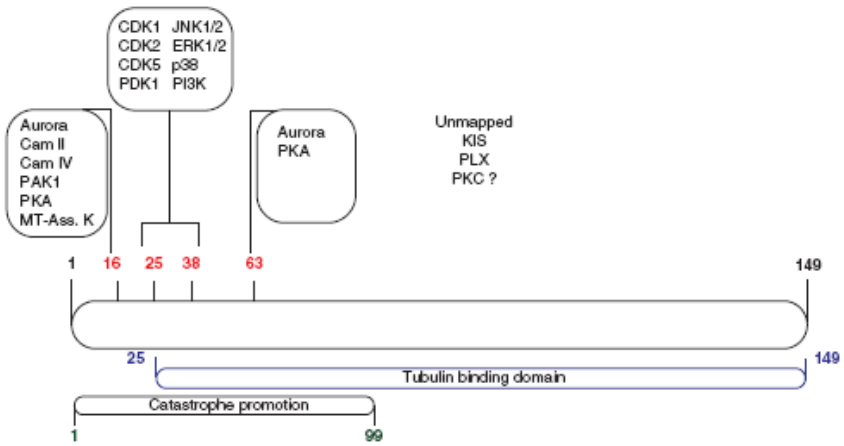

Figure 8. *Schematic representation of the stathmin protein*. Its sequence comprises 149 amino-acids and two principal domains: at the N-terminus, the catastrophe promoting domain (aa 1-99, depicted in green), responsible for the binding to microtubules; at the C-terminus, the tubulin binding domain (aa 25-149, depicted in blue) responsible for the sequestration of free α/β tubulin heterodimers. The four serines (S16, S25, S38 and S63, in red) and the kinases responsible for their phosphorylation are indicated, as well. (*from Belletti et al., 2011*).

3.1 Stathmin in the control of cell cycle progression

Stathmin has been proved to play a fundamental role in the control of cell division. Consistent with its extensive phosphorylation on four Ser residues during mitosis, which serves to inhibit its destabilizing activity during spindle assembly, alterations in stathmin expression levels are associated with severe mitotic spindle abnormalities and results in altered M phase progression (reviewed in Rubin et al., 2004).

During mitosis, stathmin becomes phosphorylated on S16 by a yet unidentified microtubule-associated kinase (Kuntziger et al., 2001) and by Aurora B kinase (Gadea et al., 2006), formally demonstrating that stathmin inactivation by serine-phosphorylation represents a key event for the formation of the mitotic spindle. Accordingly, it has been demonstrated that stathmin S25 and S38 are phosphorylated at the G2/M transition by the master regulator of the M phase progression, CDK1, thus reinforcing the idea that inactivation of stathmin represents an essential condition for the initiation of metaphase. Further studies also showed that CDK2 (Brattsand et al., 1994) and CDK5 (Hayashi et al., 2006) phosphorylate these two serine residues, suggesting that CDK-dependent regulation of stathmin activity represents a conserved mechanism necessary for proper progression throughout the entire cell cycle. The currently accepted model of M phase progression related to stathmin function is that CDK-dependent phosphorylation of S25 and S38 precede that of S16 and S63, thus allowing correct formation of the mitotic spindle. However, stathmin phosphorylation can be observed also during the G1 to S phase transition by other serine-threonine kinases belonging to the MAPK family (ERK 1 and 2, p38, JNK-1 and 2), PDK-1 and PI3K pathways (reviewed in Belletti et al., 2011). Stathmin has also been suggested to be involved in the microtubule-dependent events of cytokinesis. In fact when cytokinesis is blocked cells become polyploidy and multinucleated (Johnson et al., 1999). This was associated with an increase in the level of stathmin expression and its level of phosphorylation. This study suggests that the microtubule regulatory function of stathmin may also be required for the morphological changes associated with cytokinesis and the entry into a new cell cycle.

3.2 p27-stathmin interaction in the control of cell motility and morphology

Although p27 and stathmin were originally discovered as important regulators of the eukaryotic cell cycle, both are now suggested to be involved in the process of cell migration.

Many authors have demonstrated a role of p27 in cell migration, but the conclusions appear in contrast. It was shown that p27 seems to reduces cell migration in endothelial cells, vascular smooth muscle cells, mesangial cells, sarcoma and glioblastoma tumor cells and normal mouse fibroblasts (Daniel et al., 2004; Goukassian et al., 2001; Sun et al., 2001; Baldassarre et al., 2005; Schiappacassi et al., 2008).

On the other hand, cytoplasmic p27 was shown to positively regulate cell migration in bi-dimensional assays (Denicourt et al., 2004). In fact, different research groups demonstrated that p27 stimulated the scatter motility of hepatocellular carcinoma cells and mouse embryonic fibroblasts in wound healing assay (McAllister et al., 2003; Besson et al., 2004), proposing that p27 can induce rearrangements of the actin cytoskeleton, either in a Rac- (McAllister et al., 2003) or RhoA-dependent manner (Besson et al., 2004). Although all these studies suggest that p27 plays a role in cell migration, it is not clear whether the discrepancy between these reports (i.e. whether p27 inhibits or promotes cell migration) might reflect differences in the activity of cytoplasmic p27 in different cell types and/or of differences in the migration assays that were used.

Besides its role in mitotic spindle formation, many literature data support the pro-migrative role of stathmin. A dual role for stathmin in the regulation of cell proliferation and cell migration should not be surprising as microtubules are known to be important in both processes. For example, the RNA interference inactivation of Drosophila stathmin expression resulted in germ cell migration arrest and induced important anomalies in nervous system development (Ozon et al., 2002). Stathmin expression is also required in border cells of the Drosophila ovary for normal migration (Borghese et al., 2006). Moreover, reducing the expression of stathmin with an antisense oligonucleotide, results in the inhibition of migration of new neurons from the sub-ventricular zone to the olfactory bulb via the rostral migratory stream, suggesting a role for stathmin in the migration of newborn neurons in the adult rodent brain (Jin et al., 2004).

Baldassarre et al. (2005) have demonstrated that p27 expression inhibits the migration of HT-1080 fibrosarcoma cells and murine fibroblasts and that the migration-inhibitory activity of p27 is localized to the C-terminal 28 amino acids of the protein. Using a yeast two-hybrid assay, they identified stathmin as a partner protein that binds to p27 C-terminus and confirmed their *in vivo* interactions in HT-1080 sarcoma cells, pork brain, mouse fetal brain and normal mouse fibroblasts adherent to fibronectin. This work demonstrated that p27, binding the C-terminus of stathmin, interferes with its ability to sequester tubulin, leading to increased microtubule stabilization that in turn impairs migration function. In fact, stathmin has a pivotal role in cell migration regulation: Stathmin-knock out mouse embryo fibroblasts (MEFs) showed migration defects rescued by transfection of stathmin cDNA, and stathmin inhibition reduces cell motility, while its over-

expression increases migration in HT-1080 cells (Baldassarre et al., 2005). But intriguingly, in their system stathmin activity in cell migration results to be regulated by p27 expression and together these data represent the first indication that cytoplasmic p27 regulates migration by a direct effect on microtubule dynamics, via stathmin. The same mechanism of migration modulation by p27-stathmin interaction was also demonstrated in a model of glioblastoma tumor (Schiappacassi et al., 2008). Two other works pubblished by Baldassarre's group described the involvement of stathmin and p27 in the regulation of cell motility and morphology in 3D-matrix. In the first work (Belletti et al., 2008) they found that stathmin stimulates cell motility in and through the extracellular matrix (ECM) *in vitro* and increased the metastatic potential of sarcoma cells *in vivo*. On contact with the ECM, stathmin was negatively regulated by phosphorylation. Accordingly, a less phosphorylable stathmin point mutant (stathmin Q18E) impaired ECM-induced microtubule stabilization and conferred a higher invasive potential, inducing a rounded cell shape coupled with amoeboid-like motility in three dimensional matrices.

Moreover (Belletti et al., 2010) they demonstrate that p27 inhibition of stathmin activity also influences morphology and motility of cells immersed in three-dimensional 3D-matrices. 3T3 p27 knock-out cells display a decrease in MT stability, a rounded shape when immersed in 3D environments, and a mesenchymal-amoeboid conversion in their motility mode. Upon cell contact to extracellular matrix, the decreased MT stability observed in p27 null cells results in accelerated lipid raft trafficking and increased RhoA activity. Importantly, cell morphology, motility, MT network composition, and distribution of p27 null cells were rescued by the concomitant genetic ablation of stathmin, implicating that the balanced expression of p27 and stathmin represents a crucial determinant for cytoskeletal organization and cellular behavior in 3D contexts.

Another question raised is whether p27 and stathmin could also interact indirectly to regulate cell motility. Figure 9 illustrates four possible interactions between p27 and stathmin (Iancu-Rubin et al., 2005). The first is a direct interaction that represents the binding of p27 to stathmin, as suggested by Baldassarre and colleagues. The second is an indirect interaction between p27 and stathmin through the Rho GTPase pathway. Rac was previously shown to stabilize microtubules by phosphorylation-dependent inactivation of stathmin (Wittmann et al., 2004). Thus, p27 might regulate cell migration by activating Rac, which can promote phosphorylation of stathmin and lead to microtubule stabilization. In a third possible interaction, p27 might modulate stathmin activity indirectly through its inhibitory effects on cyclin–CDK complexes. As stathmin is a substrate for CDK1, inhibition of CDK1 by p27 might prevent the inactivation of stathmin or, alternatively, considering that E2F transcription factors are known to activate the stathmin promoter (Polzin et al., 2004), inhibition of the CDK–Rb–E2F pathway by p27 might result in decreased stathmin

expression and lead to microtubule stabilization. Finally, a fourth way in which p27 and stathmin might interact is through the human kinase interacting stathmin (hKIS) which has been described to bind and phosphorylate stathmin. Interestingly, KIS was also shown to phosphorylate p27 and promote its translocation from the nucleus to the cytoplasm, where it has to be to regulate the activity of stathmin (Figure 9).

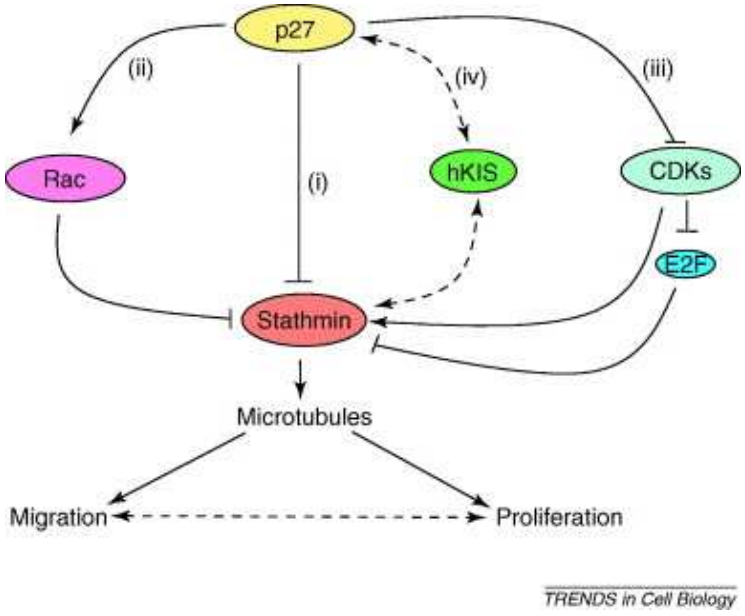

Figure 9. *Potential interactions between p27 and stathmin in the regulation of cell motility.* Four different mechanisms are described: (i) p27 might directly interact with stathmin and prevent its microtubule-destabilizing activity, (ii) p27 activates Rac, which can promote the phosphorylation of stathmin and inhibit its microtubule-destabilizing activity, (iii) the inhibitory effect of p27 on Cyclin-Dependent Kinases (CDKs) might result in either E2F-mediated downregulation of stathmin expression or increased stathmin activity by means of CDK1 inactivation; (iv) p27 and stathmin might interact through the human Kinase Interacting stathmin (hKIS) that phosphorylates p27 and induces its translocation to the cytoplasm where stathmin is localized (*from Iancu-Rubin et al., 2005*).

4. SUMOylation

Post-translational modification of cellular proteins by the SUMO (small ubiquitin-related modifier) is involved in numerous modes of regulation in widely different biological processes. In contrast with ubiquitination, SUMO conjugation does not target proteins for proteasomal degradation and is highly specific in terms of target lysine residues, but many aspects of substrate and lysine selection by the SUMO conjugating machinery are still poorly understood (Sistonen et al., 2007). Like ubiquitin, SUMO proteins are covalently and reversibly conjugated to specific lysine residues in the target proteins. In particular SUMO has been found to bind to the lysine residue on the consensus sequence ΨKxD/E (where Ψ corresponds to a large hydrophobic amino acid, K is a lysine residue, x is any amino acid and D/E is an aspartic/glutamic acid residue) on the target protein (Hannoun et al., 2010). However SUMOylation can also occur at lysine residues outside this motif and not all *ψ*KxD/E motifs are SUMOylated. Thus although useful as an initial predictor, the presence of a *ψ*KxD/E motif on potential SUMO substrates is certainly not a definitive indicator that a protein is SUMO-modified. SUMOylation is involved in surprisingly diverse biological pathways, such as genome integrity, chromosome packing and dynamics, and various aspects of signal transduction.

4.1 The SUMO family

SUMO proteins are ~10 kDa in size and resemble the three-dimensional structure of ubiquitin. However, they share less than 20% amino-acid sequence identity with ubiquitin and are different in their overall surface-charge distribution. All SUMO proteins carry an unstructured stretch of 10–25 amino acids at their N termini that are not found in any other ubiquitine-related proteins. The human genome encodes four distinct SUMO proteins: SUMO 1–SUMO 4. Of these, SUMO 1–SUMO 3 are ubiquitously expressed, whereas SUMO 4 seems to be expressed mainly in the kidney, lymph node and spleen. All SUMO proteins are expressed in an immature proform, in which they carry a C-terminal stretch of variable length (2–11 amino acids) after an invariant Gly-Gly motif that marks the C terminus of the mature protein. Removal of this C- terminal extension by SUMO-specific proteases is a prerequisite for the conjugation of SUMO to targets. The expression of the peptidic modifiers as precursors appears to be a common characteristic of ubiquitin-like modifiers. Whether maturation is a regulated or constitutive process remains to be shown. The mature forms of SUMO 2 and SUMO 3 are 97% identical, but share only 50%

sequence identity with SUMO 1. SUMO 1 and SUMO 2/3 serve distinct functions, as they are conjugated to different target proteins *in vivo*. The role of SUMO 4 remains enigmatic, as it is presently unclear whether it can be processed to its mature conjugation-competent form *in vivo* (Geiss-Friedlander et al., 2007). SUMO 2 and 3 have the ability to form polySUMO chains, covalently binding to themselves via the lysine residue at the N terminus consensus motif ΨKxE. SUMO-1 lacks this consensus site and as a consequence is unable to form polychains and acts as a polySUMO chain terminator (Hannoun et al., 2010).

Sumoylation is an essential process in most organisms, including *S. cerevisiae*, *C. elegans*, and mice. Whether individual SUMO proteins are essential in organisms that have multiple SUMO proteins remains to be seen. However, disruption of SUMO1 in mice causes embryonic lethality, and SUMO1 haploinsufficiency induces a developmental defect (split lip and palate) in mice and possibly in humans.

4.2 The SUMO cycle: SUMO conjugation and deSUMOylation

The reversible SUMOylation pathway is outlined in Figure 10. The first step is the activation of a mature SUMO protein at its C terminus by the SUMO-specific E1 activating enzyme heterodimer AOS1–UBA2. This reaction uses ATP for the formation of a SUMO–adenylate conjugate, which functions as an intermediate in the formation of a thioester bond between the C-terminal carboxy group of SUMO and the catalytic Cys residue of UBA2. Next, SUMO is transferred from UBA2 to the E2 conjugating enzyme UBC9, forming a thioester linkage between the catalytic Cys residue of UBC9 and the C- terminal carboxy group of SUMO. Finally, UBC9 transfers SUMO to the substrate: an isopeptide bond is formed between the C-terminal Gly residue of SUMO and a Lys side chain of the target. This process is usually facilitated by SUMO E3 ligases, which are enzymes that catalyse the transfer of SUMO from UBC9 to a substrate. Owing to the action of specific proteases, SUMOylation is a reversible modification. So far, a single gene family that encodes SUMO-specific Cys proteases has been identified. In mammals there are six SENPs, designated SENP 1–3 and SENP 5–7, which vary in their cellular distribution, SUMO paralogue specificity and selectivity for SUMO maturation compared with deconjugation activities (Mukhopadhyay et al., 2007).

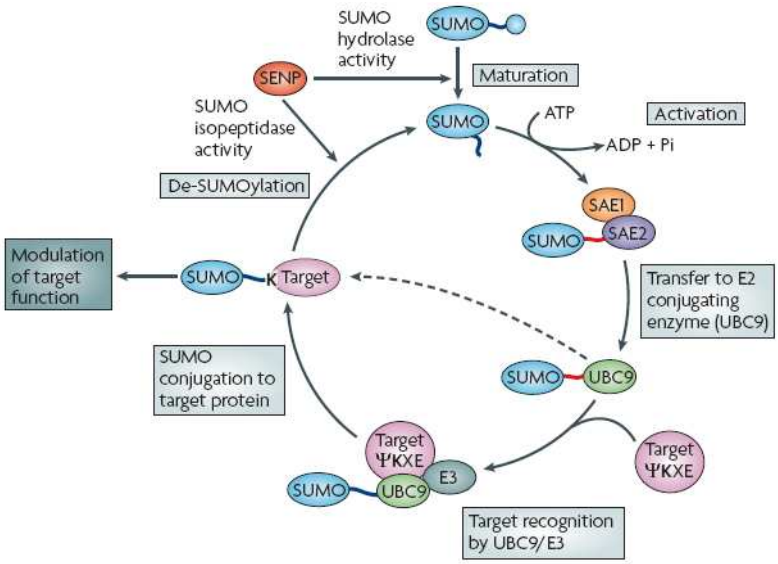

Figure 10. *Schematic representation of the SUMO conjugation pathway (from Martin et al., 2007).*

4.3 Molecular consequences of SUMOylation

The functional consequences of SUMOylation for a target are impossible to predict, as modification can alter localization, activity or stability. However, protein modification by SUMO may lead to one of three none mutually exclusive effects (Figure 11). First, SUMOylation may mask the binding site of a protein that interacts with the substrate protein, essentially acting to occlude the interaction in a SUMOylation-dependent manner. Second, and conversely, the covalently attached SUMO may act as an interaction 'hub' that recruits new interacting proteins to the substrate either by direct non-covalent interaction with the SUMO moiety, or via a novel interaction domain created at the SUMO-substrate interface. Third, SUMOylation can lead to a conformational change in the SUMOylated substrate, directly regulating its function (Wilkinson et al., 2010).

An initially intuitive observation regarding SUMOylation is that only small proportion of the available substrate protein need be SUMOylated to achieve maximal effect. This phenomenon has been referred to as the 'SUMO enigma' (Hay, 2005). Although the underlying mechanisms for this effect on many SUMO-modified proteins have not been determined, elegant explanations based on the highly dynamic nature of the SUMOylation cycle have been proposed. In fact it is important to

keep in mind that targets can undergo rapid cycles of modification and de-modification. Although the equilibrium might lie on the side of the unmodified form, the whole pool of a given protein might be affected by SUMOylation in a short window of time (Geiss-Friedlander et al., 2007).

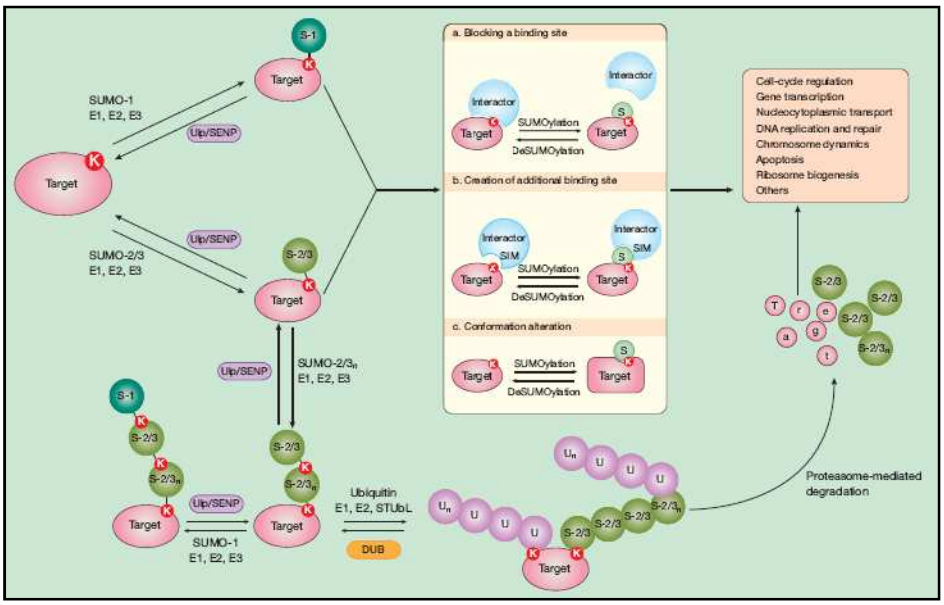

Figure 11. *SUMOylation confers multiple fates to target protein (from Wang et al., 2009).*

MATERIALS AND METHODS

1. Cell culture, Transfection and Treatments

HT-1080 fibrosarcoma cells (ATCC CCL-121), HEK 293 (ATCC CRL- 1573), HeLa (ATCC CCL-2) and MCF-7 (ATCC HTB-22) were grown in DMEM supplemented with 10% heat-inactivated FBS (Sigma). 3T3 fibroblasts were obtained from primary MEFs following the 3T3 immortalization protocol (Todaro et al., 1963). 3T3 p27 null ($p27^{KO}$) fibroblasts were grown in DMEM supplemented with 10% heat-inactivated FBS. U87MG malignant glioma cells (ATCC HTB-14) and MDAH 2774 ovarian adenocarcinoma cells (ATCC CRL-10303) were maintained in RPMI-1640 medium supplemented with 10% heat inactivated FBS. SCC9 squamous cell carcinoma cells (ATCC CRL-1629) were grown in a 1:1 mixture of DMEM and HAM'S F12 supplemented as described by the provider. The cells were transfected with the indicated expression vectors using FuGENE HD Transfection Reagent (Roche). When indicated, cells were treated with 10 µg/ml cycloheximide (Sigma) for 3, 6 and 9 hours, 50 µM MG132 (Calbiochem) for 6 and 9 hours and recombinant human TGFβ (Peprotech) for 3 hours.

2. Construction of Expression Vectors

The T198 mutants of p27 were generated by PCR on $p27^{wt}$ vector using oligonucleotides carrying the indicated mutations (Table 1). Amplified fragments were cloned into pGEM-T Easy Vector (Promega). The Y/F and K/R p27 mutants were generated with the QuickChange XL Site-Directed Mutagenesis kit (Agilent-Stratagene), using oligonucleotides carrying the indicated mutations (Table 1). All the mutants generated were checked by sequencing. The expression vectors utilized were pEGFP-C (Clontech), pFLAG-CMV 6 (Sigma), pDNR-CMV (Clontech), pQE-30 (Qiagen) and pTNT (Promega). In the same way stathmin coding sequence was cloned in the DsRed-Monomer-C expression vector (Clontech) and FLAG-CMV 6 (Sigma).
SUMO1, SUMO2 and SUMO3 cDNAs were retrotranscribed from HEK293 total RNA, using specific oligonucleotides (Table 1), and cloned into pCMV-HA expression vector (Clontech). Untagged Ubc9 constructs were generated with the QuickChange XL Site-Directed Mutagenesis kit on pCMVhuman Ubc9 wt HA and pCMV human Ubc9 C96S HA (Addgene), using oligonucleotides carring a stop codon (Table 1).

3. Recombinant Adenoviruses

Recombinant adenoviruses for p27 overexpression were produced with two systems: the Adeno-X Tet ON Expression System 2 (Clontech) and the Adeno-X ViraTrak Expression System 2 (Clontech), according provider's instructions. To obtain regulated p27 expression, in the first

method target cells were co-transduced with two viruses: the AdTet-ON (Clontech), that provides the constitutive expression of the reverse tetracycline-controlled transactivator (rtTA), and the AdTRE that encodes for the $p27^{WT}$ or mutant proteins. Recombinant protein production was induced using Doxycycline (Sigma) at 1 µg/ml added to cell culture medium. In the other system the gene of interest and the gene for the green fluorescence protein are under the control of distinct CMV promoter, allowing the simultaneous but not fused expression of the two proteins. The control (AdNeg, Clontech) and Skp2 siRNA adenoviruses were generated using the BD Knockout Adenoviral RNAi System 2 (Clontech) following the manufacturer's procedures and inserting the appropriate target sequence: human Skp2: 5'-GCCTAAGCTAAATCGAGAGAA-3' (NM_032637, pos nt 428-449). Adenovirus production, titration and characterization were performed as previously described (20). Briefly, adenoviruses were produced by transfecting with FuGENE (Roche) recombinant adenoviral vectors into HEK 293 cells. Before transfection, the vectors were digested with Pac I (Clontech) to linearize the DNA and to expose the inverted terminal repeats (ITRs) that flank the Adeno-X genome. Then HEK 293 cells were checked every day for cytopathic effect (CPE), and once detached from the plate were harvested and centrifuged at 3000 rpm for 5 min. Because adenovirus remains associated with cells until late in the infection cycle, high titer virus was obtained by lysing cells with a series of freeze-thaw cycles. After the third cycle, the pellet debris was centrifuged to recover the viral suspensions, which stored at -20°C. Then recombinant adenoviruses were amplified to prepare high-titer stocks.

4. Expression and Purification of Recombinant Proteins

For the production of bacterial recombinant proteins $p27^{WT}$ and p27 mutants cDNAs were cloned in the pQE-30 vector (Qiagen). *Escherichia coli* (M15) cells were transformed with the expression plasmid to produce recombinant proteins containing His-tag at the N-terminus. Briefly, 25 ml LB medium containing 100 µg/ml ampicillin and 25 µg/ml kanamycin was inoculated with a positive transformant and grown overnight at 37°C. Next day 500 ml of prewarmed media with antibiotics was inoculated with 25 ml of the overnight culture and grow at 37°C until the OD600 was 0.6. At this point IPTG (final concentration 1 mM) was added to induce the expression of the recombinant protein and the culture was grown for additional 4–5 hours. Finally cells were harvested by centrifugation at 5000 rpm for 20 min.

Purification of His-tagged p27 was performed with the Ni-nitrilotriaceticacid (NiNTA) resin (Qiagen), following manufacturer's instructions. Briefly, bacterial pellet was resuspended in sonication buffer (50 mM Tris-HCl pH 7.4, 20 mM Imidazole) added with protease inhibitor cocktail (Complete™, Roche), 1 mM sodium orthovanadate, and 1 mM dithiothreitol and sonicated

ten times for 10 seconds. Then the pellet debris was centrifuged at 10000 rpm for 30 minutes and the supernatant was recovered and incubated overnight at 4°C with 1.5 ml of NiNTA resin, at gentle shaking. The next day NiNTA was washed 6 times in wash buffer (50 mM Tris-HCl pH 7.4, 500 mM NaCl, 20% glycerol). To elute 6xHis-tag p27, NiNTA resin was incubated for 30 minutes at 4°C with 1 ml of elution buffer (200 mM Imidazole, 20 mM Hepes pH 7.4, 1 mM KCl, 100 mM EDTA). This step was repeated four times and finally the eluted fractions were loaded into polyacrylamide gel to check which fraction contained the recombinant protein. Elution buffer of recombinant proteins was always exchanged with kinase assay buffer using Ultrafree MC centrifugal filter units (cut off MW 10000, Millipore) according to manufacturer's instructions.

5. Preparation of Cell lysates, Immunoblotting, Immunoprecipitation and Kinase assay

5.1 Total protein extraction

Total cell proteins were extracted using cold NP-40 lysis buffer (0.5% NP-40, 50 mM HEPES [pH 7], 250 mM NaCl, 5 mM EDTA, 0.5 mM EGTA [pH 8]) plus a protease inhibitor cocktail (Complete™, Roche), 1 mM sodium orthovanadate, and 1 mM dithiothreitol.

For the analysis of SUMOylation, total cell proteins were extracted using an 1:3 ratio mix of SDS buffer I (5% SDS, 150 mM Tris-HCl pH 6.8, 30% glycerol) and SDS buffer II (25 mM Tris-HCl pH 8.3, 50 mM NaCl, 0.5% NP40, 0.1% SDS, 1mM EDTA) plus a protease inhibitor cocktail (Complete™, Roche), 1 mM sodium orthovanadate, 1 mM dithiothreitol and 20 mM *N*-Ethylmaleimide (Sigma). Lysates were sonicated two times for 5 seconds.

After incubation on ice for 20 min, the lysates were centrifuged at max speed for 10 min at 4°C to recover the supernatant.

5.2 Cytoplasmic and nuclear protein fractions extraction

The differential extraction of cytoplasmic and nuclear fractions of proteins was performed scraping cells at 4°C in cold PBS. Cell suspensions were centrifuged at 1500 rpm for 3 min at 4°C and the pellets were resuspended in buffer A (10 mM Hepes pH 7.9, 0,1 mM EDTA pH 8, 0.1 mM EGTA pH8, 10 mM KCl, 1 mM DTT) containing a protease inhibitor cocktail (*Complete*™, Roche) and 1mM sodium orthovanadate. Samples were then keeped on ice for 15 min, then NP40 was added to a final concentration of 0.5% and lysates vortexed for 10 seconds and centrifuged at max speed for 1 min at 4°C, to recover the supernatant, which represents the cytoplasmic protein

fraction. The pellets were washed three times with sucrose buffer (0.32 M sucrose, 3 mM $CaCl_2$, 2 mM MgAcetate, 0.1 mM EDTA, 10 mM Tris-HCl pH 8, 1 mM DTT, 0.5% NP40), resuspended in buffer C (20 mM HEPES pH 7.9, 1 mM EDTA pH 8, 1 mM EGTA pH 8, 400 mM NaCl, 1 mM DTT) containing a protease inhibitor cocktail and 1mM sodium orthovanadate. The lysates were incubated on ice for 20 min and centrifuged at max speed for 15 min at 4°C, to recover the supernatant, which represent the nuclear protein fraction.

5.3 Immunoprecipitation and Kinase assay

Immunoprecipitation experiments were performed using 0.5-2 mg of total cell lysate in HNTG buffer (20 mM HEPES, 150 mM NaCl, 10% glycerol, 0.1% Triton X-100) or in PBS-0,2% NP40 (for stathmin and RhoA immunoprecipitates) plus the specific agarose-conjugated primary antibody (FLAG-M2 Affinity gel) and incubating overnight at 4°C. When primary antibodies were not agarose conjugated, protein A or protein G Sepharose 4 Fast Flow (Amersham Biosciences) was added during the last 2 hours of incubation. Immunoprecipitates were washed six times in HNTG buffer, and then nine parts were resuspended in 3X Laemmli sample buffer with 50 mM dithiothreitol and one part was resuspended in kinase buffer (20 mM TrisHCl pH 6.8, 10 mM $MgCl_2$).

For the evaluation of kinase activity samples were mixed with a kinase reaction solution containing 50 µM not labelled ATP, ATP γ-^{32}P (PerkinElmer Life Sciences) and 2 µg of H1-Histone H1 or recombinant retinoblastoma protein (RB) as substrate, in kinase buffer. The reaction was carried out at 30°C for 30 min and then 2X Laemli Sample Buffer was added. After denaturation at 95°C for 5 min, proteins were loaded on a 4-20% SDS-PAGE (Criterion Precast Gel, Biorad). The gel was then dried and exposed on an autoradiographic film (Amersham-Hyperfilm MP) at -80°C and developed after different time intervals.

p27 kinase inhibitory activity was also tested with an *in vitro* assay using recombinant cyclin-CDK complexes. Different amounts of recombinant p27 mutants were incubated with 40 ng of recombinant cyclin A_2-CDK2 complex (SignalChem) or with 300 ng of cyclin D_1-CDK4 (SignalChem) complex, on ice for 1.5 hrs. Then samples were subjected to kinase assay using, respectively, histone H1 or Rb protein as the substrate.

5.4 Immunoblotting

For immunoblotting, 40 µg of proteins was separated by 4-20% SDS-PAGE (Criterion precast gel; Bio-Rad) and transferred to nitrocellulose membranes (Hybond C; Amersham Inc.). Membranes were incubated with primary antibodies as indicated and then with horseradish

peroxidase-conjugated secondary antibodies (GE Healthcare) for ECL detection (GE Healthcare) or Alexa-conjugated secondary antibodies (Invitrogen) for Odyssey infrared detection (Licor). For immunoprecipitates, rabbit immunoglobulin G and mouse immunoglobulin G True Blot (eBioscience) secondary horseradish peroxidase-conjugated antibodies were used. Quantification of the immunoblots was done using the QuantiONE software (BioRad) or the Odyssey infrared imaging system (Licor Biosciences). Primary antibodies were from: Transduction Laboratories (p27, metablastin/stathmin, CDK2 and Ubc9), Santa Cruz (p27 C19, p27 N20, CDK4, vinculin, Skp2,), Clontech (Zs green polyclonal antibody), Sigma (Op18/stathmin, SUMO1), Upstate (RhoA). As marker of nuclear extracts we used an anti-HMG2A polyclonal antibody kindly provided by Prof. G. Manfioletti.

6. *In vitro* transcription and translation

In vitro transcription-translation was performed using the TNT T7 Quick Coupled Reticulocyte Lysate System (Promega). $p27^{WT}$ and p27 mutants cDNAs were cloned in the pTNT vector (Promega) and 1 µg of circular plasmid was added directly to TNT Lysate and incubated in a 50 µl reaction for 1.5 hs at 30°C. The reaction mix contained [^{35}S] methionine (PerkinElmer Life Sciences) for the detection of translated proteins. Before doing the experiment, 100 ng of each plasmid were loaded into an agarose gel for mass standardization.

7. *In vitro* protein degradation assay

In vitro degradation of p27 was carried out essentially as previously described (Loda et al., 1997). Briefly, HT1080 cells were transfected with pHA-Ubiquitin vector and lysed 48 hs later in ice-cold double-distilled water. The sample was frozen and thawed 3 times, and then spun down to pellet debris. The supernatant was retrieved and frozen at -80°C. 1 µg of histidine-tagged p27 was incubated at 37°C for different times in 50 µl of degradation mix containing 200 µg of lysate from HT1080 cells, 50 mM Tris-HCl (pH 8.0), 5 mM $MgCl_2$, 1 mM DTT and 2 mM ATP. After the indicated times, reactions were stopped by adding 5X Laemmli buffer and loaded onto 4-20% polyacrylamide gel. p27 degradation was analyzed by immunoblotting with an anti-p27 monoclonal antibody.

8. RNA Extraction, RT-PCR and Real-Time PCR

Total RNA from transfected cells was extracted using the RNeasy kit (Qiagen). Two micrograms of total RNA was retrotranscripted using AMV Reverse Transcriptase and random

hexamers according to the provider's instruction (Promega); 1/20 of the obtained cDNAs were then amplified using the upstream primer for the human p27 sequence and the M13 reverse primer that target pDNR vector, to not amplify endogenous p27 transcript, or with primers for human GAPDH mRNA. Quantitative Real-Time PCR analysis was performed amplifying 100 ng of the same cDNAs using SYBR Green PCR Core Reagents (Applied Biosystems). Standard curves (10-fold dilution from 10^{1} to 10^{-4} attomoles) were prepared both for target gene and for more than one housekeeping gene. The incorporation of the SYBR Green dye into the PCR products was monitored in real time using the Applied Biosystems ABI PRISM 7700 Sequence Detector, and the resulting threshold cycles (Ct) (the PCR cycle number at which the fluorescent signal of the report dye crosses an arbitrarily placed threshold ensures that the PCR is in the exponential phase of amplification) were computed. Ct values were converted into attomoles and the normalized target gene value was obtained by dividing target gene with the housekeeping amount.

9. Cell cycle analysis

To evaluate cell cycle progression 3T3 $p27^{KO}$ cells were transduced with the indicated mutants and 24 hrs after transduction cells were starved and then released in DMEM complete. Collected cells were fixed with 70% ice-cold ethanol and maintained at -20°C until ready for the staining procedure. Cells were then twice washed with PBS and labeled with propidium iodide staining solution (50 µg/ml Propidium Iodide and 0.1 mg/ml RNaseA, in PBS 1X) for 30 minutes at RT. The stained cells were subjected to flow cytometry analysis (FACS) with a FACScan and a FACSCalibur instrument (BD Biosciences). Data were analyzed with a cell cycle analysis software program (WinMDI2.8) to calculate the distribution of cells in G1, S and G2/M phases of the cell cycle.

10. Colony assay

For colony assay, 24 hrs post-transduction SCC9 cells were trypsinized, counted and seeded at density 1000 and 5000 cell/100mm dish and incubated in their complete growth medium. Two weeks later plates were stained with crystal violet and colonies counted. Results were expressed as percentage of growth inhibition comparing the colony numbers of each condition to the colony numbers formed in the plate transduced with AdGFP control vector. Experiments were performed in quadruplicate and data represents the mean value of three independent experiments. The transduction efficiency was calculated counting the number of green cells in 10 randomly selected

fields, 24 hs after transduction. After 15 days, 60-80 colonies were counted for each mutants and the percentage of green colonies was determined.

11. Immunofluorescence analysis

For immunofluorescence staining, cells seeded on coverslips were fixed in PBS 4% paraformaledehyde (PFA) at room temperature (RT), permeabilized in PBS 0.2% Triton X-100 and blocked in PBS-1% BSA or 10% normal goat serum. Incubation with primary antibodies (anti Flag-M2, Sigma, anti-SUMO 1, Sigma, and anti-p27, DABKO) was performed overnight at 4°C in PBS-1% BSA or 1% normal goat serum, then samples were washed in PBS and incubated with secondary antibodies (Alexa Fluor 488-, 546- or 633-conjugated anti-mouse or anti-rabbit, Invitrogen) for 1 hour at RT. In some cases antibody incubation was followed by nuclear staining with 5 μg/ml Propidium Iodide (PI) in PBS for 45 min at RT. Coverslips were mounted in Mowiol 488 (Calbiochem-Novabiochem) containing 2.5% (w/v) 1,4-diazabicyclo(2,2,2)octane (DABCO, Sigma). Stained cells were then observed using a confocal laser-scanning microscope (TSP2 Leica) interfaced with a Leica DMIRE2 fluorescent microscope. Images were acquired using a Nikon Diaphot 200 epifluorescent microscope equipped with distinguishing filters.

12. Morphology in 3D

For the evaluation of cellular morphology in 3D matrix, U87MG cells were included in Matrigel (6 mg/ml; BD) 10μl-drops on a coverslip (5000 cells/drop) and maintained for 1 hour upside down at 37°C, to allow Matrigel polymerization. Then, complete medium was added. Drops were incubated for 24 hours and photographed using a phase-contrast microscope to evaluate cell morphology.

13. Time-Lapse video microscopy

For the evaluation of cell motility following adhesion to FN cells were transfected with EGFP-p27 fusion proteins in the presence or not of DsRed-stathmin protein and 24 hours later plated on FN coated glass bottom dishes (WillCo Wells BV) that allow the use of the 63X immersion glycerin objective. Cells were then incubated at 37°C in 5% CO_2 atmosphere in the Leica Time Lapse AF6000LX workstation equipped with the Leica DMI 6000 motorized microscope and an environmental chamber for the proper setting of temperature, humidity and CO_2 concentration. The microscope allows the acquisition of multiple fields on the X, Y and Z axes and is computer assisted. The AF6000 Software (Leica) allows the acquisition of the images on the

desiderate frames and periods of time. Images were collected every 2 minutes for 2 hours and used to create a video (15 images per second) and analyzed with a cell tracking software (Leica) to collect different locomotion parameters (21, 24). In brief, cells were randomly selected and their x/y coordinates tracked using the IM2000 software (Leica), which allows automated or manual cell tracking in order to obtain cell speed (micron/min) and total distance covered (micron) by the cells. At least 3 independent wells/cell type have been analyzed.

14. Migration experiments

Haptotaxis was performed using Transwell-like inserts, carrying a fluorescence-shielding porous PET membrane with 0.8 m pores (HTS FluoroBlokTM, BD) which were previously coated on the bottom side with 10 μg/ml fibronectin, overnight at 4°C, and then saturated 2 hrs at room temperature with PBS 1% BSA. Cells were seeded in the Fluoroblok^{TM} upper chamber and then incubated at 37°C for the indicated times. Migrating cells were evaluated by reading at different time points the lower (migrated cells) and the upper sides (non migrated cells) of the membrane with the SPECTRAFluor Plus microplate fluorometer (Tecan). Each experiment was performed at least 3 times, in duplicate. Migration was then blocked by fixing the Fluoroblok membranes in 4% PFA to allow the count of migrated cells.

Table 1

ATG-B		5’ ggatccccacc**atg**tcaaacgtgcga 3’
1-170		5’ aagcttttatgttctgttggctctttt 3’
T187A		5’ aagcttttacgtttgacgtcttctgaggccaggcttcttggg**cgc** 3’
T198A		5’ gatatcaagcttttta**cgc**ttgacgtc 3’
T198F		5’ gaattcaagcttttta**gaa**ttgacgtcttct 3’
T198V		5’gaattcaagcttttta**cac**ttgacgtcttct 3’
197stop		5’ gaattcaagctt**tta**ttgacgtcttctgag 3’
T198D		5’ gaattcaagcttttta**atc**ttgacgtcttct 3’
T198E		5’ gaattcaagcttttta**ctc**ttgacgtcttct 3’
T198S		5’ gaattcaagcttttta**cga**ttgacgtcttct 3’
T198G		5’ gaattcaagcttttta**tcc**ttgacgtcttct 3’
Y74F	F	5’ cccctagagggcaag**ttc**gagtggcaagaggtg 3’
	R	5’ cacctcttgccactc**gaa**cttgccctctagggg 3’
Y88F	F	5’ cagcttgcccgagttc**ttc**tacagacccccgcgg 3’
	R	5’ ccgcgggggtctgta**gaa**gaactcgggcaagctg 3’
Y89F	F	5’ cttgcccgagttctac**ttc**agacccccgcggcc 3’
	R	5’ ggccgcgggggtct**gaa**gtagaactcgggcaag 3’
K25R	F	5’ caggcggagcacccc**agg**ccctcggcctgcagg 3’
	R	5’ cctgcaggccgaggg**cct**ggggtgctccgcctg 3’
K47R	F	5’ cccgggacttggag**agg**cactgcagagacatg 3’
	R	5’ catgtctctgcagtg**cct**ctccaagtcccggg 3’
K59R	F	5’ gaggcgagccagcgc**agg**tggaatttcgattttc 3’
	R	5’ gaaaatcgaaattcca**cct**gcgctggctcgcctc 3’
K68R	F	5’ gattttcagaatcac**aga**cccctagagggcaag 3’
	R	5’ cttgccctctaggggg**tct**gtgattctgaaaatc 3’
K73R	F	5’ caaacccctagagggc**agg**tacgagtggcaagag 3’
	R	5’ ctcttgccactcgta**cct**gccctctaggggtttg 3’
K81R	F	5’ggcaagaggtggag**agg**ggcagcttgcccgag 3’
	R	5’ ctcgggcaagctgcc**cct**ctccacctcttgcc 3’
K96R	F	5’ cccccgcggcccccc**aga**ggtgcctgcaaggtg 3’
	R	5’ caccttgcaggcacc**tct**gggggccgcggggg 3’
K100R	F	5’ cccaaaggtgcctgc**agg**gtgccggcgcaggag 3’

	R	5’ ctcctgcgccggcac**cct**gcaggcacctttggg 3’
K134R	F	5’catttggtggaccca**agg**actgatccgtcggac 3’
	R	5’ gtccgacggatcagt**cct**tgggtccaccaaatg 3’
K153R	F	5’ gcgcaggaataagg**agg**cgacctgcaaccgac 3’
	R	5’ gtcggttgcaggtcg**cct**ccttattcctgcgc 3’
K165R	F	5’ cttctactcaaaac**aga**agagccaacagaac 3’
	R	5’ gttctgttggctct**tct**gttttgagtagaag 3’
K189R	F	5’ gtggagcagacgccc**agg**aagcctggcctcag 3’
	R	5’ ctgaggccaggctt**cct**gggcgtctgctccac 3’
K190R	F	5’ gagcagacgcccaag**agg**cctggcctcagaag 3’
	R	5’ cttctgaggccagg**cct**cttgggcgtctgctc 3’
SUMO1	F	5’ aagcttatgtctgaccaggaggca 3’
	R	5’ ggtaccctaaactgttgaatgacc 3’
SUMO2/3	F	5’ aagcttatgtccgaggagaagccc 3’
	R	5’ ggtaccctagaaactgtgccctgc 3’
Ubc 9stop	F	5’ gcgccctcaccgcgg**taa**ccttatgatgtgcc 3’
	R	5’ ggcacatcataagg**tta**ccgcggtgagggcgc 3’

RESULTS

1. p27 protein expression is affected by the T198A point mutation but is not dependent on the T198 phosphorylation

We recently demonstrated that the C-terminal portion of p27 is important for its ability to control MT stability, via stathmin interaction and this, in turn, impinge on cell motility (Baldassarre et al., 2005; Schiappacassi et al., 2008; Berton et al., 2009; Belletti et al., 2010). By studying the effects of $p27^{WT}$ protein on the regulation of glioblastoma cell growth and motility we observed that the WT protein was able to stimulate the formation of neuron like protrusions in U87MG cells (Video S1), thus confirming our previous observation that p27 is able to control protrusion formation in 3D context (Belletti et al., 2010), also in glioblastomas. Further data demonstrated that p27 stimulated protrusion formation in U87MG cells through its C-terminal tail, since the deleted mutant $p27^{1-170}$ was ineffective (Figure 1A). To better understand the mechanism of regulation of cell shape and motility by p27, we decided to generate specific point mutants in those residues comprised among amino-acids 170 and 198 that have been proposed to have a role in the regulation of p27 protein. Indeed, two residues appeared of particular interest in this region, namely the T187, that plays a fundamental role in CDK-mediated degradation of p27 (Tsvetkov et al., 1999) and the T198 which has been proposed to regulate protein stability (Kossatz et al., 2006), autophagy (Liang et al., 2007) and cell motility (Larrea et al., 2009).

First, we generated a $p27^{T198A}$ non-phosphorylable mutant to verify whether or not the modification of p27 last amino-acid had any role in morphological and motility phenotypes of glioblastoma cell lines. Adenoviruses expressing the WT, the 1-170 and the T198A p27 proteins were generated and used to transduce the U87MG cell line. The T198A mutation resulted in a strong abrogation of p27 protein expression (Figure 1B). This effect was independent from the phosphorylation of the T187 since it was not rescued by the concomitant mutation of T187 in alanine and was confirmed using DNA transfection instead of adenoviral transduction using 3 different cell lines (Figures 1C, 1D and 2A). Altogether these data confirm that T198 is a key residue for p27 protein stability and its effect is not dependent on the phosphorylation of T187.

In contrast with this observation several lines of evidence demonstrated that the $p27^{1-170}$ mutant (that lacks both the T198 and the T187 residues) has an expression comparable to that of the WT protein (Figures 1B, 1C, 2A, 4B) and (19, 21). In order to clarify this point the $p27^{1-197}$ mutant was generated in which only the last amino-acid was deleted. As shown in Figure 2A, $p27^{1-197}$ was expressed at levels similar to the WT protein indicating that the phosphorylation of p27 on T198 is not required to govern the protein stability (compare lane 1 with lane 11 in Figure 2A).

We then reasoned that the threonine homolog non-phosphorylable amino-acid is the valine and not the alanine while the glutamic acid (E) and aspartic acid (D) represent the pseudo-

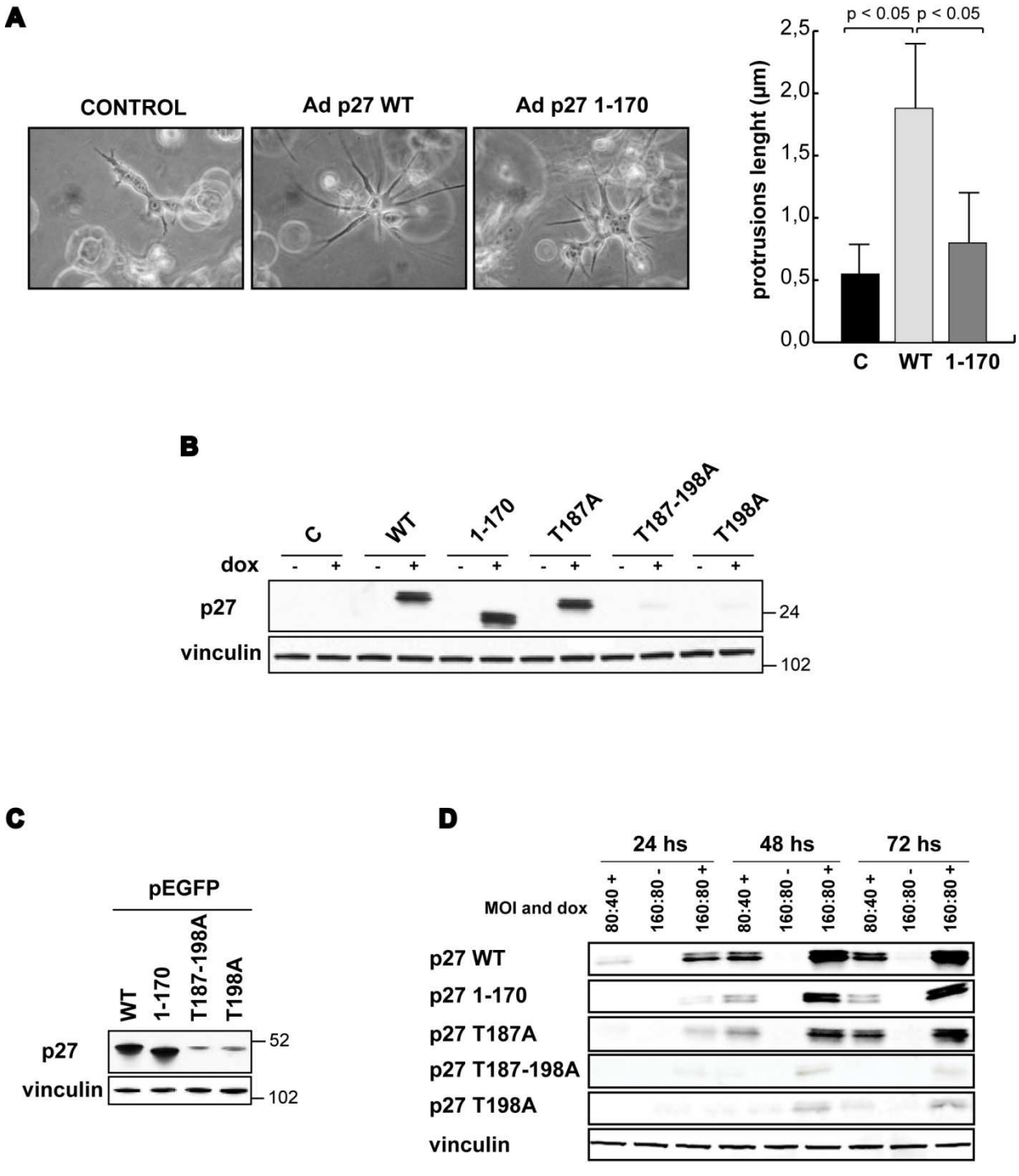

Figure 1. p27 protein expression is affected by the T198A/G point mutation. **A**. U87MG cells were transduced with the indicated Ads, included in 3D Matrigel matrix and images were taken 24 hours later (20x objective). In the graph the length of cell protrusions is reported. Data represents the mean value (± standard deviation) obtained measuring protrusions length in at least 20 cells for each type of transduction in 3 separate experiments. **B**. Western blot analysis of p27 expression in U87MG cells co-transduced with AdTRE p27s/AdTet-ON 72 hours post-transduction. Vinculin was used for loading control. **C**. Western blot analysis of p27 expression in HT1080 cells transiently transfected with different pEGFP-p27 mutants. **D**. Time course analysis of p27 expression in SCC9 cells co-transduced with AdTRE p27s/AdTet-ON (MOI 80:40 and 160:80) as indicated. The expression of p27 and vinculin (loading control) evaluated by western blot analysis is reported.

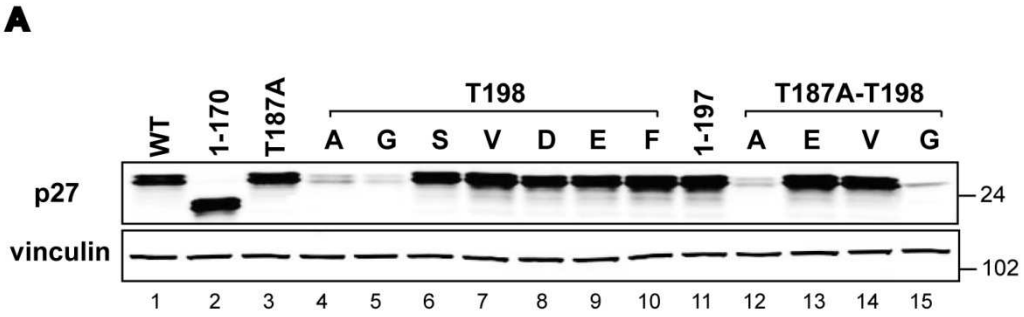

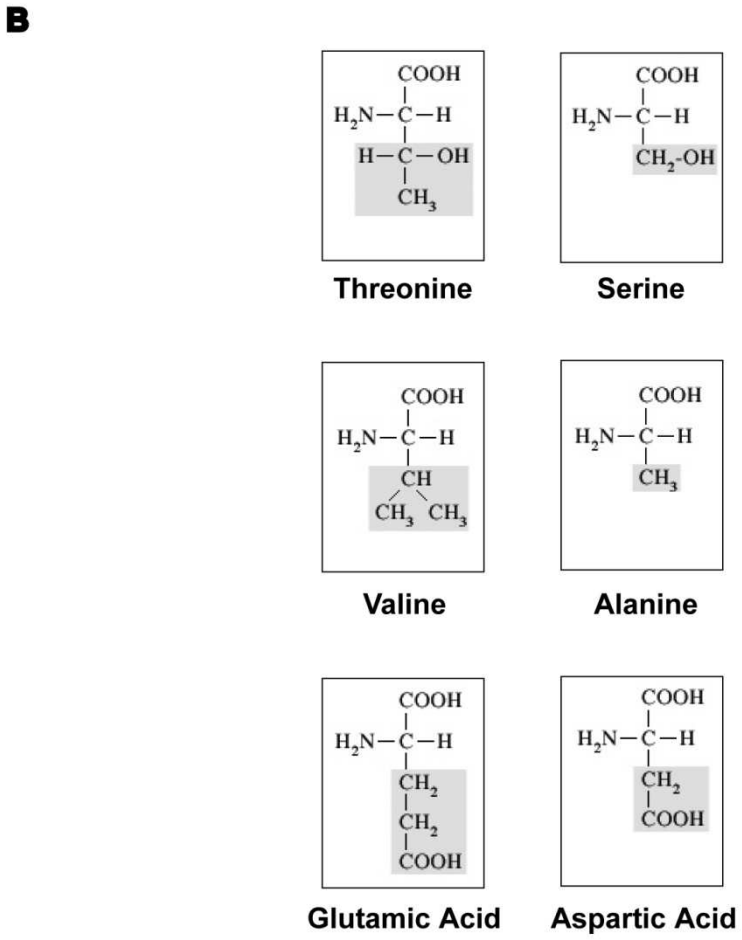

Figure 2. p27 expression is affected by the steric hindrance of the last aminoacid. A. Western blot analysis of p27 expression in SCC9 cells transiently transfected with different p27 mutants cloned in the pDNR vector and analyzed 48 hrs after transfection. Vinculin was used as the loading control. (A=alanine, G=glycine, S=serine, V=valine, D=aspartic acid, E=glutamic acid, F=phenylalanine). **B**. Comparison of Amino-acids lateral chains. As shown by the structural formula, valine and glutamic acid are, respectively, the non-phosphorylable and phospho-mimetic homolog of threonine, while alanine and aspartic acid are those of serine.

phosphorylated mutation of threonine and serine, respectively (Figure 2B). In accord with the observation obtained with the deletion $p27^{1-170}$ and $p27^{1-197}$ mutants, both T198V and T198E mutants displayed an expression level similar to that of the WT p27 protein (compare lane 1 with lanes 7 and 9 in Figure 2A). Similarly, the double mutants T187A-T198E and T187A-T198V were expressed as the WT protein (Figure 2A).

Being the alanine the smallest of the 20 amino-acids after the glycine, we hypothesized that the steric hindrance of the last amino-acid in p27 rather than the addition of a phosphate group to the T198 was important for the correct expression of the protein. To prove this hypothesis the p27 T198 was changed either in glutamic acid (D), serine (S), phenylalanine (F) or glycine (G). All the mutants but T198G displayed level of expression similar to that of the WT protein (Figure 2A). Consistently, the double mutant T187A-T198G was expressed at very low level when compared to the expression of the WT protein (Figure 2A). Thus, only the substitution of T198 with A or G, the two smallest amino-acids, resulted in the reduced p27 expression, confirming that the size of the last amino-acid rather than the threonine phosphorylation was important for the regulation of its expression.

2. $p27^{T198A}$ displays an increased proteasome-dependent degradation that is not dependent on the T198 phosphorylation

We tried to understand the mechanism by which the T198A/G substitution could regulate p27 expression. We first looked at the transcription of the different constructs that, as expected, was similar in all mutants as indicated by semiquantitative RT-PCR (Figure 3A). These results were confirmed by quantitative Real Time PCR experiments coupled with western blot analyses in the same transfectants. The results of three independent experiments showed in Figure 3B obtained by comparing the protein expression (in arbitrary units) with the fentomoles of p27 mRNA present in each transfectant, demonstrated that when the T198 in p27 was mutated in G or A only 1/10 of the protein was found per each fentomole of mRNA as compared with the ratio observed for the WT protein (Figure 3B). In any of the other mutants tested we were not able to find any significant difference with the ratio observed for the WT protein.

Using *in vitro* transcription-translation assays we also excluded that the differences in protein expression resided in the ability of the mRNA to be correctly translated in protein since similar amount of protein was produced *in vitro* per each nanogram of plasmid used (Figure 3C).

Collectively these data suggested that the different expression of $p27^{T198A/G}$ mutants could be linked to differences in protein stability. To test this hypothesis we looked at the stability of $p27^{WT}$ and mutant proteins in cells treated with cycloheximide (10 µg/ml) for different times. This

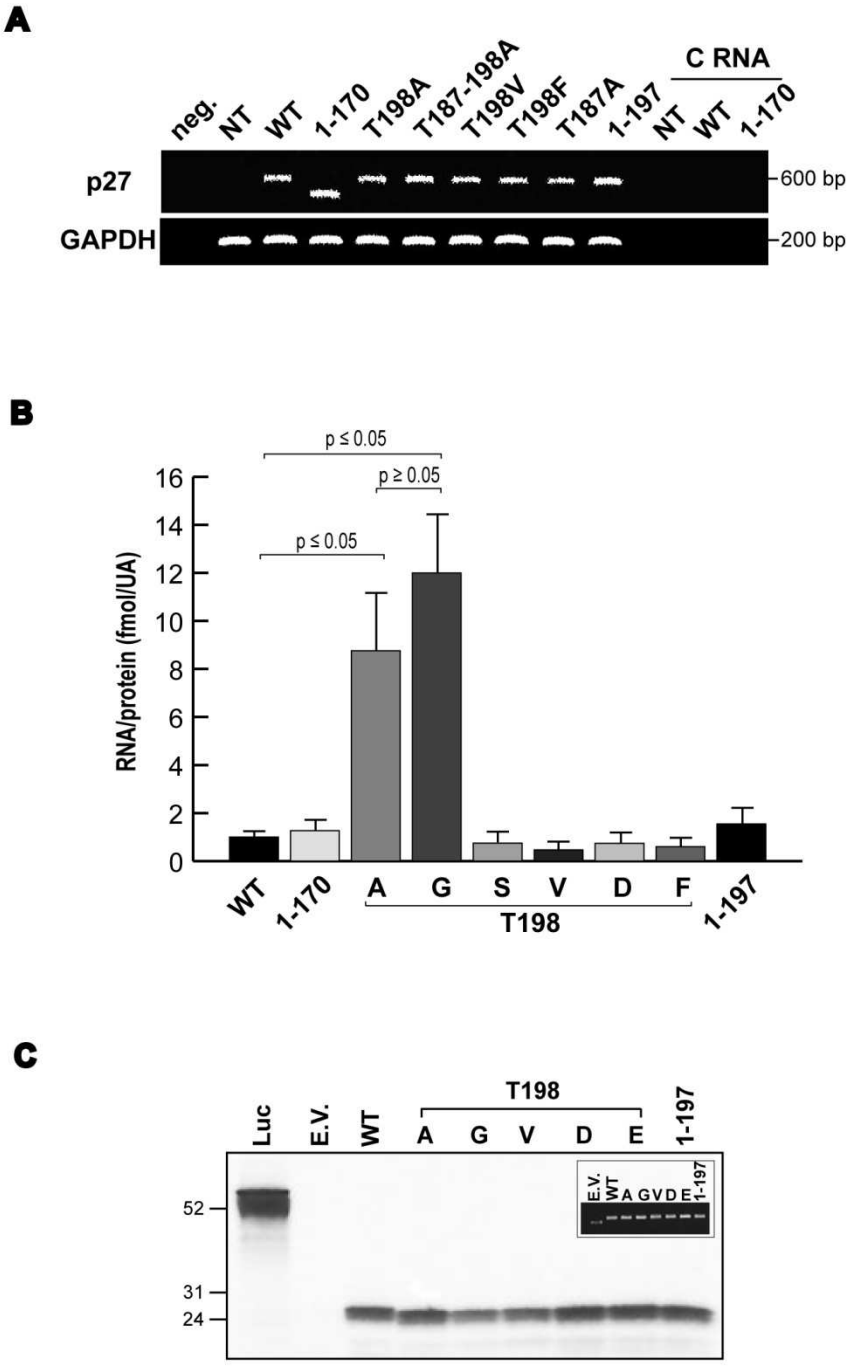

Figure 3. p27T198A/G low protein expression is not due to decreased transcription. **A**. RT-PCR on RNA extracted from SCC9 cells transiently transfected with different p27 mutants cloned in the pDNR vector and analyzed 48 hrs after transfection. GAPDH was used as internal control. NT = Non Transfected cells, C RNA= amplification of non retro-transcribed RNA. **B**. SCC9 cells were transfected with pDNR p27WT and with the indicated mutants and 48 hs later RNA and protein extracts were prepared from each plate. Results represent the ratio between the fentomoles of p27-mRNA evaluated by qRT-PCR analysis and the amount of p27 protein expression evaluated by densitometric analysis of the blots and normalized to the loading control vinculin. Data represents the mean value (± standard deviation) of three independent experiments. Statistical analysis was carried out using Student's t test. **C**. p27WT and the indicated T198 mutants cDNAs were in vitro transcribed and translated, loaded into SDS-PAGE gels and subjected to autoradiography. Inset shows control of plasmidic DNA quantification used in this experiment. Luc= luciferase positive control vector, E.V. = empty vector.

experiment clearly showed that the stability of mutants containing either G or A as last amino-acid was lower than that observed for the WT protein, with an half life of about 4,5 hours for the A/G containing mutant respect to about 12 hours for the WT or the non A/G T198 (T198E and T198V) mutants (Figure 4A).

As a complementary approach we utilized recombinant p27 proteins produced in *E. coli* and analyzed them in a proteasome dependent degradation assay. Western blot analysis demonstrated that the degradation rate of $p27^{T198A/G}$ mutants tested in the presence of proteasomal extract derived from HT-1080 cells transfected with HA-tagged ubiquitin was higher respect to that of the WT protein or substituted with the V or E amino-acids (Figure 4B). Quantitative analysis demonstrated that mutants containing $p27^{T198A/G}$ displayed a half-life of about 2.5 hours respect to the 7-9 hours of $p27^{T198V}$, $p27^{WT}$ or $p27^{T198E}$. Also in this case the concomitant mutation of T187 was not able to rescue p27 stability (Figure 4B), demonstrating that the presence of A/G in the last position of p27 was dominant respect to the mutation of T187. Accordingly, the $p27^{1-170}$ mutant that lacks both T198 and T187 resulted even more stable in the same assay (Figure 4B).

These data suggested that the presence of a small amino-acid in the last residue of p27 protein resulted in increased proteasome dependent degradation and that this process was independent from the phosphorylation of T187. Since phosphorylation of T187 is an event necessary for the Skp2 mediated degradation of p27 (Montagnoli et al., 1999; Carrano et al., 1999; Tsvetkov et al., 1999), our data pointed to a Skp2 independent pathway leading to p27 down-modulation.

This hypothesis was sustained by subsequent results coming from experiments using MDAH 2774 cells where the Skp2 silencing level was optimal. The use of shRNA directed against Skp2 resulted in increased expression of the $p27^{WT}$, $p27^{T198V}$ or $p27^{T198E}$ proteins but produced only minor effects on the half-life of $p27^{T198A}$ or $p27^{T198G}$ (Figure 5A). However, the experiments confirmed that the low levels of $p27^{T198A/G}$ were due to their enhanced protein degradation since their expression could be rescued by the treatment of the cells with the proteasome inhibitor MG132 (Figure 5B).

3. Mutation of T198 in alanine increased proteasome dependent degradation of p27 independently by its CDK binding ability

We also tested the possibility that CDK2 binding could be involved in the regulation of $p27^{T198A/G}$ stability. To this aim we generated $p27^{CK-}$ mutants in which the 30-32 and 62-64 amino-acids were mutated and the p27 binding ability to the CDK2/cyclin A/E complexes abolished (Vlach et al., 1997). The expression levels of $p27^{CK-}$ were similar to those of the WT protein (data not shown). When $p27^{CK-}$ was also mutated in the last amino-acid in either A, G or V, only the

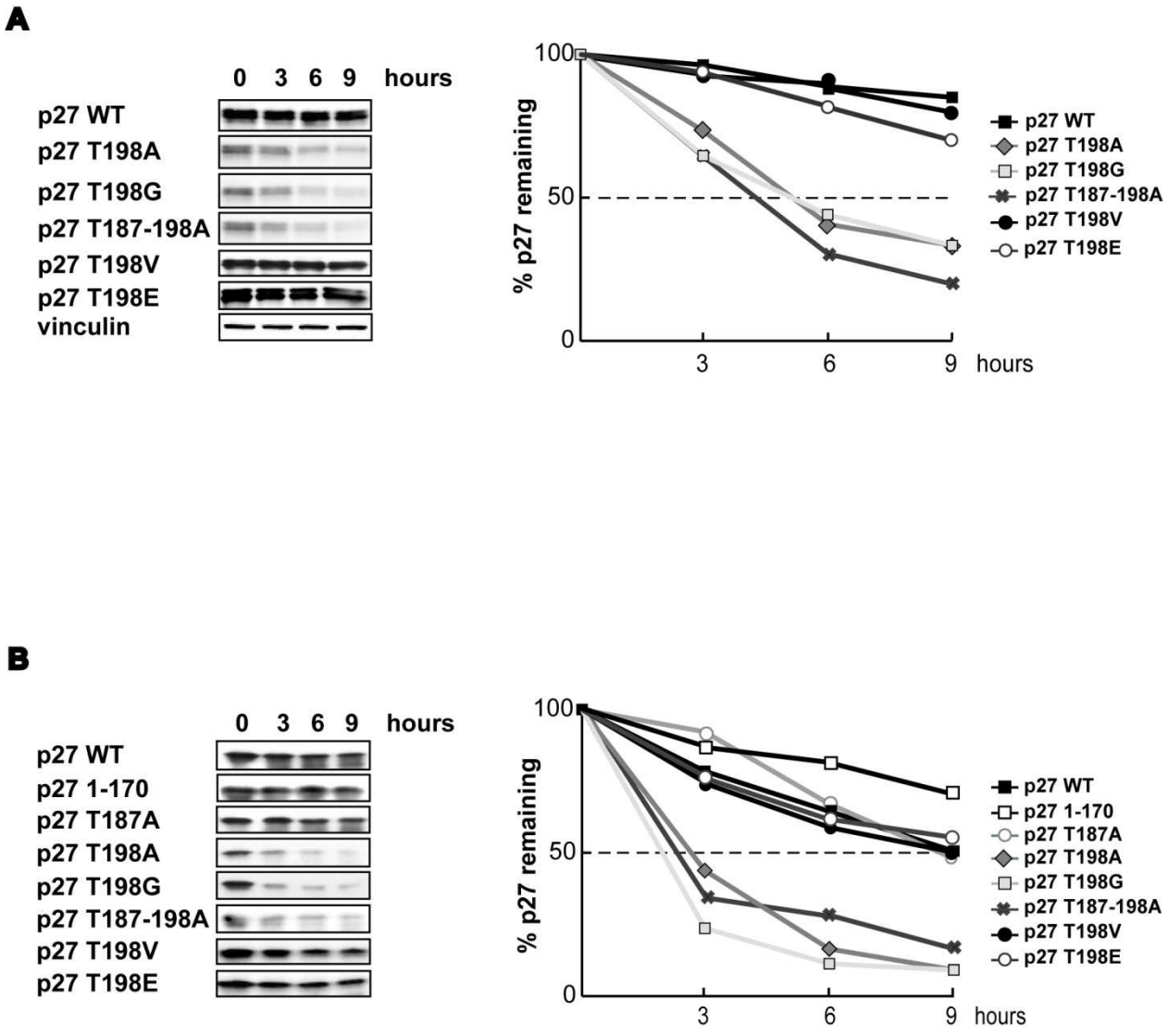

Figure 4. T198A/G substitution markedly decreases p27 protein stability. **A**. Western Blot analysis of p27 expression in SCC9 cells transfected with the indicated p27 mutants and 48 hrs later treated with cycloheximide (CHX) for 3, 6 and 9 hrs. The densitometric analysis of the blots of a representative experiment is reported in the graph (right) and is expressed as percentage of remaining protein respect to untreated cells. **B**. Western Blot analysis of p27 recombinant proteins in in vitro degradation assay using bacterial His-tagged recombinant p27 proteins incubated with proteasome extracts for 3, 6 and 9 hrs. Quantification of a representative degradation assay is reported in the right graph and expressed as described in A.

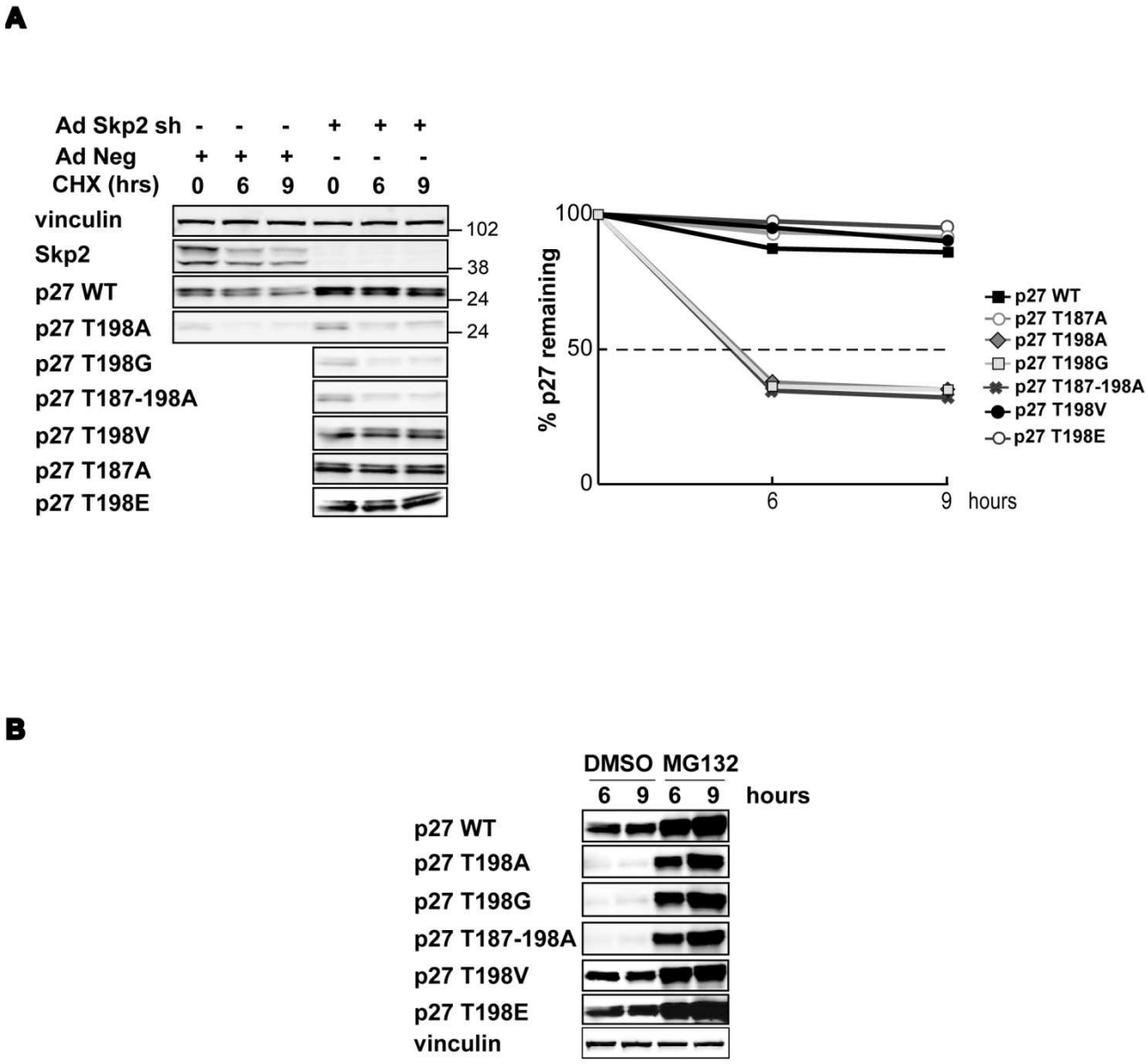

Figure 5. p27T198A/G down-modulation is due to Skp2-independent increased proteasome degradation. **A**. Western blot analysis of p27 and Skp2 expression in MDAH cells transduced with AdSkp2 or with AdNeg (Control) shRNAs in which the different p27 proteins were expressed and treated or not with CHX for 6 and 9 hs. Total protein extracts were analyzed by western blot using the indicated antibodies (left). The densitometric analysis of a representative Skp2 silencing experiment is reported in the graph (right) and expressed as in A. **B**. Western blot of 3T3 p27KO fibroblasts expressing the different p27 mutants as indicated and treated with MG132 (50 μM) or DMSO for 6 and 9 hours. A typical experiment is shown.

$p27^{CK-/T198V}$ mutant was expressed at levels similar to that of the control protein (Figure 6A). Immunoprecipitation experiments demonstrated that as expected the CK- p27 mutants did not bind the CDK2 protein (Figure 6B) and the analysis of protein stability in the presence of cycloheximide demonstrated that the CK- mutation did not alter the stability of $p27^{T198A/G}$ mutants in two different cell lines (HT1080, Figure 6C and HEK293 cells, data not shown).

It has also been proposed that the phosphorylation of tyrosines 74, 88 and 89 is important for p27 protein degradation and is related to conformational changes in its C-terminal tail (Chu et al., 2007; Grimmler et al., 2007). We thus hypothesized that they could be involved in the generation of the phenotype observed with the T198A/G mutants. Preventing the phosphorylation of either Y74 or Y88 did not alter the stability of the T198A mutant although the single substitution in Y74 or in Y88 slightly increased p27 protein stability, as judged by experiments of cycloheximide treatment (Figure 6D). In this setting, the half life of $p27^{Y74F-T198A}$ and $p27^{Y88F-T198A}$ was about 5 hours, thus similar to the $p27^{T198A}$ mutant, while that of the single $p27^{Y74F}$ and $p27^{Y88F}$ was about 15 hours, thus longer than that of the WT protein (12 hours of half-life).

Altogether these data demonstrate that the T198A/G substitution causes an increased degradation of p27 protein but that this effect is not related to the binding with the Cyclin/CDK complexes.

4. The lack of p27 phosphorylation on T198 does not affect cancer cell proliferation

The phosphorylation of p27 on T198 has been linked to the control of cell growth and motility (Kossatz et al., 2006; Larrea et al., 2009). To verify whether or not this was true also in our model system we compared the effects of the overexpression of the $p27^{T198A}$ mutant with that of $p27^{WT}$, $p27^{T198E}$ and $p27^{T198V}$ proteins on the regulation of both cell proliferation and motility.

To evaluate cell growth we transduced SCC9 squamous cell carcinoma with an adenovirus encoding the ZsGreen fluorescent protein together with the different p27 mutants, under the control of two different CMV promoters (Adeno-X™ ViraTrak™ Expression System 2, Clontech). Using this tool it is possible to follow the transduced cells that express the exogenous protein avoiding the influence of the fluorescence protein on the studied transgene. Moreover, the expression of the ZsGreen protein is not influenced by the protein stability of the transgene, as occurs with the fusion proteins. Accordingly, we observed similar levels of ZsGreen protein in the transduced cells coupled with high expression of $p27^{WT}$, $p27^{1-170}$, $p27^{T198E}$ and $p27^{T198V}$ proteins while, as expected, with low expression of the T198A mutants (Figure 7A). The colony assay experiment demonstrated that overexpression of $p27^{WT}$, $p27^{1-170}$, $p27^{T198E}$ and $p27^{T198V}$ proteins resulted in about the 60% of

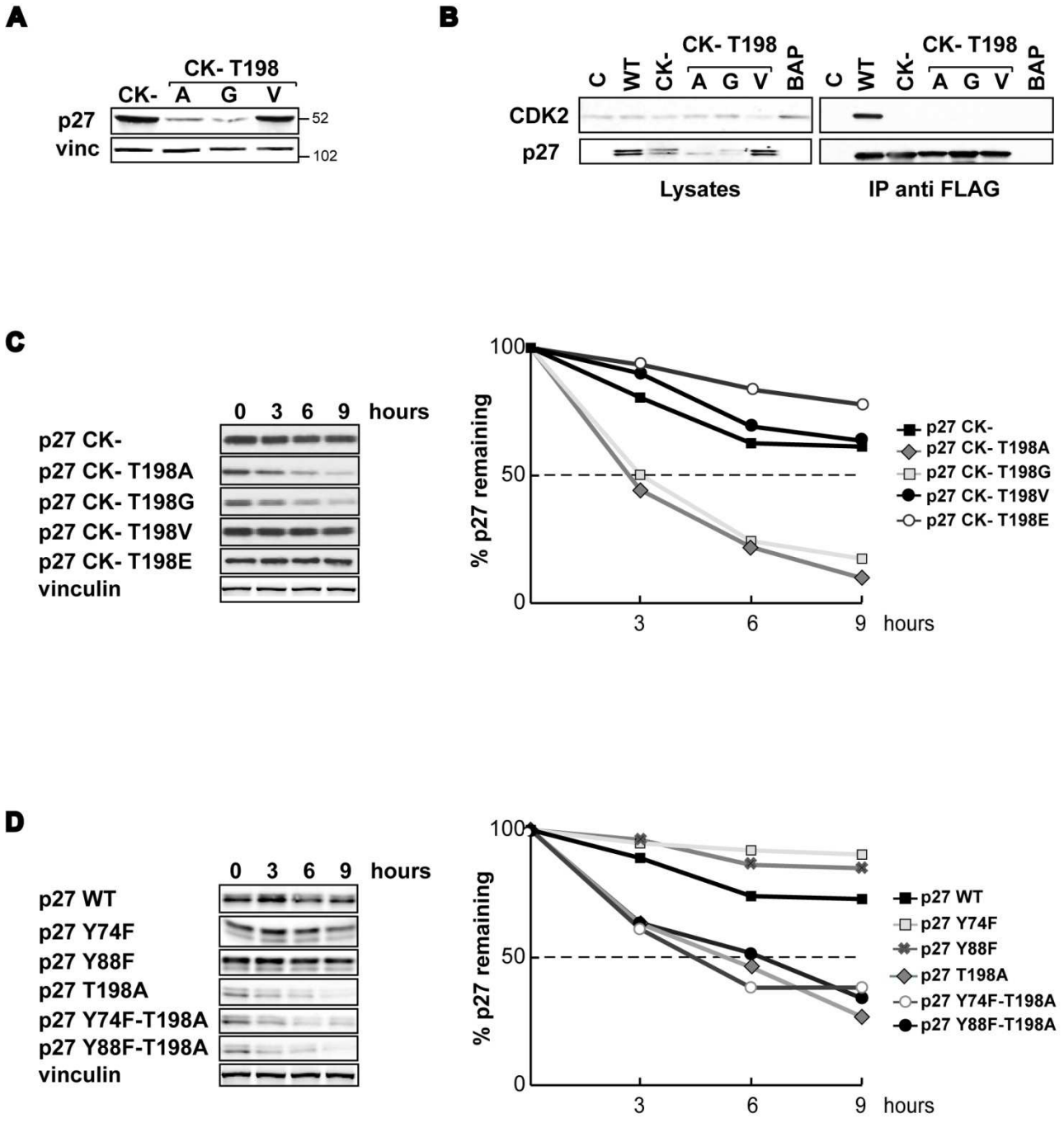

Figure 6. p27T198A/G increased proteasome-dependent degradation is not dependent on CDK-binding. **A**. Western blot analysis of p27 expression in HT1080 transfected with the indicated vectors and analyzed 48 hours after transfection. **B**. Western blot analysis of p27 and CDK2 expression in SCC9 cells transfected with the indicated FLAG-p27 or control (pFLAG-BAP) vectors analyzed 48 hours after transfection. The amount of CDK2 bound to the different p27 mutants is shown in the right blots (IP anti-FLAG). **C** and **D**. Western blot analysis of p27 expression in HT1080 transfected with the indicated vectors treated with CHX for 3, 6 and 9 hours. In the graph is reported the densitometric of a typical experiment.

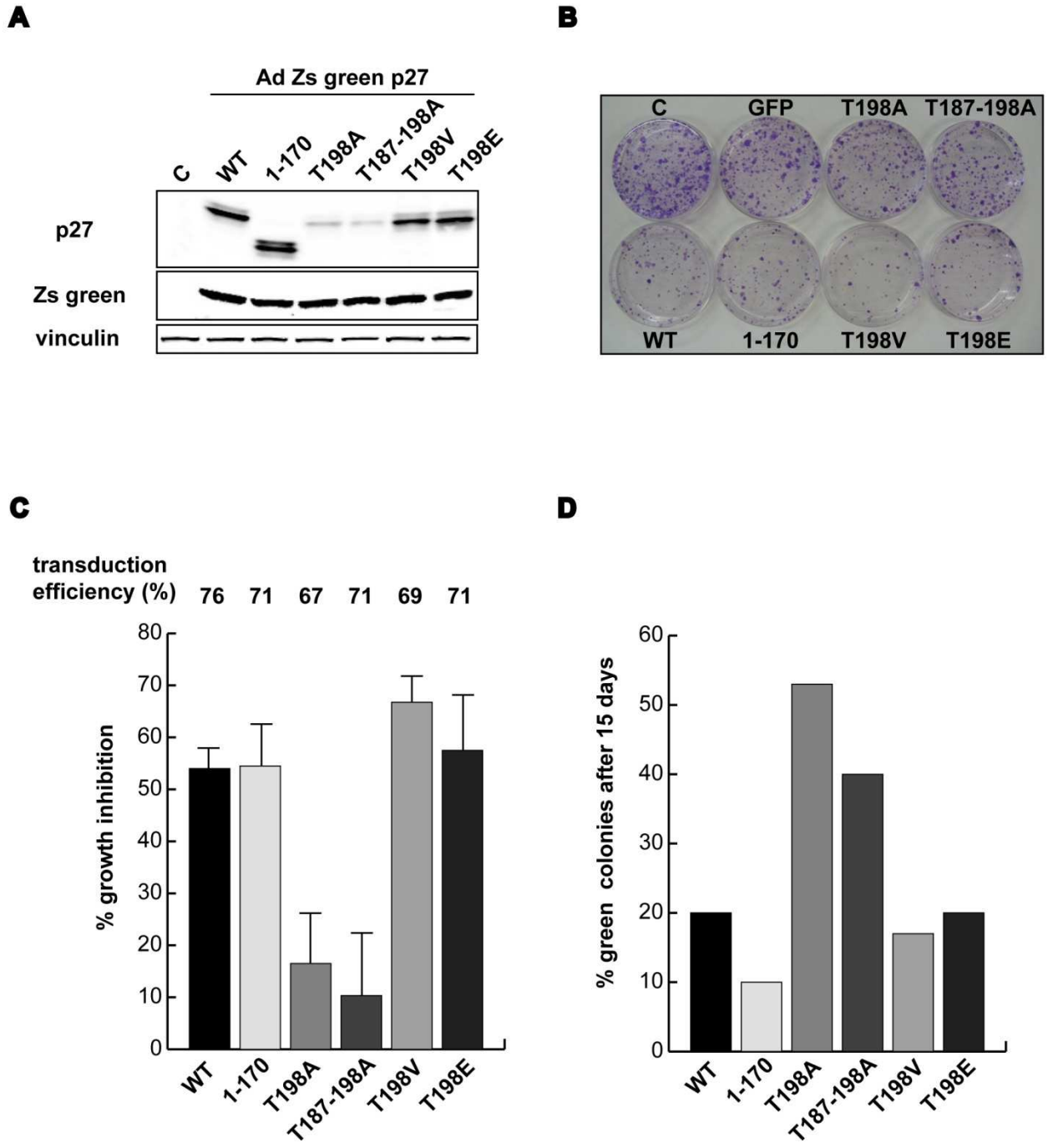

Figure 7. p27 is able to inhibit cell growth independently from phosphorylation of T198, but only when expressed over a threshold level. **A** Western blot analysis of p27 and Zs green expression in SCC9 cells transduced with the indicated AdZsgreen viruses and analyzed 24 hours post-transduction. **B**. Typical image of colony assay analysis in SCC9 cells transduced as in A and allow to grow for 15 days. **C**. Quantification of growth inhibition induced by the different p27 proteins respect to control cells evaluated by colony assay. Data represents the mean value of three independent experiments performed in quadruplicate. The mean transduction efficiency (% of green cells over the total) is reported. **D**. Percentage of colonies expressing the Zs Green protein 15 days post-transduction as determined counting at least 80 colonies for each mutants. A representative experiment is shown.

growth inhibition (Figures 7B and C) when compared with controls (non-transduced and GFP-transduced cells). This growth inhibition was directly related to the percentage of transduced cells, (69-76% of ZsGreen-positive cells by using the different Adenoviruses) (Figure 7C). The inhibition exerted by the T198A mutants was less than 20%, thus lacking any significant effect on cancer cell growth (Figures 7B and C). The absence of cell growth inhibition by $p27^{T198A}$ (and $p27^{T187\text{-}198A}$) was likely due to the low levels of proteins expression, as demonstrated by the count of green colonies in cells transduced with the different Adenoviruses and allowed to grow for 15 days. This experiment showed that while less than 20% of cells expressing the WT protein or the $p27^{1\text{-}170}$, $p27^{T198E}$ and $p27^{T198V}$ were green, more than 50% of the colonies in cells expressing the $p27^{T198A}$ protein were ZsGreen-positive (Figure 7D), thus demonstrating that the overexpression of p27 in SCC9 cells was able to inhibit cell growth independently from phosphorylation of T198, but only when expressed over a threshold level.

To further analyze the effects of these mutants overexpression in cell cycle, and being p27 mainly involved in G1/S transition, we studied more in details how T198 substitution affects this event. For this purpose 3T3 $p27^{KO}$ were transduced with $p27^{WT}$, $p27^{T198E}$ and $p27^{T198V}$ serum starved for 24 hours and released in complete medium. Cell cycle reentry was evaluated by FACS analysis and biochemically looking at the expression of cyclin A, used as marker of S phase entry. Data showed that no significant differences could be observed in the ability to enter into the cell cycle among the different mutants analyzed. In fact at 16 hours the percentage of S phase cells was 18%, 17%, and 16% for $p27^{WT}$, $p27^{T198E}$ and $p27^{T198V}$, respectively (Figure 8) coupled with a similar increase in the levels of the S phase marker cyclin A. Moreover, the levels of p27 expression at the same time points were not affected by the mutation of the T198, confirming the results obtained in exponentially growing cells (Figures 1 and 2).

It has been proposed that the T198A mutation results in a higher inhibition of CDK2 containing complexes (Kossatz et al., 2006). We thus tested whether or not T198A substitution could change the ability of p27 to bind CDK2- or CDK4-containing complexes and whether this effect could be related to the lack of T198 phosphorylation.

To this aim 3T3 p27 knock-out cells have been transduced with vectors encoding for $p27^{WT}$, $p27^{T198A}$, $p27^{T187\text{-}198A}$ or $p27^{T198V}$ and the exogenous proteins immunoprecipitated (Figure 9A). The amount of CDK2 and CDK4 bound to the different mutants was then evaluated and normalized respect to the amount of the immunoprecipitated protein (Figure 9B). Results show that T198A protein displays a 3 fold higher affinity for CDK2 respect to the WT one ($p< 0.01$), while the affinity for CDK4 was similar for all mutants ($p>0.05$) (Figure 9B), thus confirming the results obtained from others (Kossatz et al., 2006). However, an *in vitro* assay performed using either

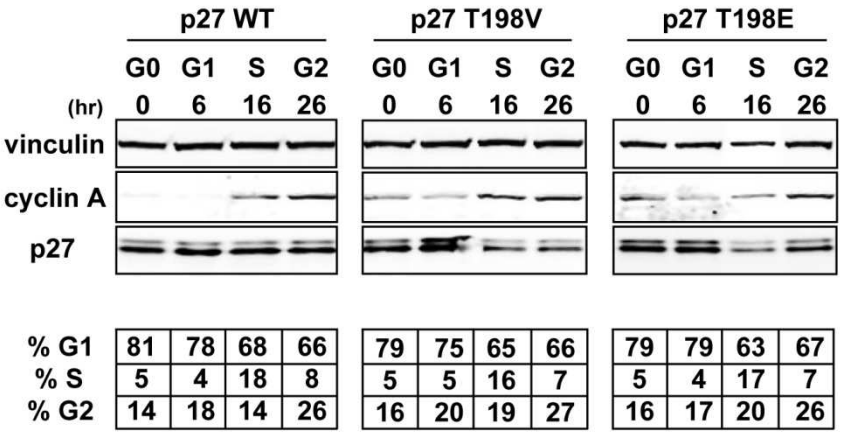

	p27 WT				p27 T198V				p27 T198E			
% G1	81	78	68	66	79	75	65	66	79	79	63	67
% S	5	4	18	8	5	5	16	7	5	4	17	7
% G2	14	18	14	26	16	20	19	27	16	17	20	26

Figure 8. The lack of p27 phosphorylation on T198 does not affect cell cycle progression. 3T3 p27KO fibroblasts were transduced with the indicated Ad ZsGreen p27s. 24 hr later cells were serum starved in DMEM 0,1% BSA for 24 hr and then released in complete medium. At the indicated time points cells were fixed and analyzed by flow cytometry for their DNA content and total cell protein extracts were prepared. Cyclin A and p27 levels are reported in the upper panels as evaluated by western blot analyses. Vinculin was used as loading control. The percentage of cells in G1, S and G2/M phases of the cell cycle at each time point is reported in the lower tables. Data represents the mean of three independent experiments.

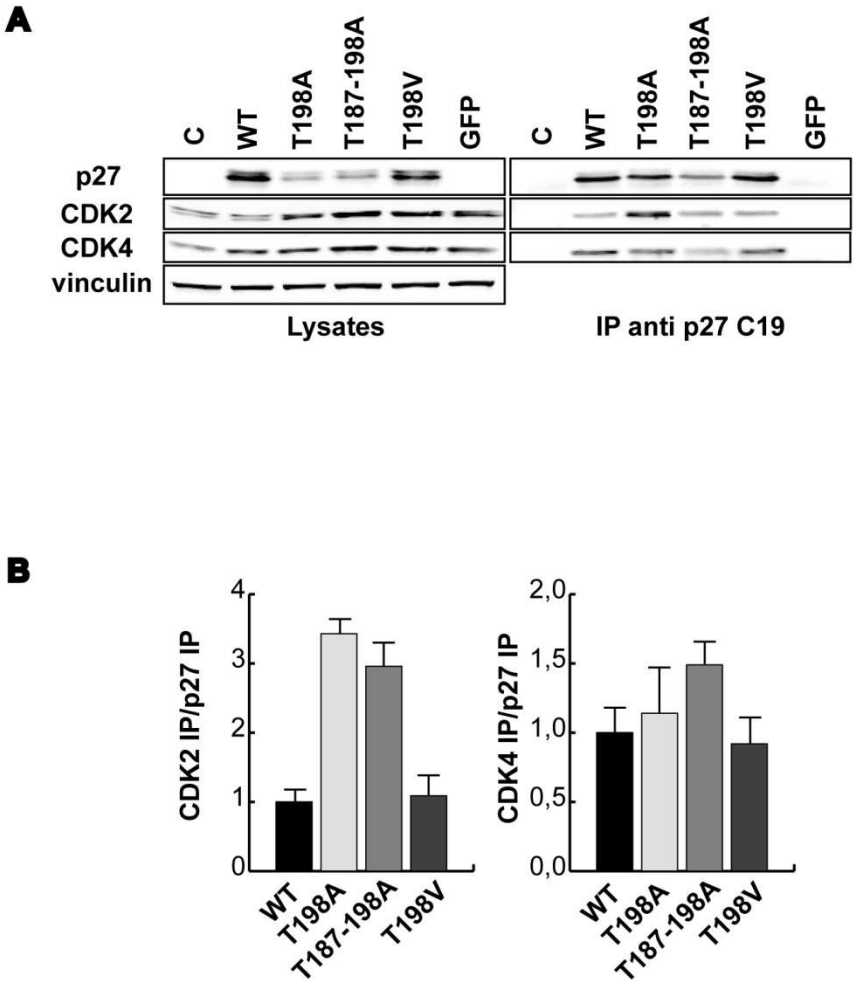

Figure 9. p27T198A and p27T187-198A bind CDK2 with high affinity. **A**. Immunoprecipitation analysis of 3T3 p27KO fibroblasts transduced with the indicated Ad ZsGreen p27 and lysed 48 hours post-transduction. IP and lysates were analyzed by western blot using anti-CDK2, anti-CDK4 and anti-p27 antibody. **B**. Quantification of p27/CDK2-4 interaction as evaluated by IP and western blot analysis. Data represents the mean value (± standard deviation) of three independent experiments and are expressed as fold increase respect to the p27WT/CDK binding value.

$CyclinA_2$/CDK2 or Cyclin D_1/CDK4 recombinant complexes, demonstrated that the ability of $p27^{WT}$, $p27^{T198A}$, $p27^{T198G}$, $p27^{T198D}$ or $p27^{T198V}$ recombinant proteins to inhibit the CDKs kinase activity was comparable in all mutants (Figures 10A and 10B). These data demonstrated that although the T198A mutation increased the ability of p27 to bind the CDK2 containing complexes it did not alter its ability to inhibit the kinase activity and that the effects observed with the T198A mutation cannot be related to the lack of T198 phosphorylation since the T198V and T198D mutants displayed an activity similar to that of the WT protein.

5. The T198 phosphorylation in p27 regulates cells motility

In the last years, a role in the regulation of cell motility has been proposed for p27. In particular, some studies reported a role for T198 phosphorylation in cell motility (Larrea et al., 2009). To avoid any possible misinterpretation due to the increased proteasomal degradation of $p27^{T198A}$, we compared the activity of $p27^{T198E}$ and $p27^{T198V}$ that have a similar expression and a similar half-life in our cell lines (Figures 1-4). We thus tested whether or not $p27^{WT}$, $p27^{T198E}$ or $p27^{T198V}$ proteins had any effect on the ECM-driven motility using different experimental settings. We already demonstrated that p27 is able to inhibit the motility of several human cancer cell lines, including HT-1080 fibrosarcoma cells (Figure 8 and Baldassarre et al., 2005) and U87MG (data not shown and Schiappacassi et al., 2008) in transwell migration assays. As already reported, the $p27^{1-170}$ deletion mutant did not affect the ability of these cells to respond to haptotactic stimuli (Figure 11 and Baldassarre et al., 2005; Schiappacassi et al., 2008; Berton et al., 2009). The use of $p27^{1-170}$, $p27^{T198E}$ or $p27^{T198V}$ revealed that the phosphorylation of T198 plays a role in the regulation ECM-driven motility. As shown in Figure 11A both $p27^{1-170}$ and $p27^{T198V}$ were unable to properly inhibit HT-1080 and U87MG cell migration through a FN-coated transwell while the pseudo-phosphorylated mutant $p27^{T198E}$ display an activity similar to the WT protein (Figure 11 and data not shown). To confirm these results we used video time-lapse microscopy to track the motility of p27-EGFP-fusion proteins expressing cells. In these conditions we have been able to look also at the subcellular localization of the transgene, during the migration. Thus, cells were transfected with EGFP-$p27^{T198E}$ or -$p27^{T198V}$ and 1 day later plated on FN-coated dishes and followed for 2 hours using a fluorescence-based time lapse analysis. Video time lapse coupled with cell tracking analyses demonstrated that the expression of EGFP-$p27^{T198V}$ both into the nucleus and into the cytoplasm did not interfere with the ability of U87MG cells to properly move on FN (Video S2 and Figure 11B). On the contrary, the expression of the T198E mutant in the cytoplasm (Video S3 and Figure 11B) but not in the nucleus (Video S4 and Figure 11B) almost completely blocked cell motility.

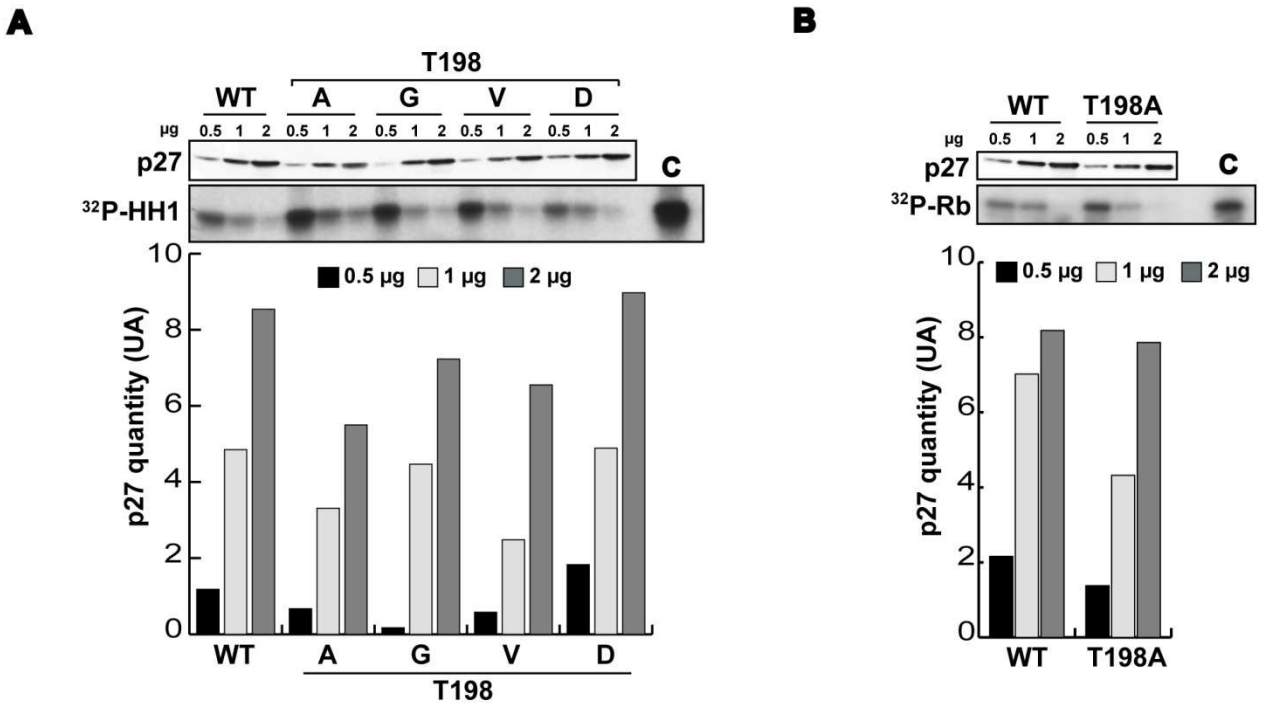

	% inhibition of CDK2 activity respect C				
protein amount (µg)	WT	A	G	V	D
0,5	90,23	63,25	66,83	75,75	89,79
1	96,01	94,47	97,04	95,97	96,41
2	99,28	97,04	99,15	99,18	98,85

	% inhibition of CDK4 activity respect C	
protein amount (µg)	WT	A
0,5	79,65	58,41
1	84,96	89,38
2	100,00	100,00

Figure 10. T198 substitution does not alter p27 ability to inhibit the CDK2/4 kinase activity. A. *In vitro* kinase assay of recombinant cyclin A2/CDK2 complex in the presence of increasing amounts (0.5, 1 and 2 µg) of recombinant His-tagged p27WT and mutants proteins as indicated using histone H1 as substrate. In the upper panel the expression of p27 in each reaction is shown. In the lower panel the phosphorylated Histone H1 is shown. A typical assay is reported. In the lower graph the amount of p27 proteins present in each reaction as evaluated by densitometric scanning of the blots is shown. In the lower table the percentage of kinase activity inhibition by the different p27 mutants respect to control kinase activity is reported. **B**. Same as in A using as kinase the recombinant cyclin D1/CDK4 complex and pRB fragment as substrate.

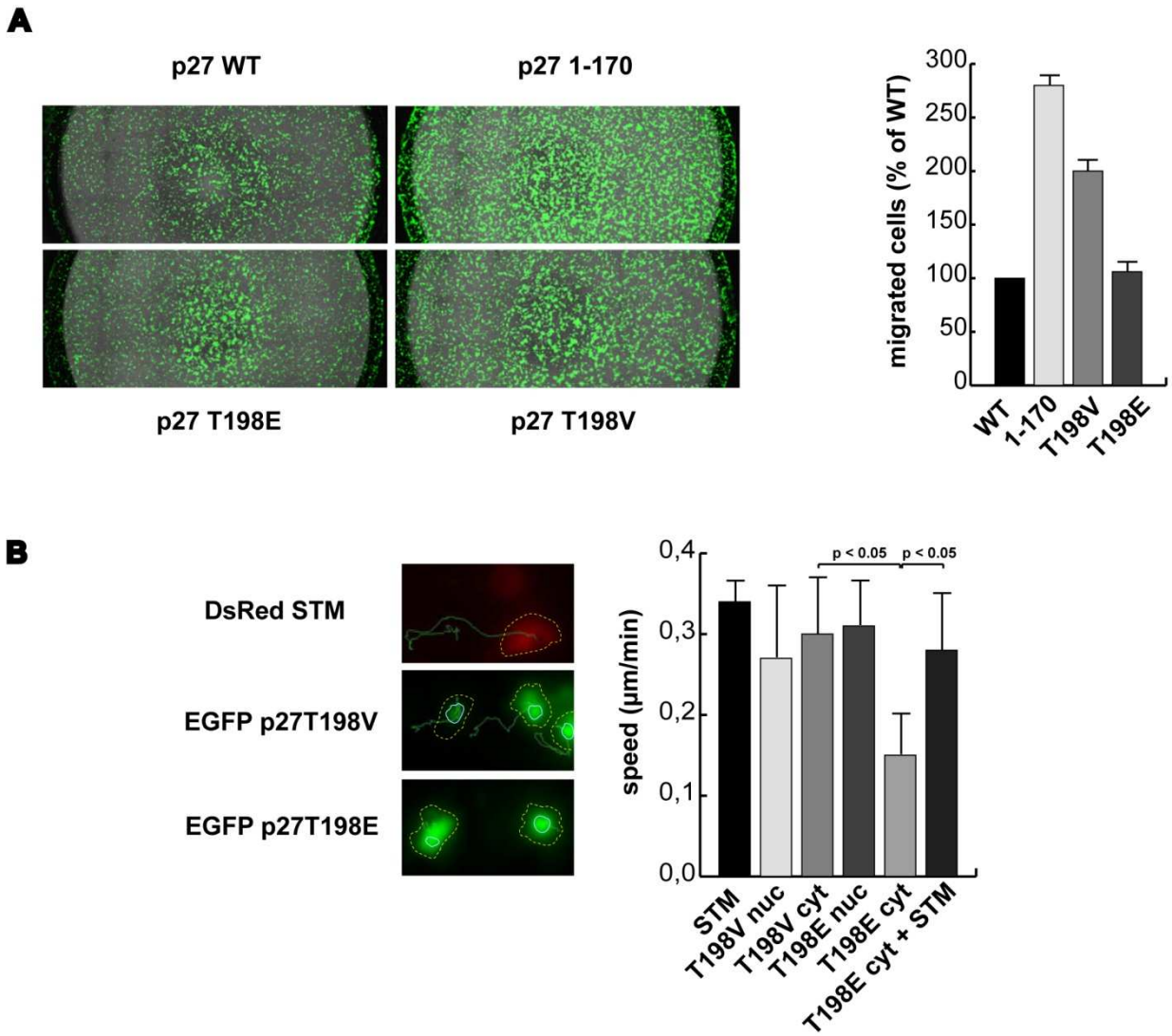

	% N	% C
WT	37	63
T198V	37	63
T198E	35	65

Figure 11. p27 T198 phosphorylation participates in the regulation of cell motility by p27. **A**. HT1080 cells were transduced with the indicated Ad Zs-green p27s and 24 hours later allowed to migrate on FN-coated Fluoroblok. A typical image of Fluoroblok bottom (Migrated cells) is shown. In the graph the quantification of migrated cells is reported. Results are expressed as fold induction respect to control cells. **B**. Orthotopical projection of cell paths of U87MG cells transfected with DsRed-Stathmin, EGFP-p27T198V and EGFP-p27T198E allowed to adhere on FN and followed for two hours (left). In the figures yellow dashed lines delimitate the cytoplasm and blue lines the nucleus positions at time 0. In the graph (right) the speed of the transfected cells is reported and represents the mean (±SD) of three independent experiments in which at least 10 cells/experiment were tracked. Statistical analysis was carried out using Mann-Whitney U-Test. **C**. Western blot analysis of p27 expression in nuclear/cytoplasmic extracts of HT1080 cells transfected with the indicated FLAG-p27 mutants and adhered 48 hr later on fibronectin for 1 h. Vinculin was used as control for cytoplasmic fractions and HMG2A as controls for nuclear fractions. **D**. Evaluation of EGFP-p27 localization in U87MG cells transfected with the indicated pEGFP-p27 vectors and adhered to FN for two hours. Data are expressed as percentage of cells with nuclear or cytoplasmic localization.

We also verified whether T198 phosphorylation may affect cell motility by favoring p27 nucleo-cytoplasm shuttling (Larrea et al., 2009). However, in our model system both time-lapse video-microscopy and western blot analyses did not confirm a primary role of T198 phosphorylation in the regulation of p27 subcellular localization following cell adhesion (Figure 11C).

The ability of p27 to modulate cell migration has been previously ascribed by its ability to bind other proteins more directly implicated in the regulation of cellular motility, namely RhoA and stathmin (Baldassarre et al., 2005; Schiappacassi et al., 2008; Berton et al., 2009). First we focused on the possible binding of p27 with the small GTPase RhoA that has been already reported to be influenced by the T198 phosphorylation (Larrea et al., 2009). To this purpose, we overexpressed in HT-1080 cells both GFP-RhoA and flag-tagged $p27^{WT}$, $p27^{1-170}$, $p27^{T198E}$ or $p27^{T198V}$ proteins and adhered them to FN for 1 hour. No detectable direct association between the two proteins was appreciable in our system (Figure 12A). Similarly, in cells adhered to FN for 1 hour we did not observe the binding of endogenous p27 and RhoA proteins (data not shown). It has been demonstrated that p27 C-terminal tail binds also the MT-destabilizing protein stathmin (Baldassarre et al., 2005; Schiappacassi et al., 2008; Berton et al., 2009). We thus speculated that T198 phosphorylation may favor this interaction in cells adhered to FN. Cells expressing $p27^{T198E}$ or $p27^{T198V}$ proteins, or the $p27^{1-170}$ deletion mutant both as untagged or EGFP-tagged proteins, were co-transfected with FLAG- or DS-Red-tagged stathmin vectors and then adhered to FN for 1 hour. Protein extracts have then been immunoprecipitated using either the anti-stathmin (Figure 12B) or the anti-p27 (Figure 12C) antibodies. Data unveiled that while the association between $p27^{T198E}$ and stathmin was readily detectable (Figure 9B and Figure 9C) the T198V mutation strongly impaired this association (Figure 12B and Figure 12C). As expected and already reported (Baldassarre et al., 2005; Schiappacassi et al., 2008; Berton et al., 2009), the deletion of the last 28 amino-acids almost completely prevented it (Figure 12C). Importantly, stathmin/p27 interaction was observed only in the cytosolic (Figure 12B) and not in the nuclear fraction (data not shown). To further prove that the interaction between p27 and stathmin plays a role in the control of adhesion dependent cell motility and that this interaction is, at least, in part regulated by T198 phosphorylation we co-expressed in U87MG cells the DsRed-stathmin and the EGFP-$p27^{T198E}$ protein. Cells were then allowed to adhere to FN coated plates and followed by video-time lapse microscopy. As shown in Figure 11B stathmin expression completely abrogated the ability of cytoplasmic $p27^{T198E}$ to inhibit cell motility (Figure 11B and Video S5). Moreover, the two proteins co-localize in the cytoplasm in response to cell-FN interaction as evaluated by time-lapse confocal video-microscopy (Video S6).

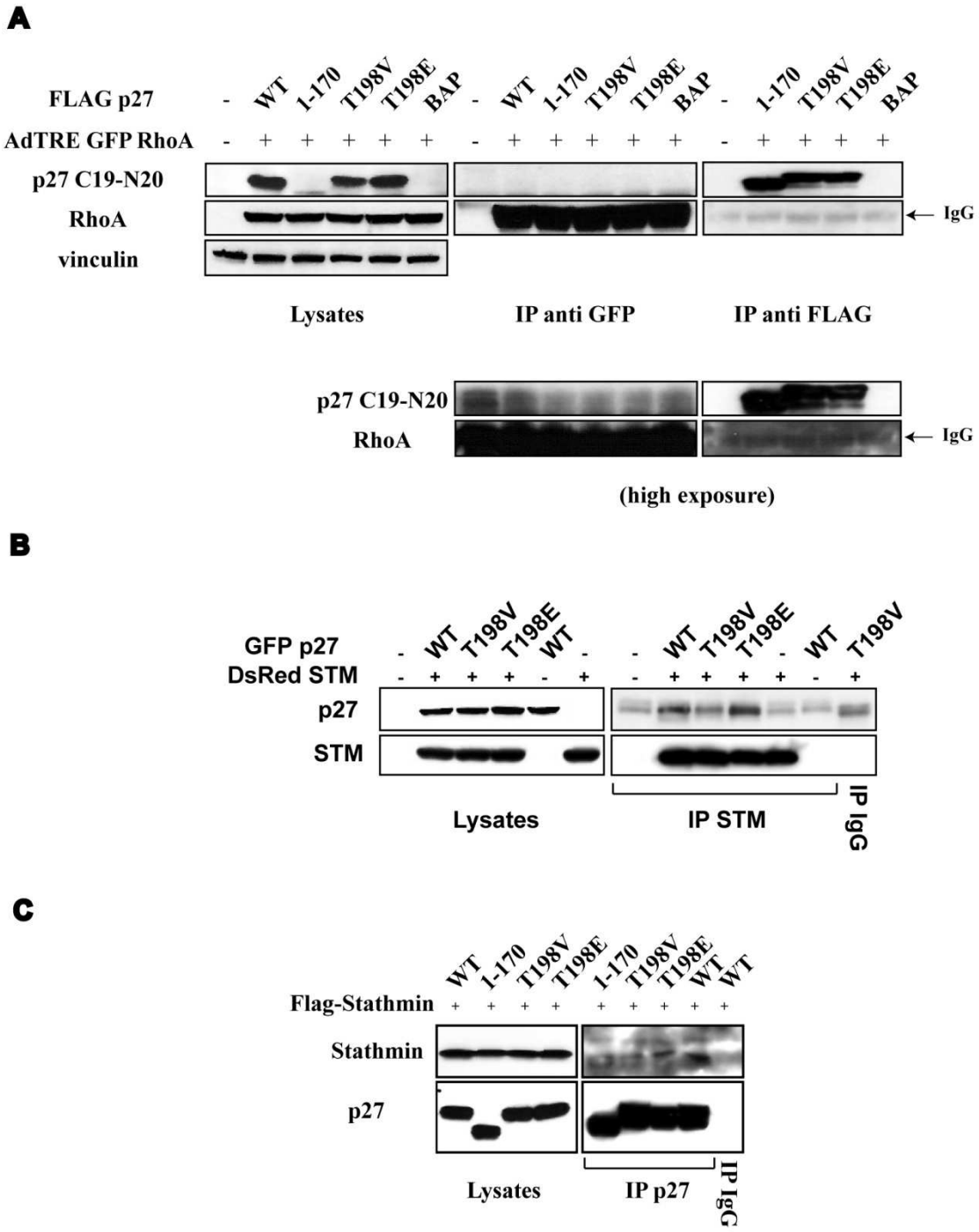

Figure 12. T198 phosphorylation favors p27 binding to stathmin. A. Immunoprecipitation (IP) analysis of HT1080 expressing FLAG-p27 and EGFP-RhoA proteins as indicated and adhered on FN for one hour. Total cell lysates and IP proteins were then evaluated by western blot analysis using anti-p27 and anti-Rho antibodies. IPs were performed using both an anti-GFP antibody and the FLAG-M2 affinity gel antibody. No co-precipitation was observed in both the conditions. **B**. IP analysis on cytoplasmic fractions of HT1080 expressing pEGFP-p27 mutants and DsRed-stathmin as indicated and adhered on FN for one hour. Cytosolic lysates and IP proteins were then evaluated by western blot analysis using anti-p27 and anti-stathmin antibodies. **C**. IP analysis of HT1080 expressing p27 and FLAG-tag stathmin proteins as indicated and adhered on FN for one hour. Total cell lysates and IP proteins were then evaluated by western blot analysis using anti-p27 and anti-stathmin antibodies.

Altogether these data demonstrated that T198 phosphorylation is an important event that may favor the p27/stathmin interaction eventually influencing ECM-driven cell motility.

6. p27 is predicted to have five possible SUMOylated sites contained in non-consensus SUMO sequences

How T198 modification could favor p27/stathmin interaction is still under investigation. Several interest was raised in the last years by a different reversible post-translational protein modification known as SUMOylation (**S**mall **U**biquitin-related **MO**difier). SUMOylation has been described to target unfolded proteins involved in microtubules stability such as tau (Dorval et al., 2006.) or the stathmin-related protein SCG10 (Gocke et al., 2005). Moreover, SUMOylation is involved in the regulation of protein stability, and localization usually favoring nuclear accumulation. We thus speculated that SUMOylation could be implicated in the regulation of p27 unfolded C-terminus and therefore in the regulation of its stability and localization. The role of SUMOylation in the regulation of p27 function is unknown, although it has been reported that inhbition of SUMO specific protease 1 (SENP1) results in increased p27 levels (Xu et al., 2011).

To examine whether p27 undergoes SUMOylation, we first performed an *in silico* analysis to predict possible SUMO-acceptor sites in p27. We used the SUMOplot™ analysis program (Abgent) which predicts and scores SUMOylation sites in the protein of interest. The SUMOplot™ score system is based on two criteria: direct aminoacid match to SUMO consensus sequence (Figure 13B) or by substitution of the consensus residues with aminoacids exhibiting similar hydrophobicity. p27 coding sequence which contains thirteen lysine residues (Figure 13A) was submitted to the prediction analysis. The result was that p27 contains five putative SUMO-acceptor sites: lysine 73 (score 0.67), 134 (score 0.61), 189 (score 0.50), 153 (score 0.48) and 190 (score 0.42) (Figure 13C). All these five lysine residues are contained in non-consensus SUMO sequences. In fact these acceptor sequences do not contain a large hydrophobic residue (aliphatic branched aminoacid) before the lysine residue and three out of the five sequences do not contain a glutamic/aspartic acid in the second position downstream the lysine residue. Only K73 and K134, which obtained the highest score, are followed by E/D residue (glutamic and aspartic acid, respectively) after the x residue (tyrosine and threonine, respectively). Moreover the downstream sequence of K73 and K134 suggests that these sites could represent a NSDM motif (negatively charged amino acid-dependent SUMOylation motif), in which negatively charged residues are found predominantly at positions +3–6 (Figure 13D). In fact in both sequences there are several glutamic or aspartic acid residues downstream K73 and K134.

A

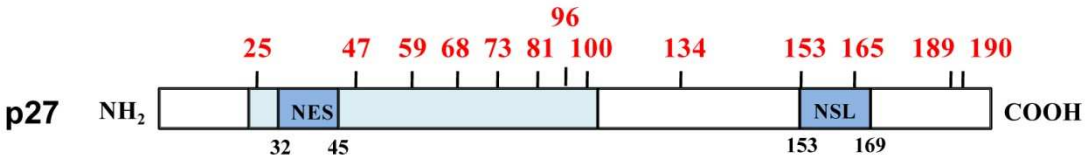

B

SUMO consensus sequence

ΨKxE/D

Ψ = large hydrophobic residue
K = Lysine
x = any residues
E/D = Glutamic or Aspartic Acid

C

SUMOplot™ Analysis Program (Abgent)

No.	Pos.	Group	Score
1	K73	HKPLE **GKYE** WQEVE	0.67
2	K134	THLVD **PKTD** PSDSQ	0.61
3	K189	SVEQT **PKKP** GLRRR	0.50
4	K153	QCAGI **RKRP** ATDDS	0.48
5	K190	VEQTP **KKPG** LRRRQ	0.42

D

NDSM (Negatively charged amino acid-Dependent SUMOylation Motif)

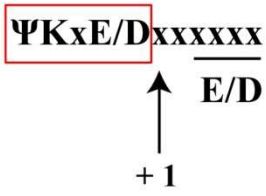

Figure 13. p27 is predicted to have five SUMOylation sites. **A**. Schematic representation of lysine residues in p27 molecule. **B**. A typical SUMO consensus acceptor site. **C**. p27 predicted SUMOylation sites and the corresponding obtained scores as resulted from SUMOplot program analysis. **D**. Representation of NSDM extended motif for SUMO conjugation.

7. p27 is covalently modified by SUMO 1 but not by SUMO 2/3

To determine whether p27 undergoes SUMOylation *in vitro* and if it could be linked to the presence of T198 and/or stathmin binding, we overexpressed Flag-p27 WT and a deleted form that lacks C-terminal domain (p27 1-170) in the presence or absence of HA-tagged SUMO 1 and SUMO 2 isoforms and untagged-Ubc9 in Phoenix 293 cells. Flag-p27 WT or 1-170 was immunoprecipitated, separated by SDS-PAGE and immunoblotted with anti-HA or anti-Flag antibodies (Figure 14A). Two slower-migrating form of p27 WT, which were immunoreactive with the anti-HA Ab, were detected only when SUMO1 is overexpressed, indicating SUMO 1 modification of p27. In particular one slower-migrating p27 has about 45 KDa-weight and the signal seemed to be constituted by double bands, and the other slow-migrating p27 was detected at about 62 KDa (Figure 14A left panel). p27 1-170 was also modified by SUMO 1 and not by SUMO 2 as demonstrated by the presence of the same two slower-migrating forms with a shift in the molecular weight proportional to that of the WT protein (Figure 14A left panel). The shift in the molecular weight was detected also in the lysates blotted with anti Flag Ab (Figure 14A right panel).

Because only one SUMO 1 can be linked to a lysine residue, the presence of two higher-weight p27 forms (with ~18 KDa and ~36 KDa increase in size, respectively) and the double bands-signal at 45 KDa suggested that p27 could be mono-SUMOylated on two lysine residues. To evaluate which region of the p27 molecule contains the two lysines we transfected 293 cells with or without HA-SUMO 1 and untagged Ubc9 together with three p27 deleted mutants: p27 42-85, p27 42-154 and p27 78-198. Lysates were subjected to immunoprecipitation with anti-Flag M2 affinity gel, followed by western blotting with anti-HA or anti-Flag antibodies to detect SUMOylated p27 (Figure 14B). Only when SUMO 1 and Ubc9 were overexpressed the three deleted p27 exhibited the two slower-migrating forms (recognized by both the anti-HA and the anti-Flag) which had an increase of ~18KDa and ~36 KDa, respectively, as for the WT protein.

However, while the signal at 45KDa was a double band for p27 42-154 and for p27 WT, p27 42-85 and p27 78-198 displayed a single band, indicating that these deleted forms have only one of the two target lysines (Figure 14B and Figure 15). We thus speculated that the SUMO-modified lysines had to be located in the 42-154 region which contains nine lysine residues (K47, K59, K68, K73, K81, K96, K100, K134, and K153) and, in particular, one site should be located in the region comprised between aa 42-85 and the other in the portion between aa 78-198.

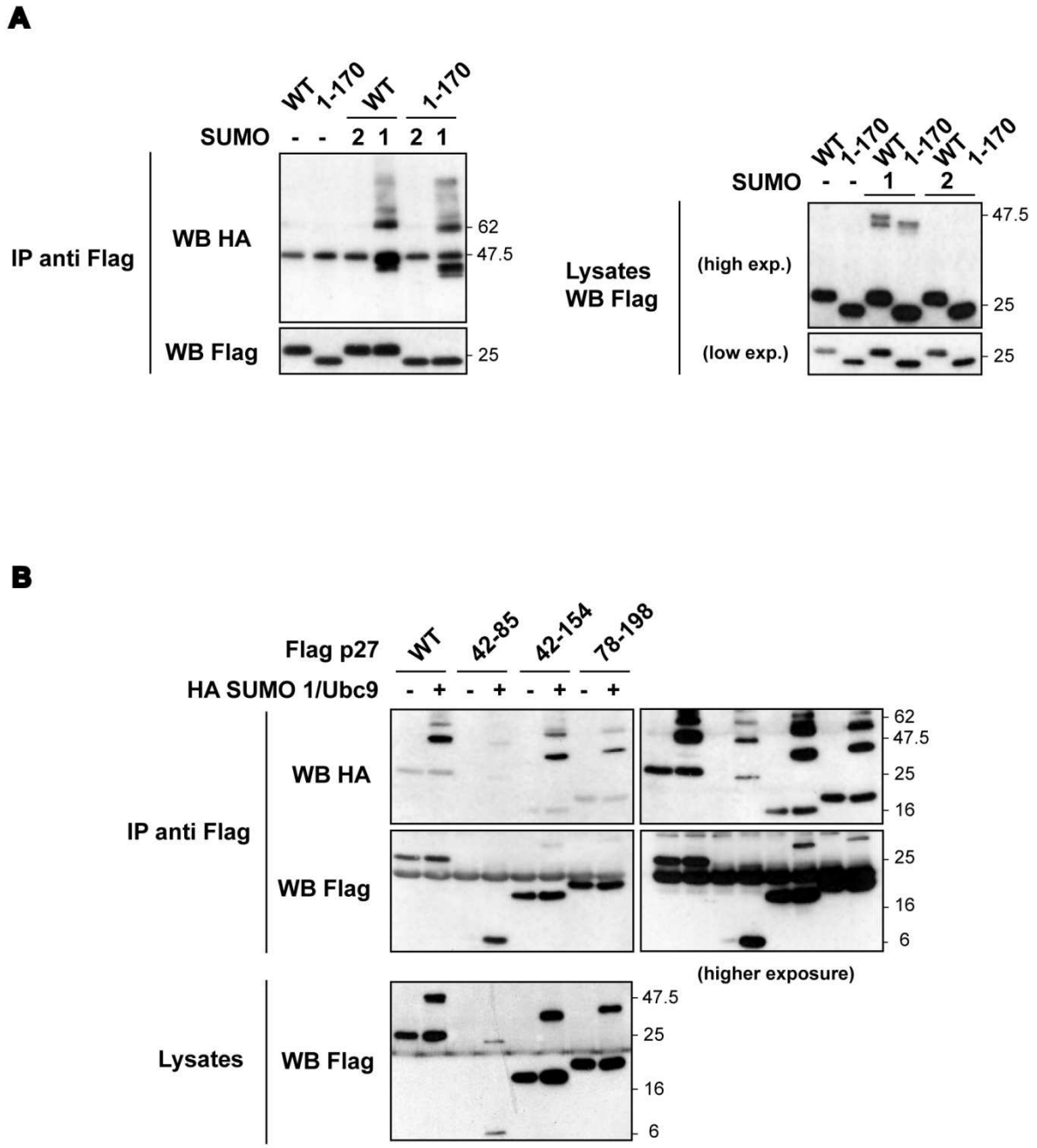

Figure 14. p27 is SUMOylated *in vitro*. **A**. Lysates of Phoenix-293 cells, overexpressing Flag-p27 WT or 1-170 together with untagged Ubc9 and HA-SUMO 1 or HA-SUMO 2, were subjected to immunoprecipitation (IP) with anti-Flag antibody, followed by western blotting with anti-HA or anti-Flag to detect SUMOylated p27. **B**. Phoenix-293 cells were transfected with Flag-p27 42-85, 42-154 or 78-198 deleted mutants together with HA-SUMO 1 and untagged Ubc9 and 48 hrs later lysates were subjected to immunoprecipitation with anti-Flag antibody, followed by western blotting with anti-HA or anti-Flag antibodies.

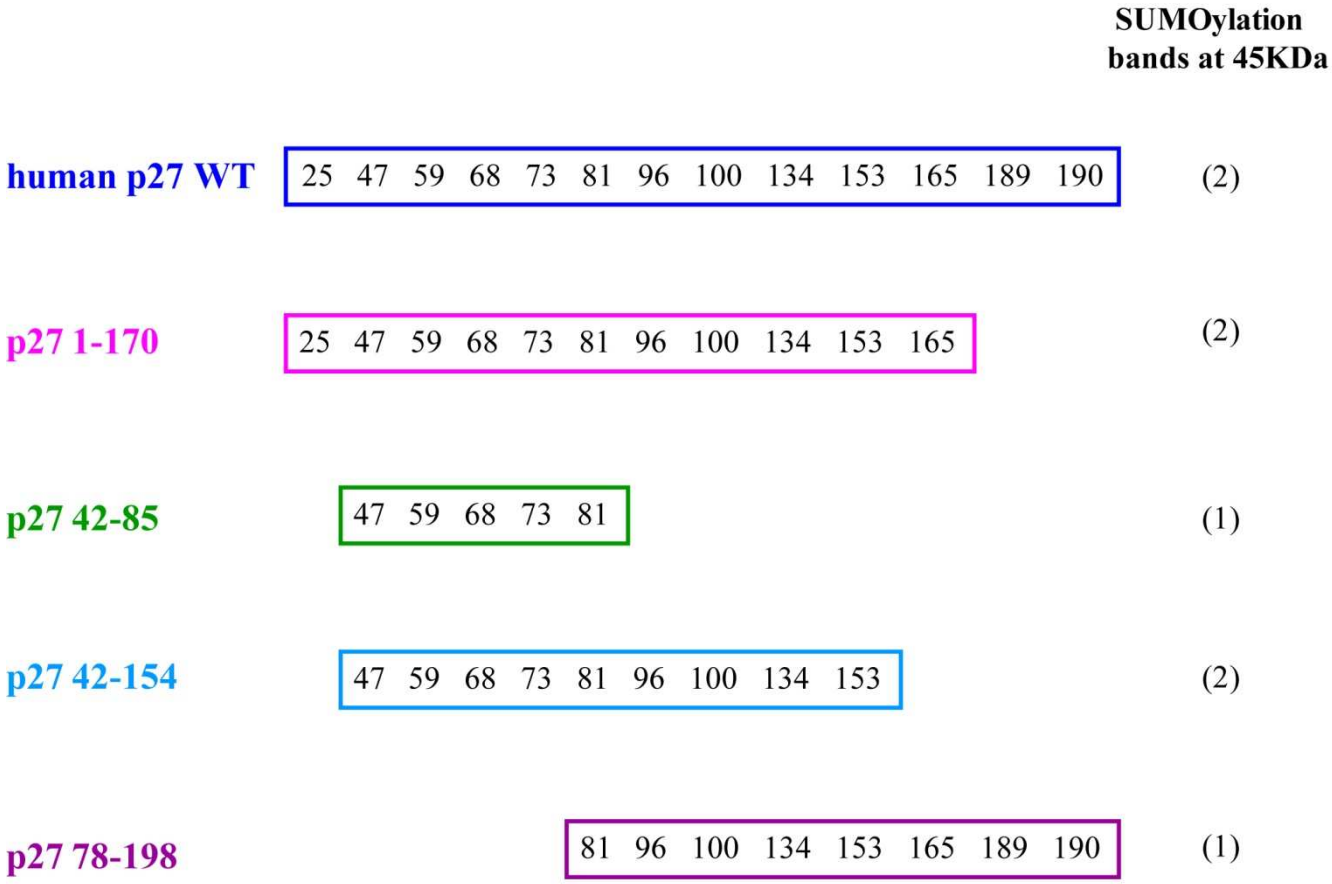

Figure 15. p27 SUMO-acceptor sites have to be comprised in the 42-154 region. Schematic representation of the lysine residues contained in p27 WT compared to 1-170, 42-85, 42-154 and 78-198 deleted p27 fragments, and the number of SUMOylation bands detected at ~45 KDa molecular weight.

8. p27 is SUMOylated *in vitro* on lysine 134

To identify p27 SUMOylated residues we combined the results obtained from the analysis of the deleted mutants with the results coming from the prediction analysis by SUMOplot™ program and we decided to begin with the analysis of lysine 73 and lysine 134. In fact these two residues have been predicted to be SUMOylated sites with the highest score and they are comprised in the region that we speculated to contain the p27 SUMO acceptor sites. To this purpose we generated K73R, K134R and the double K73-134R p27 mutants by site-directed mutagenesis and we transfected 293 cells with these Flag-tagged constructs, in the presence or absence of HA-SUMO 1 and untagged Ubc9. To analyze SUMOylated p27 we immunoprecipitated p27 with anti-Flag M2 affinity gel and probed the western blot with anti HA antibody. As shown in figure 16A, p27 K73R is SUMOylated as the WT protein since it retained all the three bands (the double at ~45KDa and the single at 62 KDa). Instead $p27^{K134R}$ has one SUMOylated band less than p27WT: in fact we did not detect a double SUMOylation band at ~45 KDa as the lower signal completely disappeared. In the same way also p27 K73-134R presented a single 45KDa SUMOylation band. All the three mutants preserved the slower migrating form of 62 KDa, even if the signal is slightly decreased for the mutants with K134R substitution. We also analyzed whether mouse p27 could be SUMOylated. We observed that mouse p27 is SUMOylated as human p27 since we detected the same SUMOylation bands as for the human protein (Figure 16A). We then tried to find out which could be the second site of SUMOylation and we focused our attention on lysine residues that where upstream K134 and comprised between aa 42 and 85, considering that this deleted p27 mutant conserved one SUMOylation band at 45 KDa. We thus generated K/R point mutations on residues 47, 59 and 68, alone or in combination with K134R substitution, we transfected 293 cells together with HA-SUMO 1 and Ubc9 and we immunoprecipitated p27 to analyze its SUMOylation with anti-HA antibody. All this point mutants were SUMOylated as they retained the 45 KDa-weight double signals, whereas the double mutants displayed only one SUMOylation band and have the 62 KDa-signal almost completely abolished as well as single K134R mutant (Figure 16B). Based on the result that we previously obtained with the p27 fragment 42-85 (Figure 14B), which was shown to be mono-SUMOylated, and considering that we have mutated four out of the five lysines contained in this region, we hypothesized that p27 could be SUMOylated on lysine 81. By mutating K81 we were not able again to completely abolish p27 SUMOylation (Figure 16C). We thus suggested that the mono-SUMOylated signal observed for the p27 42-85 fragment could be an artifact due to the fact that this small deleted fragment could not be representative of the entire molecule. To detect the second modified site we decided to mutate all the lysine residues, also those that we initially excluded by the analysis of the p27 deleted mutants. We generated K/R substitution

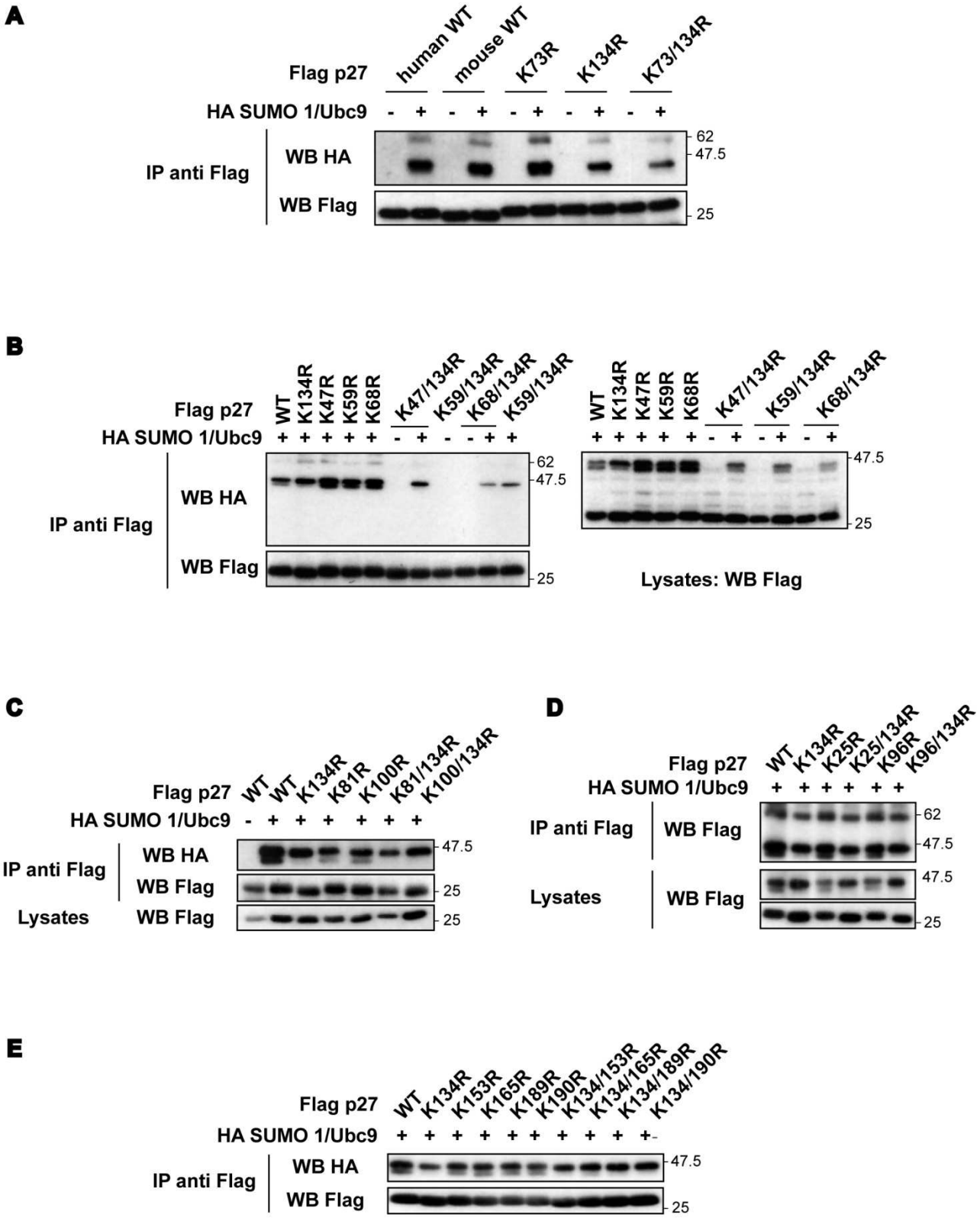

Figure 16. p27 is SUMOylated *in vitro* on lysine 134. **A-E**. Lysates of Phoenix-293 cells, overexpressing HA-SUMO 1, untagged Ubc9, Flag-tagged human and mouse p27 and the indicated p27 K/R mutants, were subjected to immunoprecipitation (IP) with anti-Flag antibody, followed by western blotting with anti-HA or anti-Flag to detect SUMOylated p27.

of lysine 25 (which was excluded by the analysis of both p27 42-85 and 42-154) (Figure 16D), lysine 96 and 100 (Figure 16C and 16D), lysine 153 and 165 (excluded by the analysis of p27 78-198) and lysine 189 and 190 (excluded by the analysis of p27 1-170) (Figure 16E). For all these mutants we obtained the same result that is a double SUMOylation band as for the WT protein and a mono-SUMOylation signal when the K/R substitution of these residues was combined with the K134R mutation. Taking together these experiments clearly demonstrated that p27 is SUMOylated *in vitro* by SUMO 1. Although the increase in molecular weight seems to indicate that p27 is mono-SUMOylated on two lysine residues, our results indicated that lysine 134 is definitely a site of SUMOylation but we were not able to identify other SUMOylated residues (Figure 17).

9. p27 SUMOylation affects protein stability

It is well known that SUMOylation could dictate different fates to its target protein. It could affect protein stability, localization, interaction with binding partners and degradation. We therefore investigated whether SUMOylation could influence p27 stability and we tested this hypothesis in a condition that it is well known to increase p27 stability that is serum starvation. HT1080 cells transfected with Flag-p27 WT or K134R mutant were starved for 24 hrs and then treated with cycloheximide (10 µg/ml) for different times to evaluate protein stability. As shown in Figure 18, the un-SUMOylable K134R mutant displayed a decreased stability respect p27 WT which is evident just 3 hours after the inhibition of its synthesis. No difference in the stability of the K134 mutant respect the wild-type protein was detected in exponentially growing condition (data not shown). This result indicated that SUMOylation participates in the regulation of p27 stability in response to serum-starvation. Moreover the fact that the accelerated degradation was evident after 3 hrs could indicate that this modification is an important early event in the regulation of p27 stability during growth factor deprivation.

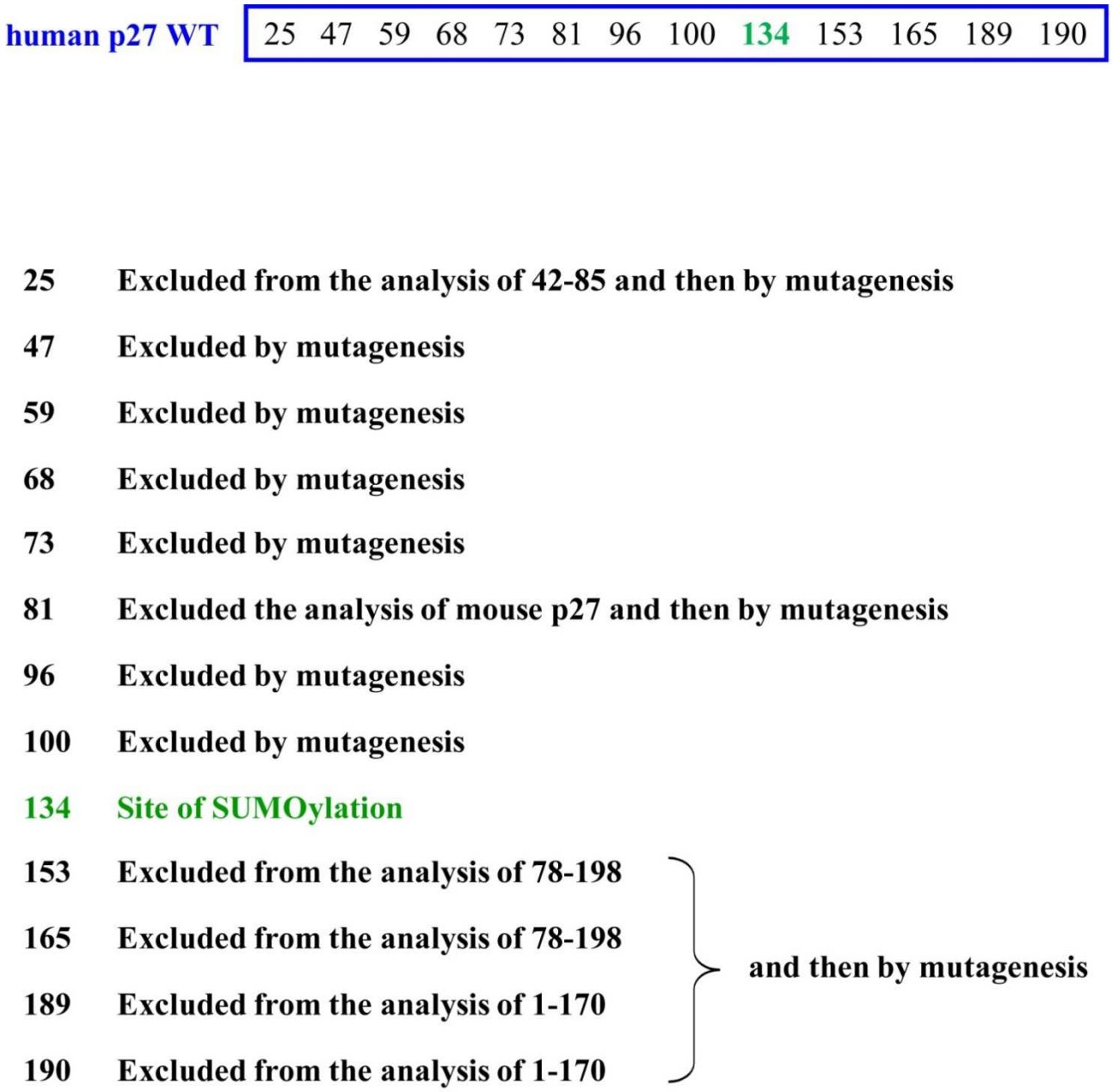

Figure 17. Lysine 134 is the only SUMO-modified p27 residue. Summary of the results obtained from the analysis of p27 lysine residues. Site-directed mutagenesis was performed on all the thirteen residues to evaluate their involvement in p27 SUMOylation, also those initially excluded by the analysis of the deleted mutants. From this analysis the only confirmed SUMO acceptor site is lysine 134.

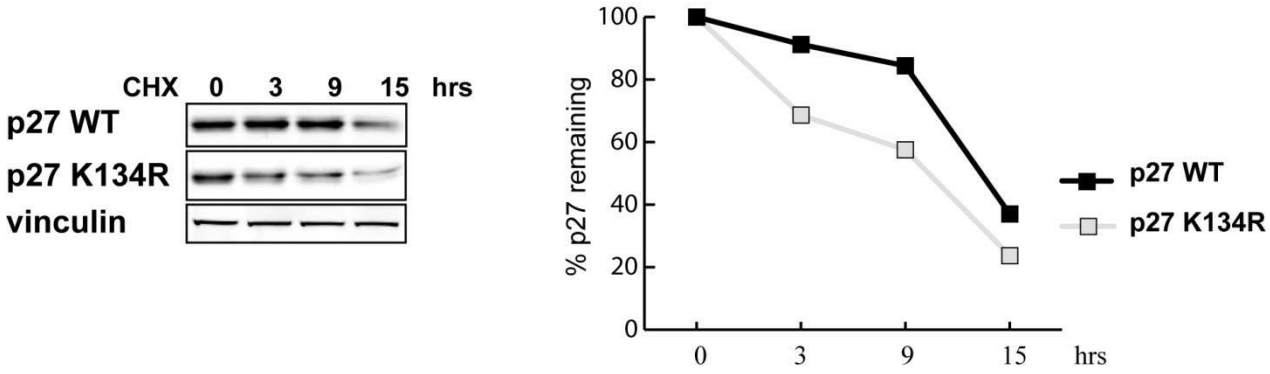

Figure 18. K134R substitution decreases p27 protein stability. Western Blot analysis of p27 expression in HT1080 cells transfected with p27 WT and K134R mutant and 48 hrs later treated with cycloheximide (CHX) for 3, 9 and 15 hrs. The densitometric analysis of the bands of a representative experiment is reported in the graph (right) and is expressed as percentage of remaining protein respect to untreated cells.

10. TGFβ increases p27 SUMOylation

The notions that SUMOlatyon is often associated with the regulation of protein stability and nuclear localization along with the collected data indicating that SUMOylation could be a signal necessary to increase p27 protein stability after serum starvation, raised the possibility that p27 SUMOylation is an important modification able to dictate its stability and nuclear accumulation following anti-mitogenic stimuli.

One of the most important and studied stimulus able to increase p27 stability and nuclear localization is the growth factor TGFβ (Lecanda et al., 2009). We thus tested whether TGFβ could represent a signal able to stimulate p27 SUMOylation. To this aim we transfected HeLa cells, that is a well known model system to study TGFβ signaling, with Flag-p27, HA-SUMO 1 and untagged Ubc9 and 48 hours later cells were treated or not with human recombinant TGFβ (20 ng/ml) for 5 hours. Lysates were then collected and p27 was immunoprecipitated to analyze the SUMO-modified levels. We observed that TGFβ signaling, whose activation was demonstrated by the phosphorylation of its downstream effector Smad2 (Figure 19A, right panel), induced an increase in the levels of p27 SUMOylation, as demonstrated by the greater intensity of the higher-molecular weight bands immunoreactive for both HA and p27 antibodies (Figure 19, left panel). Next we also verified whether the effect of TGFβ on p27 SUMOylation was time-dependent. Therefore we performed a time-course analysis treating HeLa cells overexpressing p27, SUMO and Ubc9 with TGFβ for 3 or 5 hours. Using this approach we found that TGFβ-induced increase of p27 SUMOylation was already evident after 3 hours of treatment (Figure 19B).

Next we compared SUMOylation level of p27 WT with that of K134R mutant in response to TGFβ to confirm that its effect on p27 specifically involved this post-translational modification. HeLa cells transfected with Flag-p27 WT or K134R together with HA-SUMO 1 and UBC9 where treated 48 hrs later with recombinant TGFβ for 3 hrs and then subjected to immunoprecipitation with anti-Flag resin. As shown in Figure 20, TGFβ treatment increased p27 SUMOylation (see the lower band detected with anti SUMO 1 antibody) whereas no SUMO-modified band was detected for K134R mutant both in presence or absence of TGFβ. Collectively these results indicated that TGFβ stimulation is able to increase p27 SUMOylation.

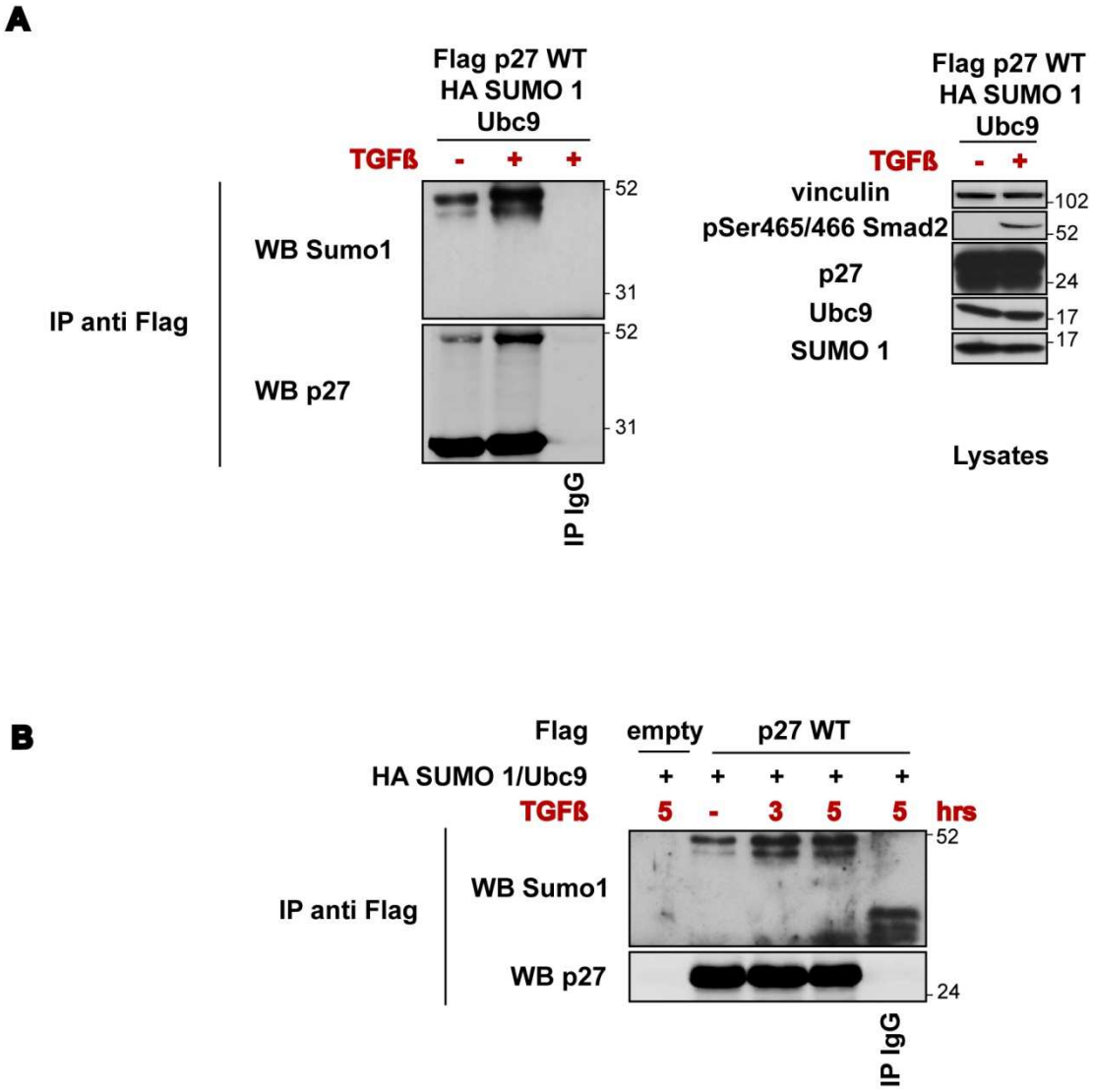

Figure 19. TGFβ increases p27 SUMOylation. **A**. HeLa cells were transfected with Flag-p27 WT, HA-SUMO 1 and untagged Ubc9 and 48 hrs later treated or not with human recombinant TGFβ (20 ng/ml) for 5 hrs. Lysates were then subjected to immunoprecipitation with anti-flag antibody and western blot analysis of IPs (left) and total lysates (right) was performed with both SUMO 1 and monoclonal p27 antibodies to detect p27 SUMOylation. Phosphorylated Smad 2 on serine 465/466 was used as marker of TGFβ signaling activation and vinculin was used as the loading control. **B**. IP analysis of HeLa cells transfected as in A and treated with TGFβ (20 ng/ml) for 3 and 5 hrs. SUMOylated p27 was evaluated by western blot analysis using anti-SUMO 1 and anti p27 antibodies.

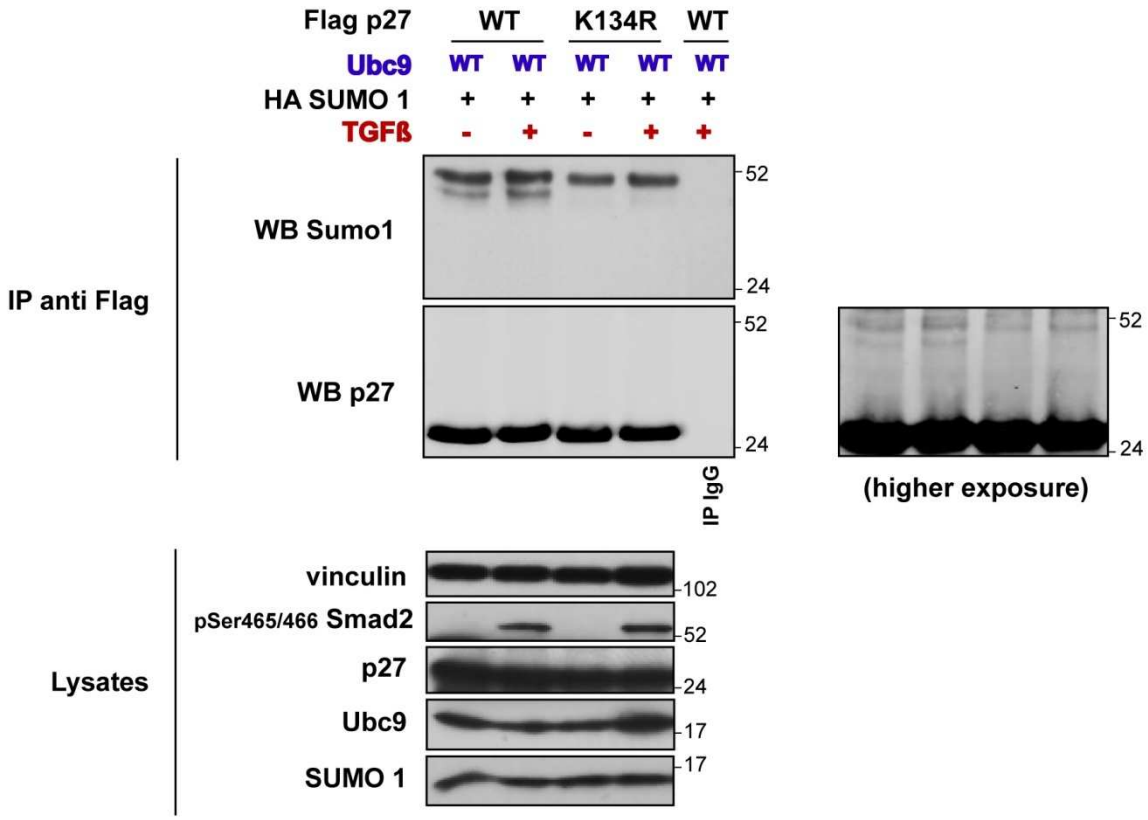

Figure 20. TGFβ induces an increase of p27 WT SUMOylation but not on p27 K134R. HeLa cells were transfected with Flag-p27 WT or K134R mutant together with HA-SUMO 1 and untagged Ubc9 WT. 48 hrs later cells were treated or not withTGFβ (20 ng/ml) for 3 hrs and then lysates were subjected to immunoprecipitation with anti-flag antibody. Total cell lysates and IPs were analyzed by western blot using SUMO 1 and monoclonal p27 antibody. Phosphorylated Smad 2 on serine 465/466 was used as marker of TGFβ signaling activation and vinculin was used as the loading control.

11. Endogenous p27 colocalizes with SUMO 1 in the nucleus and its nuclear localization is increased by TGFβ

As mentioned before, it has been demonstrated that TGFβ accumulates nuclear p27 by preventing its degradation to mediate cell cycle arrest in late G1. Considering this effect we asked whether p27 SUMOylation induced by TGFβ could affect p27 localization. To answer this question we decided to use MCF-7 breast adenocarcinoma cell line which presents high level of endogenous p27 and which has been demonstrated to respond to TGFβ signaling with p27 nuclear accumulation (Donovan et al., 2002). Cells treated with TGFβ (20 ng/ml) for 3 hrs were subjected to both immunofluorescence and nucleus/cytoplasm differential protein extraction to evaluate p27 localization. According to literature p27 translocated into the nucleus of MCF-7 treated cells and its nuclear accumulation was appreciable after 1 hour treatment, as demonstrated by nuclear localization after immunofluorescence staining (Figure 21A, yellow arrow), and became evident after 3 hrs treatment as shown by the increase of p27 amount in the nuclear protein fraction (Figure 21C). In the same experiment we also looked at SUMO 1 localization. We found that SUMO 1 is predominantly located in the nucleus of MCF-7 cells (Figure 21A) and in particular it seemed to be localized in specific nuclear regions, as we detected several small brilliant red dots in the nucleus that resemble PML-nuclear bodies (Figure 21B, yellow arrow). By the use of confocal microscopy analysis we were able to detect co-localization between endogenous p27 and endogenous SUMO 1 after TGFβ treatment. It is worth to note that we detected p27-SUMO 1 co-localization after TGFβ treatment just in the nuclear regions where SUMO 1 is accumulated.

Therefore these results confirmed p27 nuclear accumulation induced by TGFβ and showed for the first time an endogenous colocalization between p27 and SUMO 1 in the nucleus. Considering that we have detected the co-localization after TGFβ stimulation we hypothesized that TGFβ could affect p27 localization regulating its SUMOylation.

12. SUMOylation affects p27 localization in response to TGFβ

Taking into account the previous results we next assessed whether SUMOylation could affect p27 localization in response to TGFβ. To this aim HeLa cells were transfected with GFP-p27 WT or K134R together with HA-SUMO 1 and Ubc9 and 48 hrs later treated with TGFβ for 30 minutes, 1 hour or 3 hours. Cells were then fixed and subjected to immunofluorescence (Figure 22A). 10 fields per condition were counted for nuclear and cytoplasmatic p27 localization and results were expressed as percentage respect to the total number of cells overexpressing p27. As reported in the table (Figure 22B) in untreated cells p27 WT was distributed in the same amount between nuclear and cytoplasmic compartment as well as $p27^{K134R}$ mutant (47% nucleus and 53%

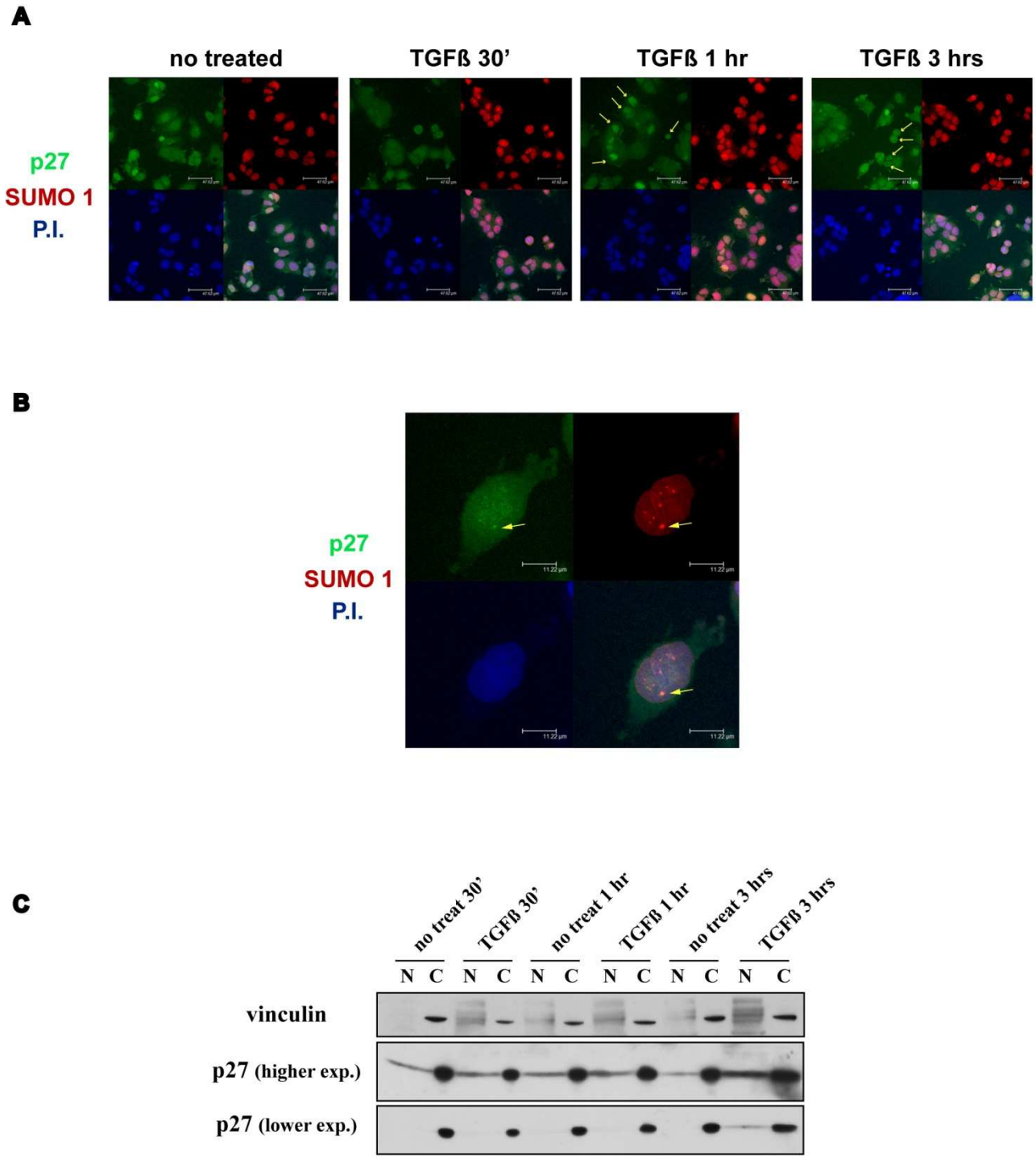

Figure 21. Endogenous p27 colocalizes with SUMO 1 in the nucleus and its nuclear localization is increased by TGFβ. MCF-7 cells were treated or not with TGFβ (20 ng/ml) for 30 minutes, 1 or 3 hrs to analyze p27 and SUMO 1 nucleus/cytoplasm distribution. **A**. Immunofluorescence analysis of endogenous p27 (green), SUMO 1 (red) and nuclei (blue). Yellow arrows indicate p27 nuclear accumulation. **B**. Confocal images at higher magnification. Yellow arrows indicate p27 and SUMO 1 nuclear co-localization. **C**. western blot analysis of nuclear and cytoplasmic extracts was performed with monoclonal p27 antibody and using vinculin as marker of cytoplasm.

cytoplasm for WT, 46% nucleus and 54% cytoplasm for K134R). When cells were treated with TGFβ, not significant difference in the p27 localization, both WT and K134R, was noted after the first hour of treatment. However after 3 hours p27 WT strongly accumulated in the nucleus (73% nuclear vs 27% cytoplasmic) while $p27^{K134R}$ was not able to shuttle into the nucleus, as demonstrated by the fact that its nucleus-cytoplasm distribution did not change after TGFβ stimulation. This result indicates that SUMOylation affects p27 ability to translocate into the nucleus in response to TGFβ stimulus as the un-SUMOylable mutant $p27^{K134R}$ did not accumulate in the nucleus as well as WT protein after 3 hrs TGFβ treatment.

A

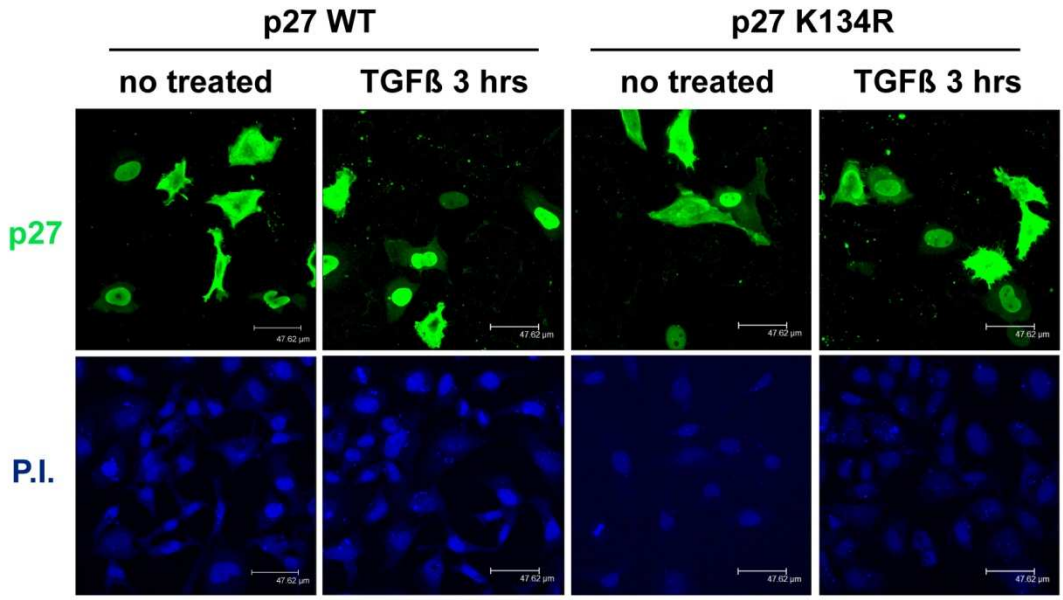

B

	WT		K134R	
	% N	% C	% N	% C
no treat	47	53	46	54
TGFß 30'	46	54	47	53
TGFß 1 hr	48	52	49	51
TGFß 3 hrs	73	27	46	54

Figure 22. p27 WT but not the SUMO-defective K134R mutant is able to translocate into the nucleus in response to TGFβ. **A**. Immunofluorescence analysis of p27 (green) in HeLa cells transfected with HA-SUMO 1, untagged Ubc9 and GFP-p27 WT or K134R mutant and 48 hrs later treated with TGFβ (20 ng/ml) for 3 hrs. Nuclear staining performed with propidium iodide is also shown. **B**. 10 fields per condition were counted for nuclear and cytoplasmatic p27 localization in HeLa cells described in A. Results were expressed as percentage respect the total amount of cells overexpressing p27.

SUPPORTING VIDEOS LEGENDS

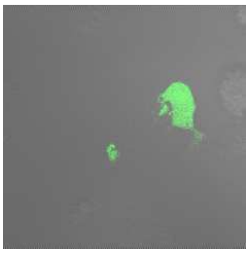

Video S1: video time-lapse of U87MG cells transfected with EGFP $p27^{WT}$ and adhered on FN for 2 hours. $p27^{WT}$ was able to stimulate the formation of neuron-like protrusions and localizes in the protrusions.

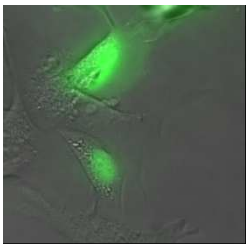

Video S2: video time-lapse of U87MG cells transfected with EGFP $p27^{T198V}$ and adhered on FN for 2 hours. Expression of $p27^{T198V}$ both in the nucleus and in the cytoplasm did not interfere with the ability of U87MG cells to properly move on FN.

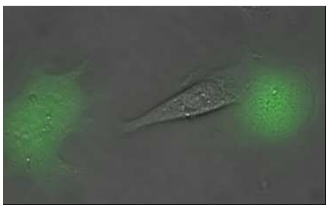

Video S3: video time-lapse of U87MG cells transfected with EGFP $p27^{T198E}$ and adhered on FN for 2 hours. Expression of the T198E mutant into the cytoplasm almost completely blocked cell motility.

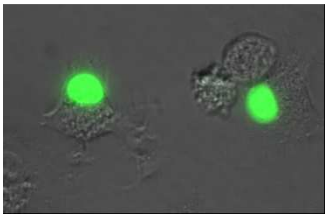

Video S4: video time-lapse of U87MG cells transfected with EGFP $p27^{T198E}$ and adhered on FN for 2 hours. Expression of the T198E mutant into the nucleus did not interfere with U87MG motility.

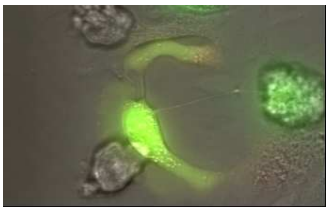

Video S5: video time-lapse of U87MG cells cotransfected with EGFP $p27^{T198E}$ and with DsRed Stathmin and adhered on FN for 2 hours. Stathmin expression completely abrogated the ability of cytoplasmic $p27^{T198E}$ to inhibit cell motility.

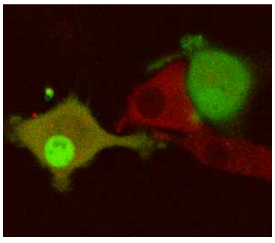

Video S6: time lapse confocal video microscopy of U87MG co-transfected with EGFP $p27^{T198E}$ and with DsRed Stathmin in adhesion on FN for 2 hs. Yellow dots represented the colocalization of $p27^{T198E}$ (green) and stathmin (red) in response to cell-FN interaction. Cells expressing only stathmin (red) or p27 (green) are also present in the field. A single confocal plane was taken during the experiment.

DISCUSSION

The role of post-translational modifications in the regulation of p27 functions was investigated in this PhD thesis, trying to evaluate how they could contribute to its deregulation in cancer progression. We studied two different p27 post-translational modifications, namely the significance of T198 phosphorylation and SUMOylation. These two aspects will be discussed separately.

1. The roles of T198 in the regulation of p27 functions

By studying the effects of $p27^{WT}$ protein on the regulation of glioblastoma cell growth and motility we observed that the WT protein was able to stimulate the formation of neuron like protrusions in U87MG cells, thus confirming our previous observation that p27 is able to control protrusion formation in 3D context (Belletti et al., 2010), also in glioblastomas. Further data demonstrated that p27 stimulated protrusion formation in U87MG cells through its C-terminal tail, since the deleted mutant $p27^{1-170}$ was ineffective (Schiappacassi and Lovisa et al., 2011). To better understand the mechanism of regulation of cell shape and motility by p27, we generated specific point mutants in T187 and T198 residues, which are comprised among amino-acids 170 and 198 and have been proposed to have a role in the regulation of p27 protein. In fact threonine 187 plays a fundamental role in CDK-mediated Skp2-dependent proteasomal degradation of p27 (Tsvetkov et al., 1999) and phosphorylation of threonine 198 by several kinases has been linked to p27 dislocation in the cytoplasm (Fujita et al., 2002 and 2003; Motti et al., 2004), cell motility (Larrea et al., 2009) and protein stability (Liang et al. 2007, Kossatz et al. 2006).

First, we generated a $p27^{T198A}$ non-phosphorylable mutant to verify whether or not the modification of p27 last amino-acid had any role in morphological and motility phenotypes of glioblastoma cell lines and we observed that the T198A mutation resulted in a strong abrogation of p27 protein expression as reported by others (Kossatz et al., 2006; Liang et al., 2007).

Several approaches (semi-quantitative RT-PCR, Real-time PCR and *in vitro* transcription and translation) indicated that this effect does not reflect a difference in the transcriptional level of the mutant respect to the wild-type protein. Our experiments confirmed that the difference in the stability of the $p27^{T198A}$, observed after the treatment with the protein synthesis inhibitor cycloheximide, is due to enhanced protein degradation since its expression could be rescued by the treatment of the cells with the proteasome inhibitor MG132. However this effect is not dependent on the T187 phosphorylation, since it was not rescued by the concomitant mutation of T187 in alanine, and it is not dependent on the binding with the cyclin-CDK complexes or with the Skp2 protein, as previously suggested (Kossatz et al. 2006). On the contrary our data support the possibility that the increased proteasome-dependent degradation of the $p27^{T198A}$ mutant does not

reflect a lack of phosphorylation but the presence of a small aminoacid in the last position of p27. In fact by the use of different approaches and several mutants differing one to each other only for the residue chosen for the substitution of T198, we demonstrated that only when T198 was mutated in alanine or glycine, the smallest aminoacids, the stability of the p27 protein dramatically decreased. In fact when T198 was substituted with the non-phosphorylable valine or when it was completely deleted ($p27^{1-197}$) the stability was restored. We thus speculated that the size of the last amino-acid rather than the threonine phosphorylation is important for the regulation of its expression. Accordingly, by increasing the size of the last amino-acid from glycine to phenylalanine, that contains a big aromatic ring in its structure, the stability of the proteins increased. This evidence was independently reached by others who recently demonstrated how p27 with a premature stop codon at amino-acid 177 did not display any defect in protein stability when compared to the WT protein (Molatore et al., 2010).

Moreover, a recent work showed that the C-terminal domain of p27 adopts a disordered and quite highly extended conformation when p27 is bound to CDK2/cyclin A and this conformation allows p27 C-terminus to function as a regulatory domain that is structurally independent of the N-terminal domain (Galea et al., 2007). We thus hypothesize that it is not the lack of T198 or the lack of its phosphorylation that is responsible for higher protein degradation but only the conformation assumed by p27 when a small amino-acid, such as alanine or glycine is present at the very end of the unstructured tail. Considering that the observed increased proteasomal degradation is Skp2-independent, we speculate that the T198A/G substitution results in an unstable conformation of the C-terminal tail of p27 which is then more rapidly recognized and degraded via the unfolded protein degradation system. Accordingly, it has been demonstrated that under particular stress conditions p27 is recognized by the heat-shock protein Hsp27 and this interaction eventually results in accelerated protein degradation (Parcellier et al., 2006).

We also focused our attention on the role of the phosphorylation of the last p27 aminoacid on cell proliferation. Although phosphorylation of p27 on Thr 198 has been described to be required for the timely exit of p27 from the nucleus after mitogenic stimulation (Fijita et al., 2002 and 2003; Motti et al., 2004; Kossatz et al., 2006), our results suggest that phosphorylation of T198 has no effect on cell proliferation. In fact colony assay experiment on cells overexpressing p27 WT and mutated forms showed that $p27^{1-170}$, $p27^{T198E}$ and $p27^{T198V}$ mutants were able to inhibit proliferation as well as the wild type protein while the absence of cell growth inhibition by $p27^{T198A}$ (and $p27^{T187-198A}$) was likely due to the low expression levels, indicating that the overexpression of p27 was able to inhibit cell growth independently from phosphorylation of T198, but only when expressed over a threshold level. Moreover the analysis of G1/S transition in a starvation-and-

release experiment demonstrated that no significant differences could be observed in the ability to enter into the cell cycle among the different mutants analyzed. This observation is in accord with previous studies demonstrating that the C-terminus of p27 is involved in the control of migration but not of cell cycle progression (Baldassarre et al., 2005; Schiappacassi et al., 2008; Berton et al., 2010).

We also investigated the role of threonine 198 in p27 regulation of cell motility since its phosphorylation by RSK1 kinase has been proposed to increase p27-RhoA binding and thus cell motility (Larrea et al., 2009). To avoid any possible misinterpretation due to the increased proteasomal degradation of $p27^{T198A}$, we compared the activity of $p27^{T198E}$ and $p27^{T198V}$ that have a similar expression and a similar half-life in our cell lines and we tested whether or not $p27^{WT}$, $p27^{T198E}$ or $p27^{T198V}$ proteins had any effect on the ECM-driven motility using different experimental settings. We observed that $p27^{1-170}$ and $p27^{T198V}$ were unable to properly inhibit HT-1080 cell migration through a FN-coated transwell while the pseudo-phosphorylated mutant $p27^{T198E}$ displays an activity similar to the WT protein. These results were also confirmed by the use of video time-lapse microscopy to track the motility of p27-EGFP-fusion proteins expressing cells.

The ability of p27 to modulate cell migration has been previously ascribed by its ability to bind other proteins more directly implicated in the regulation of cellular motility, namely RhoA and stathmin (Besson et al. 2004; Baldassarre et al., 2005; Schiappacassi et al., 2008; Berton et al., 2009). We demonstrated that p27 T198 phosphorylation favors the interaction between p27 and stathmin following cell adhesion to ECM, thus proposing the mechanism by which the T198 modification could affect cell motility. These data are in agreement with our (Belletti et al., 2008) and others' (Langenickel et al., 2008; Delaloy et al., 2010) observations, showing that stathmin activity plays a pivotal role in the regulation of cell migration and metastasis formation. We also provide evidence that in our experimental setting the p27/RhoA interaction is not implicated, since no direct binding between the two proteins was detectable, even after overexpression of both proteins. However, our group recently demonstrated that the interaction between p27 and stathmin indirectly affects RhoA activity in mouse fibroblasts (Belletti et al., 2010). In the absence of p27 increased MT-dynamics results in increased RhoA activity, following cell adhesion to ECM. We cannot exclude that this mechanism works also in the model system we used in the present thesis and that RhoA activity participates to the motile phenotype observed in the cells expressing the different p27 mutants. It is to note that the inhibition of the Rho-Rock1 activity results in the formation of cell protrusion in several model system (Ridley et al., 2006; Woo et al., 2006; Machacek et al., 2009; Belletti et al., 2010), and we demonstrated here how overexpression of p27

induced protrusion formation in U87MG included in 3D matrices and/or adhered to ECM substrates. This event is dependent on the presence of the last 28 amino-acids and partially on the phosphorylation of T198. In fact we noticed some differences between the activity of $p27^{1-170}$ deletion mutant and the $p27^{T198V}$ point mutant in the regulation of cell motility and protrusion formation and also in stathmin binding capacity. These observations suggest that other residues are important in the regulation of cell motility within the C-terminal portion of p27 and future work will better define the modifications required for proper regulation of cell motility. The relevance of the p27-stathmin-MT dynamics-Rho axis we recently highlighted (Belletti et al., 2010) in the generation of cell protrusion is confirmed by several experimental evidences that demonstrate how p27 (Nguyen et al., 2006; Kawauchi et al., 2006) and stathmin (Ozon et al., 2002; Watabe et al., 2006) participate in the neurite protrusion formation and in the regulation of neuronal migration, at least in part by modulating Rho small GTPase activity.

Therefore this work provides new unexpected results on the role of T198 in modulating the functions of p27. In fact we evidenced that the complex regulation of p27 functions include not only the phosphorylation of threonine 198 but also the three dimensional conformation of its unstable C-terminal tail and how these events eventually play a role in the control of ECM-driven cell motility.

This study also raises concerns on the correct interpretation of the results coming from studies focused on phosphorylation of threonine and/or serine only by the use of T/A or S/A substitution.

2. The role of K134 SUMOylation in the regulation of p27 stability and localization

Considering that p27 is predominantly regulated at post-translational level we also decided to investigate whether p27 could undergo other post-translational modifications in addition to phosphorylation. In particular we focused our attention on SUMOylation, a highly dynamic post-translational modification which consists in the covalent attachment of SUMO (Small Ubiquitin-like protein MOdifier) to lysine residues of target protein by an enzymatic cascade. More than a decade after its discovery, the small ubiquitin-like protein modifier (SUMO) has emerged as a key regulator of proteins and the search for SUMO substrate has produced a long list of targets, which appear to be involved in most cellular functions. Lysine residue targeted by SUMO is frequently found in the sequence motif ΨKxE/D (in which Ψ is a large aliphatic aminoacid, x is any aminoacid and D/E is aspartic/glutamic acid), which has been identified as the consensus SUMO-acceptor site (Geiss-Friedlander et al., 2007).

In silico analysis with SUMOplot™ program (Abgent), which predicts and scores SUMOylation sites in the protein of interest, revealed that five out of the thirteen lysines contained

in p27 molecule are predicted to be SUMOylated even if they do not lie within the classical SUMO acceptor site. It is known from literature that many functionally important SUMO sites are contained in no consensus sequences and that some variants of the canonical sequence exist such as the E/DxKΨ inverted SUMOylation motif and the hydrophobic cluster SUMOylation motif (HCSM) in which the modified lysine is preceded by a cluster of at least three hydrophobic aminoacids (Matic et al., 2010). Moreover two different extensions of the simple SUMO acceptor site have been described (PDSM and NDSM, phosphorylation-dependent and negative charged aminoacid-dependent, respectively, SUMOylation motifs) which both have a negative charged aminoacid next to the basic consensus site that has been demonstrated to enhance SUMOylation (Anckar et al., 2007).

The functional analysis of SUMOylation is hampered by the low amount of the SUMOylated protein of interest in the cell. One observation regarding SUMOylation is that only small proportion of the available substrate protein need to be SUMOylated to achieve maximal effect. This phenomenon has been referred to as the 'SUMO enigma' (Hay, 2005). As a consequence most SUMO targets are modified at a very low level at any given time. This implicate the need to analyze by immunoprecipitation a great amount of the target protein to detect the small modified proportion, a fact that could explain the difficulty to analyze the SUMOylation levels of endogenous proteins. For this reason to test whether p27 could be *in vitro* SUMOylated we immunoprecipitated p27 from Phoenix-293 cells transiently transfected with Flag-p27 together with Ubc9, which is the unique enzyme known to transfer SUMO to the acceptor site, and with HA-SUMO 1 or SUMO 2. Western blot analysis clearly showed that p27 is SUMOylated *in vitro* by SUMO 1 as indicated by the presence of a higher-weight p27, which corresponds to the SUMO covalently modified p27, when SUMO 1 but not SUMO 2 is overexpressed. In particular we detected one slower-migrating p27 at about 45 KDa with the signal that seemed to be constituted by double band, and another slow-migrating p27 was detected at about 62 KDa. Considering that SUMO 1 typically does not form poly-SUMO chains because it lacks SUMO consensus sequence, only one SUMO 1 can be linked to a lysine residue (Ulrich, 2008). As a consequence the presence of two higher-weight p27 forms (45 and 62 KDa) and the shift of their molecular weight (about 18 KDa and 36 KDa, respectively) together with the double band-signal at 45 KDa we suggested that p27 could be mono-SUMOylated on two lysine residues. The analysis of SUMOylation of some p27 deleted mutants indicated that one site should be located in the region comprised between aa 42-85 and the other in the portion between aa 78-198, a result consistent with the prediction analysis, which indicated K73 and K134 as the most probable modified sites. By site-directed mutagenesis we identified lysine 134 as SUMOylated residue since $p27^{K134R}$ mutant did not display

a double SUMOylation band at ~45 KDa. In fact the lower band completely disappeared and also the band at 62 KDa was slightly decreased.

Our results indicated that lysine 134 is definitely a site of SUMOylation and are corroborated by two important biochemical considerations. First, K134 is preceded by proline which is one of aminoacid most frequently observed before SUMOylated lysine and second, considering the role of phosphorylated or negatively-charged residues in enhancing protein SUMOylation, we noticed that four positions downstream K134 there are two serine separated by one aspartic acid, which are the most frequently occurring aminoacids found in these positions downstream the SUMOylated lysine. However our incapability to completely abolish p27 SUMOylation by mutagenesis raises some questions about the significance of the upper 45 KDa-band and the 62 KDa band. A good explanation could come from the observation reported by others (Wilson et al., 2008) that site-directed mutagenesis method is unable to discriminate between SUMOylation sites and sites whose mutation alters in somehow the substrate and results in SUMOylation at distal lysines. Another explanation could simply be that these bands are aspecific. In fact if p27 had two SUMOylated lysines the signal at 62 KDa would completely disappeared by mutating just one of the two residues, but our results did not clearly show this abrogation. To exclude the presence of aspecific signals it will be necessary to generate the so-called p27 SUMO-defective mutant which could not be SUMOylated since all its thirteen lysines have been mutated. This strategy has been used for other proteins as reported in the oral presentation by Aragon et al. during the 6th Conference on SUMO, Ubiquitin and UBL proteins helded in Houston (TX-USA) last february. Mass spectrometry-based proteomic analysis would also provide us a more precise way for better clarify the lysines involved in p27 SUMO-modification. The analysis of mouse p27, which is SUMOylated as human p27 since we detected the same SUMOylation bands as for the human protein but from which it differs because it lacks lysines 73, 81 and 134, suggested that SUMOylation is an evolutionary conserved post-translational modification of p27 even if the involved lysines are not the same between the two species.

Next step was the understanding of the upstream pathways that induce p27 SUMOylation and the biological effect on p27 activity. The consequences of SUMOylation for a target are impossible to predict, as modification can alter localization, activity or stability. Considering that p27 function is highly regulated by various extracellular stimuli we first assessed which could be the stimulus inducing p27 SUMOylation. We started our analysis from the most important stimulus that regulates p27, TGFβ, which has been described to accumulate nuclear p27 to mediate cell cycle arrest in late G1 (Lecanda et al., 2009). Our results from TGFβ treatment of HeLa cells overexpressing both p27 and the SUMO-machinery indicated that TGFβ signaling increased the

SUMOylation of p27 WT but not of K134R mutant. Then we asked whether p27 SUMOylation induced by TGFβ could affect its localization. This hypothesis was confirmed by two different experimental approaches. First we observed that endogenous p27 accumulates in the nucleus of MCF-7 breast adenocarcinoma cell line, where it co-localizes with SUMO 1 after 3 hrs-treatment with TGFβ, and second, the un-SUMOylable K134R mutant was not able to shuttle into the nucleus of HeLa cells after TGFβ stimulation. Altogether these results suggested that TGFβ could affect p27 localization through a SUMOylation-dependent mechanism. Moreover we also demonstrated that K134-SUMOylation participates in the regulation of p27 stability in response to serum-starvation, which is another well-known condition stabilizing p27. In fact the analysis of p27 stability in HT1080 cells revealed that the un-SUMOylable K134R mutant is less stable than the WT protein as it was observed by cell treatment with the protein synthesis inhibitor cyclohexamide.

TGFβ has been described to induce G1-arrest by accumulating nuclear p27 and by preventing its proteasomal degradation. Moreover p27 has been described to be the sole mediator of this growth inhibition, since knocking down p27 by siRNA completely obviated TGFβ response (Lecanda et al., 2009). Considering these evidences together with the results outlined in this thesis, we hypothesized that TGFβ regulation of p27 function and localization is exerted through the modulation of its SUMOylation. This hypothesis is supported by our results which demonstrate that TGFβ increases p27 SUMOylation and that the SUMO-defective $p27^{K134R}$ mutant is not able to translocate into the nucleus in response to TGFβ signaling. Some more experiments are needed to further demonstrate our hypothesis and to better elucidate the intracellular effectors involved in the TGFβ-induced signaling pathway inducing p27 SUMOylation. In particular we will address whether or not the phosphorylation/modification of T198 could be a signal involved in the regulation of p27 SUMOlatyon induced by TGFβ, since this signal impinge on T198 modification via SGK1 activation (Hong et al., 2008).

Finally, some other important considerations have to be done. We found that p27 is SUMOylated on lysine 134, which is also one of the three lysine residues targeted by ubiquitin for p27 proteasomal degradation. Since our results regarding p27 stability indicated that SUMOylation stabilizes p27 as demonstrated by the decreased stability of the K134R mutant, we speculated that there could be a crosstalk between this two modification systems that could confer different fates to p27 protein, as already reported for other proteins (Ulrich, 2005). Furthermore, the interplay between p27 post-translational modifications could be much more complex if we consider that the pathways inducing its proteasomal degradation involve phosphorylation on tyrosines and threonine residues. Our results could also provide a new molecular mechanism for explaining how p27 is downregulated in several tumors. In fact considering that both SUMOylation pathway and TGFβ

signaling are altered during cancer progression (Bawa-Khalfe et al., 2010; Massaguè, 2008), we speculate that the alteration of the TGFβ-SUMO axis could be responsible for the accelerated p27 degradation found in several tumors.

Collectively the results collected in this thesis provide new insight into p27 regulation by both post-translational modifications and conformational changes in its unstructured C-terminal domain that may be helpful in the design of new anticancer therapies.

REFERENCES

Alessandrini A, Chiaur DS, Pagano M. (1997). Regulation of the cyclin-dependent kinase inhibitor p27 by degradation and phosphorylation. *Leukemia.* 11:342-5.

Anckar J, Sistonen L. (2007). SUMO: getting it on. *Biochem Soc Trans*. Dec;35(Pt 6):1409-13. Review.

Baldassarre G, Belletti B, Nicoloso MS, Schiappacassi M, Vecchione A, Spessotto P, Morrione A, Canzonieri V, Colombatti A. (2005). p27(Kip1)-stathmin interaction influences sarcoma cell migration and invasion. *Cancer Cell*. Jan;7(1):51-63.

Bawa-Khalfe T, Yeh ET. (2010) SUMO losing balance: SUMO proteases disrupt SUMO homeostasis to facilitate cancer development and progression. *Genes& Cancer* 1(7), 748-752.

Belletti B, Baldassarre G. (2011). Stathmin: a protein with many tasks. New biomarker and potential target in cancer. *Expert Opin Ther Targets*. Nov;15(11):1249-66. Epub 2011 Oct 7.

Belletti B, **Nicoloso MS, Schiappacassi M, Berton S, Lovat F, Wolf K, Canzonieri V, D'Andrea S, Zucchetto A, Friedl P, Colombatti A, Baldassarre G.** (2008). Stathmin activity influences sarcoma cell shape, motility, and metastatic potential. *Mol Biol Cell.* May;19(5):2003-13.

Belletti B, Nicoloso MS, Schiappacassi M, Chimienti E, Berton S, Lovat F, Colombatti A, Baldassarre G. (2005). p27(kip1) functional regulation in human cancer: a potential target for therapeutic designs. *Curr Med Chem*. 12(14):1589-605. Review.

Belletti B, **Nicoloso MS, Schiappacassi M, Chimienti E, Berton S, Lovat F, Colombatti A, Baldassarre G.** (2005). p27(kip1) functional regulation in human cancer: a potential target for therapeutic designs. *Curr Med Chem*. 12(14):1589-605. Review.

Belletti B, Pellizzari I, Berton S, Fabris L, Wolf K, Lovat F, Schiappacassi M, D'Andrea S, Nicoloso M S, Lovisa S, Sonego M, Defilippi P, Vecchione A, Colombatti A, Friedl P, and Baldassarre G. (2010). p27kip1 controls cell morphology and motility by regulating microtubule-dependent lipid raft recycling *Mol. Cell. Biol.* May;30(9):2229-40. Epub 2010 Mar 1.

Belmont LD, **Mitchison TJ.** (1996). Identification of a protein that interacts with tubulin dimers and increases the catastrophe rate of microtubules. *Cell*. Feb 23;84(4):623-31.

Berton S, **Belletti B, Wolf K, Canzonieri V, Lovat F, Vecchione A, Colombatti A, Friedl P, Baldassarre G**. (2009). The tumor suppressor functions of p27(kip1) include control of the mesenchymal/amoeboid transition. *Mol Cell Biol*. Sep;29(18):5031-45. Epub 2009 Jul 13.

Besson A, **Gurian-West M, Schmidt A, Hall A, Roberts JM**. (2004). p27Kip1 modulates cell migration through the regulation of RhoA activation. *Genes Dev*. Apr 15;18(8):862-76.

Bienkiewicz EA, Adkins JN and Lumb KJ. (2002). Functional consequences of preorganized helical structure in the intrinsically disordered cell-cycle inhibitor p27(Kip1). *Biochemistry*. 41:752–759.

Bloom J, Pagano M. (2003). Deregulated degradation of the cdk inhibitor p27 and malignant transformation. *Semin Cancer Biol*. Feb;13(1):41-7.

Bohem M, Yoshimoto T, Crook MF, Nallamshetty S, Treu A, Nabel GJ, Nabel EG. (2002). A growth factor-dependent nuclear kinase phosphorylates p27 (Kip1) and regulates cell cycle progression. *EMBO J.* 21:3390-401.

Borghese L, **Fletcher G, Mathieu J, Atzberger A, Eades WC, Cagan RL, Rørth P.** (2006). Systematic analysis of the transcriptional switch inducing migration of border cells. *Dev Cell.* Apr;10(4):497-508.

Borriello A, Cucciolla V, Criscuolo M, Indaco S, Oliva A, Giovane A, Bencivenga D, Iolascon A, Zappia V, Della Ragione F. (2006) Retinoic acid induces p27Kip1 nuclear accumulation by modulating its phosphorylation. *Cancer Res*. Apr 15;66(8):4240-8.

Bouchard C, **Thieke K, Maier A, Saffrich R, Hanley-Hyde J, Ansorge W, Reed S, Sicinski P, Bartek J, Eilers M.** (1999). Direct induction of cyclin D2 by Myc contributes to cell cycle progression and sequestration of p27. *EMBO J*. Oct 1;18(19):5321-33.

Brattsand G, **Marklund U**, **Nylander K**, **Roos G, Gullberg M.** (1994). Cell-cycle-regulated phosphorylation of oncoprotein 18 on Ser16, Ser25 and Ser38. *Eur J Biochem.* 220:359-68.

Carrano AC, Eytan E, Hershko A, Pagano M. (1999). SKP2 is required for ubiquitin-mediated degradation of the CDK inhibitor p27. *Nat Cell Biol.* 1: 193–9.

Chassot AA, **Turchi L, Virolle T, Fitsialos G, Batoz M, Deckert M, Dulic V, Meneguzzi G, Buscà R, Ponzio G**. (2007). Id3 is a novel regulator of p27kip1 mRNA in early G1 phase and is required for cell-cycle progression. *Oncogene*. Aug 23;26(39):5772-83.

Chu I, Sun J, Arnaout A, Kahn H, Hanna W, Narod S, Sun P, Tan CK, Hengst L, Slingerland J. (2007). p27 phosphorylation by Src regulates inhibition of cyclin E-CDK2. *Cell*. 128:281-94.

Connor MK, **Kotchetkov R, Cariou S, Resch A, Lupetti R, Beniston RG, Melchior F, Hengst L, Slingerland JM.** (2003). CRM1/Ran-mediated nuclear export of p27(Kip1) involves a nuclear export signal and links p27 export and proteolysis. *Mol Biol Cell*. Jan;14(1):201-13.

Daniel C, **Pippin J, Shankland SJ, Hugo C.** (2004). The rapamycin derivative RAD inhibits mesangial cell migration through the CDK-inhibitor p27KIP1. *Lab Invest.* May;84(5):588-96.

Delaloy C, Liu L, Lee JA, Su H, Shen F, Yang GY, Young WL, Ivey KN, Gao FB. (2010). MicroRNA-9 coordinates proliferation and migration of human embryonic stem cell-derived neural progenitors. *Cell Stem Cell.* 6: 323–35.

Deng X, Mercer SE, Shah S, Ewton DZ, Friedman E. (2004). The cyclin-dependent kinase inhibitor p27Kip1 is stabilazes in G0 by Mirk/dyrk1B kinase. *J Biol Chem.* 279:22498-504.

Denicourt C, **Saenz CC, Datnow B, Cui XS, Dowdy SF.** (2007). Relocalized p27Kip1 tumor suppressor functions as a cytoplasmic metastatic oncogene in melanoma. *Cancer Res.* Oct 1;67(19):9238-43.

Donovan JC, Rothenstein JM, Slingerland JM. (2002). Non-malignant and tumor-derived cells differ in their requirement for p27Kip1 in transforming growth factor-beta-mediated G1 arrest. *J Biol Chem* Nov 1;277(44):41686-92. Epub 2002 Aug 28.

Dorval V, Fraser PE. (2006). Small ubiquitin-like modifier (SUMO) modification of natively unfolded proteins tau and alpha-synuclein. *J Biol Chem* Apr 14;281(15):9919-24.

Dunker AK, Obradovic Z, Romero P, Garner EC, Brown CJ. (2000). Intrinsic protein disorder in complete genomes. *Genome Inform Ser Workshop Genome Inform* 11:161–171.

Dyson HJ, Wright PE. (2005). Elucidation of the protein folding landscape by NMR. *Methods Enzymol*. **2005**;394:299-321.

Fotedar R, **Fitzgerald P, Rousselle T, Cannella D, Dorée M, Messier H, Fotedar A.** (1996). p21 contains independent binding sites for cyclin and cdk2: both sites are required to inhibit cdk2 kinase activity. *Oncogene*. May 16;12(10):2155-64.

Fujita N, Sato S, Katayama K, Tsuruo T. (2002). Akt-dependent phosphorylation of p27Kip1 promotes binding to 14-3-3 and cytoplasmic localization. *J Biol Chem.* 277(32):28706-13. Epub 2002 May 31.

Fujita N, Sato S, Tsuruo T. (2003). Phosphorylation of p27Kip1 at threonine 198 by p90 ribosomal protein S6 kinases promotes its binding to 14-3-3 and cytoplasmic localization. *J Biol Chem*. 278(49):49254-60. Epub 2003 Sep 22.

Gadea BB, Ruderman JV. (2006). Aurora B is required for mitotic chromatin-induced phosphorylation of Op18/Stathmin. *Proc Natl Acad Sci. USA* 103:4493-8.

Galea CA, Nourse A, Wang Y, Sivakolundu SJ, Heller WT, Kriwacki RW. (2007) Role of intrinsic flexibility in signal transduction mediated by the cell cycle regulator, p27Kip1. *J Mol Biol.* Feb 22; 376(3):827-38.

Galea CA, **Wang Y**, **Sivakolundu SG, Kriwacki RW.** (2008). Regulation of Cell Division by Intrinsically Unstructured Proteins: Intrinsic Flexibility, Modularity and Signaling Conduits. *Biochemistry*. July 22; 47(29): 7598–7609.

Geiss-Friedlander R, Melchior F. (2007). Concepts in sumoylation: a decade on. *Nat Rev Mol Cell Biol*. Dec;8(12):947-56.

Gocke CB, Yu H, Kang J. (2005). Systematic identification and analysis of mammalian small ubiquitin-like modifier substrates. *J Biol Chem.* Feb 11;280(6):5004-12.

Grimmler M, Wang Y, Mund T, Cilensek Z, Keidel EM, Waddell MB, Jakel H, Kullmann M, Kriwacki RW, Hengst L. (2007). CKD-inhibitory activity and stability of p27Kip1 are directly regulated by oncogenic tyrosine kinases. *Cell.* 128:269-80.

Gunasekaran K, Tsai CJ, Kumar S, Zanuy D, Nussinov R. (2003). Extended disordered proteins: targeting function with less scaffold. *Trends Biochem Sci*. Feb;28(2):81-5.

Hannoun Z, Greenhough S, Jaffray E, Hay RT, Hay DC. (2010). Post-translational modification by SUMO. *Toxicology* 278 (2010) 288–293

Hara T, **Kamura T, Kotoshiba S, Takahashi H, Fujiwara K, Onoyama I, Shirakawa M, Mizushima N, Nakayama KI.** (2005). Role of the UBL-UBA protein KPC2 in degradation of p27 at G1 phase of the cell cycle. *Mol Cell Biol*. Nov;25(21):9292-303.

Hara T, **Kamura T, Nakayama K, Oshikawa K, Hatakeyama S, Nakayama K.** (2001). Degradation of p27(Kip1) at the G(0)-G(1) transition mediated by a Skp2-independent ubiquitination pathway. *J Biol Chem*. Dec 28;276(52):48937-43.

Hauck L,Harms C, An J, Rohne J, Gertz K, Dietz R, Endres M, Harsdorf R. (2008). Protein kinase CK2 links extracellular growth factor signaling with the control of p27Kip1 stability in the heart. *Nat Med.* 14(3): 315-324.

Hay RT. (2005). SUMO: a history of modification. *Mol Cell.* Apr 1;18(1):1-12.

Hayashi K, Pan Y, Shu H, Ohshima T, Kansy JW, White CL 3rd, Tamminga CA, Sobel A, Curmi PA, Mikoshiba K, Bibb JA. (2006). Phosphorylation of the tubulin-binding protein, stathmin, by Cdk5 and MAP kinases in the brain. *J Neurochem.* 99:237-50

Hengst L, Reed SI. (1998). Inhibitors of the Cip/Kip family. *Curr Top Microbiol Immunol*. 227:25-41.

Hong F, Larrea MD, Doughty C, Kwiatkowski DJ, Squillace R, Slingerland JM. (2008). mTOR-raptor binds and activates SGK1 to regulate p27 phosphorylation. *Mol Cell.* Jun 20;30(6):701-11.

Iakoucheva LM, Brown CJ, Lawson JD, Obradovic Z, Dunker AK. (2002). Intrinsic disorder in cell-signaling and cancer-associated proteins. *J. Mol. Biol.* 323:573–584.

Iancu-Rubin C, Atweh GF. (2005). p27(Kip1) and Stathmin share the stage for the first time. *Trends Cell Biol.* Jul;15(7):346-8. Review.

Ishida N, Hara T, Kamura T, Yoshida M, Nakayama K, Nakayama KI. (2002). Phosphorylation of p27Kip1 on serine 10 is required for its binding to CRM1 and nuclear export. *J Biol Chem* 2002; 277(17):14355-8. Epub 2002 Mar 11.

Ishida N, Kitagawa M, Hatakeyama S, Nakayama K. (2000). Phoshorylation at serine 10, a major phpsphorilation site ok p27 (kip1), increases its protein stability. *J Biol Chem.* 275:25146-54.

Jeffrey PD, **Tong L, Pavletich NP.** (2000). Structural basis of inhibition of CDK-cyclin complexes by INK4 inhibitors. *Genes Dev*. Dec 15;14(24):3115-25.

Jin K, **Mao XO, Cottrell B, Schilling B, Xie L, Row RH, Sun Y, Peel A, Childs J, Gendeh G, Gibson BW, Greenberg DA**. (2004). Proteomic and immunochemical characterization of a role for Stathmin in adult neurogenesis. *FASEB J.* Feb;18(2):287-99.

Johnson WE, **Watters DJ, Suniara RK, Brown G, Bunce CM.** (1999). Bistratene A induces a microtubule-dependent block in cytokinesis and altered Stathmin expression in HL60 cells. *Biochem Biophys Res Commun*. Jun 24;260(1):80-8.

Jourdain L, **Curmi P, Sobel A, Pantaloni D, Carlier MF.** (1997). Stathmin: a tubulin-sequestering protein which forms a ternary T2S complex with two tubulin molecules. *Biochemistry.* Sep 9;36(36):10817-21.

Kaldis P: Another piece of the p27Kip1 puzzle. *Cell.* 2007; 128:241-244.

Kamura T, **Hara T, Matsumoto M, Ishida N, Okumura F, Hatakeyama S, Yoshida M, Nakayama K, Nakayama KI.** (2004). Cytoplasmic ubiquitin ligase KPC regulates proteolysis of p27(Kip1) at G1 phase. *Nat Cell Biol*. Dec;6(12):1229-35.

Kardinal C, Dangers M, Kardinal A, Koch A, Brandt DT, Tamura T, Welte K. (2006). Tyrosine phosphorylation modulates binding preference to cycline-dependent kinases and subcellular localization of p27Kip1 in the acute promyelocytic leukemia cell line NB4. *Blood*. 107:1144-40.

Kawauchi T, Chihama K, Nabeshima Y, Hoshino M. (2006). Cdk5 phosphorylates and stabilizes p27kip1 contributing to actin organization and cortical neuronal migration. *Nat Cell Biol*. 8: 17–26.

Koff A, **Ohtsuki M, Polyak K, Roberts JM, Massagué J.** (1993). Negative regulation of G1 in mammalian cells: inhibition of cyclin E-dependent kinase by TGF-beta. *Science*. Apr 23;260(5107):536-9.

Kortylewski M, **Heinrich PC, Mackiewicz A, Schniertshauer U, Klingmüller U, Nakajima K, Hirano T, Horn F, Behrmann I.** (1999). Interleukin-6 and oncostatin M-induced growth inhibition of human A375 melanoma cells is STAT-dependent and involves upregulation of the cyclin-dependent kinase inhibitor p27/Kip1. *Oncogene*. Jun 24;18(25):3742-53.

Kossatz U, **Dietrich N, Zender L, Buer J, Manns MP, Malek NP.** (2004). Skp2-dependent degradation of p27kip1 is essential for cell cycle progression. *Genes Dev*. Nov 1;18(21):2602-7.

Kossatz U, Vervoorts J, Nickeleit I, Sundberg HA, Arthur SJ, Manns MP, Malek NP. (2006). C-terminal phosphorylation controls the stability and function of p27Kip1. *EMBO J*. 25:5159-5170.

Kotoshiba S, **Kamura T, Hara T, Ishida N, Nakayama KI**. (2005). Molecular dissection of the interaction between p27 and Kip1 ubiquitylation-promoting complex, the ubiquitin ligase that regulates proteolysis of p27 in G1 phase. *J Biol Chem*. May 6;280(18):17694-700.

Küntziger T, Gavet O, Manceau V, Sobel A, Bornens M. (2001). Stathmin/Op18 phosphorylation is regulated by microtubule assembly. *Mol Biol Cell*. 12:437-48.

Lacy ER, Filippov I, Lewis WS, Otieno S, Xiao L, Weiss S, Hengst L, Kriwacki R. (2004). p27 binds cyclin–CDK complexes through a sequential mechanism involving binding-induced protein folding. *Nat Struct Mol Biol*. 11:358–364.

Langenickel TH, Olive M, Boehm M, San H, Crook MF, Nabel EG. (2008). KIS protects against adverse vascular remodeling by opposing stathmin-mediated VSMC migration in mice. *J Clin Invest* 118: 3848–59.

Larrea MD, Hong F, Wander SA, da Silva TG, Helfman D, **Lannigan D, Smith JA, Slingerland JM.** (2009). RSK1 drives p27Kip1 phosphorylation at T198 to promote RhoA inhibition and increase cell motility. *Proc Natl Acad Sci USA* 106: 9268–73.

Lecanda J, Ganapathy V, D'Aquino-Ardalan C, Evans B, Cadacio C, Ayala A, Gold LI. (2009). TGFbeta prevents proteasomal degradation of the cyclin-dependent kinase inhibitor p27kip1 for cell cycle arrest. *Cell Cycle* Mar 1;8(5):742-56. Epub 2009 Mar 16.

Liang J, Shao SH, Xu ZX, Hennessy B, Ding Z, Larrea M, Kondo S, Dumont D, Gutterman U, Walker CL, Slingerland JM, Mills GB. (2007). The energy sensing LKB1-AMPK pathway regulates p27kip1 phosphorylation mediating the decision to enter autophagy or apoptosis. *Nat Cell Biol*. 9(2):218-224.

Liang J, Zubovitz J, Petrocelli T, Koychetkov R, Connor MK, Han K, Lee JH, Ciarallo S, Catzavelos C, Beniston R, Frassen E, Slingerland JM. (2002). PKB/Akt phosphorylates p27, impairs nuclear import of p27 and opposes p27-mediated G1 arrest. *Nat Med* 2002; 8(10):1153-60. Epub Sep 16.

Loda M, Cukor B, Tam SW, Lavin P, Fiorentino M, Draetta GF, Jessup JM, Pagano M. (1997). Increased proteasome-dependent degradation of the cyclin-dependent kinase inhibitor p27 in aggressive colorectal carcinomas. *Nat Med.* 3(2):231-4.

Lu Z, Hunter T. (2010). Ubiquitylation and proteasomal degradation of the p21(Cip1), p27(Kip1) and p57(Kip2) CDK inhibitors. *Cell Cycle.* Jun 15;9(12):2342-52. Epub 2010 Jun 15.

Machacek M, Hodgson L, Welch C, Elliott H, Pertz O, **Nalbant P, Abell A, Johnson GL, Hahn KM, Danuser G**. (2009). Coordination of Rho GTPase activities during cell protrusion. *Nature.* 461:99–103.

Malanga D, De Gisi S, Riccardi M, Scrima M, De Marco C, Robledo M, Viglietto G. (2011). Functional characterization of a rare germline mutation in the gene encoding the Cyclin-Dependent Kinase Inhibitor p27Kip1 (CDKN1B) in a Spanish patient with Multiple Endocrine Neoplasia (MEN)-like phenotype. *Eur J Endocrinol*. Nov 30 [Epub ahead of print].

Martin S, Wilkinson KA, Nishimune , Henley JM. (2007). Emerging extranuclear roles of protein SUMOylation in neuronal function and dysfunction. *Nat Rev Neurosci.* Dec;8(12):948-59.

Maruyama S, **Hatakeyama S, Nakayama K, Ishida N, Kawakami K, Nakayama K.** (2001). Characterization of a mouse gene (Fbxw6) that encodes a homologue of Caenorhabditis elegans SEL-10. *Genomics*. Dec;78(3):214-22.

Massaguè J. (2008) TGFβ and cancer. *Cell* 134, 215-230.

Matic I, Schimmel J, Hendriks IA, van Santen MA, van de Rijke F, van Dam H, Gnad F, Mann M, Vertegaal AC. (2010). Site-specific identification of SUMO-2 targets in cells reveals an inverted SUMOylation motif and a hydrophobic cluster SUMOylation motif. *Mol Cell*. Aug 27;39(4):641-52.

McAllister SS, **Becker-Hapak M, Pintucci G, Pagano M, Dowdy SF.** (2003). Novel p27(kip1) C-terminal scatter domain mediates Rac-dependent cell migration independent of cell cycle arrest functions. *Mol Cell Biol.* Jan;23(1):216-28.

Medema RH, **Kops GJ, Bos JL, Burgering BM**. (2000). AFX-like Forkhead transcription factors mediate cell-cycle regulation by Ras and PKB through p27kip1. *Nature*. Apr 13;404(6779):782-7.

Molatore S, Kiermaier E, Jung CB, Lee M, Pulz E, Höfler H, Atkinson MJ, Pellegata NS. (2010). Characterization of a naturally-occurring p27 mutation predisposing to multiple endocrine tumors. *Mol Cancer* 9: 116.

Montagnoli A, Fiore F, Eytan E, Carrano AC, Draetta GF, Hershko A, Pagano M. (1999). Ubiquitination of p27 is regulated by Cdk-dependent phosphorylation and trimeric complex formation. *Genes Dev*. 13(9):1181-9.

Motti ML, **De Marco C, Califano D, Fusco A, Viglietto G.** (2004). Akt-dependent T198 phosphorylation of cyclin-dependent kinase inhibitor p27kip1 in breast cancer. *Cell Cycle*. Aug;3(8):1074-80.

Mukhopadhyay D, Dasso M. (2007). Modification in reverse: the SUMO proteases. *Trends Biochem Sci*. Jun;32(6):286-95. Epub 2007 May 17.

Nacusi LP, Sheaff RJ. (2006). Akt1 sequentially phosphorylates p27kip1 within conserved but noncanonical region. *Cell Division.* 1:11-38.

Nakayama K, **Nagahama H, Minamishima YA, Miyake S, Ishida N, Hatakeyama S, Kitagawa M, Iemura S, Natsume T, Nakayama KI.** (2004). Skp2-mediated degradation of p27 regulates progression into mitosis. *Dev Cell*. May;6(5):661-72.

Nguyen L, **Besson A**, **Heng JI**, **Schuurmans C**, **Teboul L**, **Parras C**, **Philpott A**, **Roberts JM**, **Guillemot F.** (2006). p27kip1 independently promotes neuronal differentiation and migration in the cerebral cortex. *Genes Dev*. 20(11):1511-24. Epub 2006 May 16.

Nigg EA. (2001). Mitotic kinases as regulators of cell division and its checkpoints. *Nat Rev Mol Cell Biol*. Jan;2(1):21-32. Review.

Nurse P. (2000). A long twentieth century of the cell cycle and beyond. *Cell*. Jan 7;100(1):71-8. Review.

Oldfield CJ, Cheng Y, Cortese MS, Brown CJ, Uversky VN, Dunker AK. (2005). Comparing and combining predictors of mostly disordered proteins. *Biochemistry.* 44:1989–2000.

Ozon S, **Guichet A, Gavet O, Roth S, Sobel A.** (2002). Drosophila Stathmin: a microtubule-destabilizing factor involved in nervous system formation. *Mol Biol Cell.* Feb;13(2):698-710.

Pagano M, Tam SW, Theodoras AM, Beer-Romeno P, Del Sa G, Chau V, Yew PR, Draetta GF, Rolfe M. (1995). Role of ubiquitin-proteasome pathway in regulating abundance of the cyclin-dependent kinase inhibitor p27. *Science*. 269:682-5.

Parcellier A, Brunet M, Schmitt E, Col E, Didelot C, Hammann A, Nakayama K, Nakayama KI, Khochbin S, Solary E, Garrido C. (2006). HSP27 favors ubiquitination and proteasomal degradation of p27Kip1 and helps S-phase reentry in stressed cells. *FASEB J.* 20: 1179–81.

Pellegata N, Quintanilla-Martinez L, Siggelkow H, Samson E, Bink K, Hofler H, Fend F, Graw F, Atkinson MJ. (2006). Germ-line mutations in p27Kip1 cause a multiple endocrine neoplasia syndrome in rats and humans. *PNAS.* 103(42): 15558–15563.

Perez-Roger I, **Kim SH, Griffiths B, Sewing A, Land H**. (1999). Cyclins D1 and D2 mediate myc-induced proliferation via sequestration of p27(Kip1) and p21(Cip1). *EMBO J*. Oct 1;18(19):5310-20.

Polyak K, **Kato JY, Solomon MJ, Sherr CJ, Massague J, Roberts JM, Koff A**. (1994). p27Kip1, a cyclin-Cdk inhibitor, links transforming growth factor-beta and contact inhibition to cell cycle arrest. *Genes Dev*. Jan;8(1):9-22.

Pruitt K, **Der CJ**. (2001). Ras and Rho regulation of the cell cycle and oncogenesis. *Cancer Lett*. Sep 28;171(1):1-10. Review.

Ridley AJ. (2006). Rho GTPases and actin dynamics in membrane protrusions and vesicle trafficking. *Trends Cell Biol.* 16: 522–9.

Rodier G, Montagnoli A, Di Marcotullio L, Coulombe P, Draetta GF, Pagano M, Meloche S. (2001). p27 cytoplasmic localization is regulated by phosphorylation on Ser10 and is not a prerequisite for its proteolysis. *EMBO J*. 20(23):6672-82.

Rubin CI, Atweh GF. (2004). The role of stathmin in the regulation of the cell cycle. *J Cell Biochem.* 93:242-50.

Russo AA, Jeffrey PD, Pavletic NP. (1996). Structural basis of cyclin-dependent kinase activation by phosphorylation. *Nat Struct Biol.* 3(8):696-700.

Sánchez-Beato M, **Camacho FI, Martínez-Montero JC, Sáez AI, Villuendas R, Sánchez-Verde L, García JF, Piris MA.** (1999). Anomalous high p27/KIP1 expression in a subset of aggressive B-cell lymphomas is associated with cyclin D3 overexpression. p27/KIP1-cyclin D3 colocalization in tumor cells. *Blood*. Jul 15;94(2):765-72.

Schiappacassi M, Lovat F, Canzonieri V, Belletti B, Berton S, Santoni A, Vecchione A, Colombatti A, Baldassarre G. (2008). p27Kip1 expression inhibits glioblastoma growth, invasion and tumor-induced neoangiogenesis. *Mol Canc Ther.* 2008 7: 1164–75.

Schiappacassi M, Lovisa S, Lovat F, Fabris L, Colombatti A, Belletti B, Baldassarre G (2011). Role of T198 modification in the regulation of p27Kip1 protein stability and function. *PLoS One*. Mar 14;6(3):e17673.

Sekimoto T, **Fukumoto M, Yoneda Y**. (2004). 14-3-3 suppresses the nuclear localization of threonine 157-phosphorylated p27(Kip1). *EMBO J.* May 5;23(9):1934-42.

Sheaff RJ, Groudine M, Gordon M, Roberts JM, Clurman BE. (1997). Cyclin E-CDK2 is a regulator of $p27^{Kip1}$. *Genes Dev.* 11(11):1464-78.

Sherr CJ, **Roberts JM.** (1995). Inhibitors of mammalian G1 cyclin-dependent kinases. *Genes Dev.* May 15;9(10):1149-63. Review.

Sherr CJ. (1993). Mammalian G1 cyclins. *Cell*. Jun 18;73(6):1059-65. Review.

Shin I, Yakes FM, Rojo F, Shin NY, Bakin AV, Baselga J, Arteaga CL. (2002) PKB/Akt mediates cell-cycle progression by phosphorylation of p27(Kip1) at threonine 157 and modulation of its cellular localization. *Nat Med***.** 8(10):1145-52. Epub 2002 Sep 16.

Sivakolundu SG, Bashford D, Kriwacki RW. (2005). Disordered p27(Kip1) exhibits intrinsic structure resembling the Cdk2/cyclin A-bound conformation. *J Mol Biol*. Nov 11;353(5):1118-28. Epub 2005 Sep 20.

Sun J, **Marx SO, Chen HJ, Poon M, Marks AR, Rabbani LE.** (2001). Role for p27(Kip1) in Vascular Smooth Muscle Cell Migration. *Circulation.* Jun 19;103(24):2967-72.

Todaro GJ, Wolman SR, Green H. (1963). Rapid transformation of human fibroblasts with low growth potential into established cell lines by SV40. *J Cell Physiol*. Dec;62:257-65.

Tomoda K, **Kubota Y, Kato J**. (1999). Degradation of the cyclin-dependent-kinase inhibitor p27Kip1 is instigated by Jab1. *Nature*. Mar 11;398(6723):160-5.

Toyoshima H, **Hunter T**. (1994). p27, a novel inhibitor of G1 cyclin-Cdk protein kinase activity, is related to p21. *Cell*. Jul 15;78(1):67-74.

Tsvetkov LM, Yeh KH, Lee SJ, Sun H, Zhang H. (1999). p27(Kip1) ubiquitination and degradation is regulated by the SCF(Skp2) complex through phosphorylated Thr187 in p27. *Curr Biol*. 9: 661–4.

Ulrich HD (2005). Mutual interactions between the SUMO and ubiquitin systems: a plea of no contest. *TRENDS in Cell Biology.* Vol.15 No.10 October 2005.

Ulrich HD (2008). The fast-growing business of SUMO chains. *Mol Cell.* Nov 7;32(3):301-5. Review.

Viglietto G, Motti ML, Bruni P, Pelillo ML, D'Alessio A, Califano D, Vinci F, Chiappetta G, Fusco A, Santoro M. (2002). Cytoplasmic relocalization and inhibition of the cyclin-dependent kinase inhibitor p27(Kip1) by PKB/Akt-mediated phosphorylation in breast cancer. *Nat Med.* 8(10):1136-44. Epub 2002 Sep 16.

Vlach J Hennecke S, Amati B. (1997). Phosphorylation-dependent degradation of the cyclin-dependent kinase inhibitor p27. *EMBO J*. 16(17):5334-44.

Vlach J, **Hennecke S, Alevizopoulos K, Conti D, Amati B.** (1996). Growth arrest by the cyclin-dependent kinase inhibitor p27Kip1 is abrogated by c-Myc. *EMBO J.* Dec 2;15(23):6595-604.

Wang Y, Dasso M. (2009). SUMOylation and DeSUMOylation at a glance. *Journal of Cell Science*.122, 4249-4252.

Watabe-Uchida M, John KA, Janas JA, Newey SE, Van Aelst L. (2006). The Rac activator DOCK7 regulates neuronal polarity through local phosphorylation of stathmin/Op18. *Neuron.* 51: 727–39.

Weinberg RA. (1995). The molecular basis of oncogenes and tumor suppressor genes. *Ann N Y Acad Sci.* Jun 30;758:331-8. Review.

Wilkinson KA, Henley JM. (2010). Mechanisms, regulation and consequences of protein SUMOylation. *Biochem. J*. **428**, 133–145.

Wilson VG, Heaton PR. (2008). Ubiquitin proteolytic system: focus on SUMO. *Expert Rev. Proteomics.* 5, 121–135.

Wittmann T, **Bokoch GM, Waterman-Storer CM**. (2004). Regulation of microtubule destabilizing activity of Op18/Stathmin downstream of Rac1. *J Biol Chem*. Feb 13;279(7):6196-203.

Wolf G, Reinking R, Zahner G, Stahl RAK, Shankland SJ. (2003). Erk 1,2 phosphorylates p27Kip1: Functional evidence for a role in high glucose-induced hypertrophy of mesangial cells. *Diabetologia*; 46:1090-9.

Woo S, Gomez TM. (2006). Rac1 and RhoA promote neurite outgrowth through formation and stabilization of growth cone point contacts. *J Neurosci.* 26:1418–28.

Xu Y, Li J, Zuo Y, Deng J, Wang LS, Chen GQ. (2011). SUMO-specific protease 1 regulates the in vitro and in vivo growth of colon cancer cells with the upregulated expression of CDK inhibitors. *Cancer Lett* Oct 1;309(1):78-84. Epub 2011 Jun 12.

Zeng Y, **Hirano K, Hirano M, Nishimura J, Kanaide H**. (2000). Minimal requirements for the nuclear localization of p27(Kip1), a cyclin-dependent kinase inhibitor. *Biochem Biophys Res Commun*. Jul 21;274(1):37-42.

PUBLICATIONS

1. Belletti B, Pellizzari I, Berton S, Fabris L, Wolf K, Lovat F, Schiappacassi M, D'Andrea S, Nicoloso MS, **Lovisa S**, Sonego M, Defilippi P, Vecchione A, Colombatti A, Friedl P, Baldassarre G. p27kip1 controls cell morphology and motility by regulating microtubule-dependent lipid raft recycling. *Mol Cell Biol*. 2010 May;30(9):2229-40. Epub 2010 Mar 1.

2. Schiappacassi M*, **Lovisa S***, Lovat F, Fabris L, Colombatti A, Belletti B, and Baldassarre G. Role of T198 modification in the regulation of p27Kip1 protein stability and function. *PLoS One*. 2011 Mar 14;6(3):e17673.

   * equally contributed